ADAPTIVE FUZZY LOGIC CONTROL
FOR
SOLAR BUILDINGS

MOHAMED MAHMOUD GOUDA NASER EL-DEEN

B.Sc. (Hons), M.Sc., AMIEE, MIEEE

A thesis submitted in partial fulfilment of the requirement of the University of Northumbria at Newcastle for the degree of Doctor of Philosophy

July 2002

In Collaboration with Smart Solar Buildings Controller Project, Non Nuclear Energy Program, JOULE III, The European Union

Declaration

No portion of the work referred to in this thesis has been submitted in support of an application for another degree or qualification of this university or any other university or other institution of learning.

All works in this thesis and the resulting publications are the sole work of the author unless otherwise stated.

Dedication

To

My Parents Sprit, My Wife,

My Sisters, and My Kids

Yasmin, Toqa and Mahmoud

Abstract

Significant progress has been made on maximising passive solar heating loads through the careful selection of glazing, orientation and internal mass within building spaces. Control of space heating in buildings of this type has become a complex problem. Additionally, and in common with most building control applications, there is a need to develop control solutions that permit simple and transparent set up and commissioning procedures. This work concerns the development and testing of an adaptive control method for space heating in buildings with significant solar input.

A simulation model of a building space to assess the performance of different control strategies is developed. A lumped parameter model based on an optimisation technique has been proposed and validated. It is shown that this model gives an improvement over existing low order modelling methods. A detailed model of a hot water heating system and related control devices is developed and evaluated for the specific purpose of control simulation.

A PI-based fuzzy logic controller is developed in which the error and change of error between the internal air temperature and the user set point temperature is used as the controller input. A conventional PID controller is also considered for comparison. The parameters of the controllers are set to values that result in the best performance under likely disturbances and changes in setpoint.

In a further development of the fuzzy logic controller, the Predicted Mean Vote (PMV) is used to control the indoor temperature of a space by setting it at a point where the PMV index becomes zero and the predicted percentage of persons dissatisfied (PPD) achieves a maximum threshold of 5%. The controller then adjusts the air temperature set point in order to satisfy the required comfort level given the prevailing values of other comfort variables contributing to the comfort sensation. The resulting controller is free of the set up and tuning problems that hinder conventional HVAC controllers.

The need to develop an adaptive capability in the fuzzy logic controller to account for lagging influence of solar heat gain is established and a new adaptive controller has therefore been proposed. The development of a "quasi-adaptive" fuzzy logic controller is developed in two steps. A feedforward neural network is used to predict the internal air temperature, in which a singular value decomposition (SVD) algorithm is used to remove the highly correlated data from the inputs of the neural network to reduce the network structure. The fuzzy controller is then modified to have two inputs: the first input being the error between the setpoint temperature and the internal air temperature and the second the predicted future internal air temperature. When compared with a conventional method of control the proposed controller is shown to give good tracking of the setpoint temperature, reduced energy consumption and improved thermal comfort for the occupants by reducing solar overheating.

The proposed controller is tested in real time using a test cell equipped with an oil-filled electric radiator, temperature and solar sensors. Experimental results confirm earlier findings arrived at by simulations, in that the proposed controller achieves superior tracking and reduces afternoon solar overheating, when compared with a conventional method of control.

Acknowledgements

I wish to express my sincere thanks and gratitude to my supervision team Dr. Sean Danaher and Dr. Chris Underwood for their support, valuable and continuous advice, guidance, weekly meetings, (and their friendship) throughout the duration of this work.

I would like to thank Dr. Nicola Pearsal, Newcastle Photovoltaic Center, University of Northumbria, and all staff in the Met Office's research department for providing the weather data used throughout the progress of this work.

All my thanks to the technician staff at the school of Engineering and school of Built Environment, University of Northumbria for their kind and helpful assistance during preparation and testing the heating system, the circuits and the sensors used in this work.

I wish to thank Dr. Chris Martin and Mr. Martin Watson, Energy Monitoring Company LTD, for their support during the implementation and testing of this work at the Cranfield test cell.

I would like to express my sincere thanks to the Egyptian Government for financial support for this research. I would also like to thank the European Union Non Nuclear Program for providing financial supports during the testing phase of this work.

My special thanks and deep gratitude to my wife Dr. Abeer, who helped me, gave me good support, and looked after our children during the hard time of this work. Also, my thanks to our children Yasmin, Toqa and Mahmoud.

I would like to give great appreciation and thanks to Dr. Maher EL-Ghotmy, faculty of Electronics Engineering Menouf, Menoufia University, Egypt, whose recent untimely death has been such a loss to me. He was of great advice and guidance in the beginning of this work.

Table of Contents

List of Symbols

A_{total}	Overall area of construction elements (m^2)
A_w	Emitter internal area (m^2)
A_a	Emitter external area (m^2)
A_{tcross}	Emitter cross-sectional area (m^2)
A	Surface area (m^2); linear inequality constraint matrix
A_{eq}	Matrix coefficients of the equality constraint
a_1, a_2	Limits of the optimised function, x
A_j	Surface area of the j^{th} construction element (m^2)

a, b	Constants
b_{inq}	Vectorised coefficients of the inequality
b_{eq}	Vectorised coefficients of the equality constraints
$C(x)$	Nonlinear inequality
$C_{eq}(x)$	Nonlinear equality constraints
C_{total}	Overall thermal capacity (JK^{-1})
C_1	Thermal capacity of the 1st layer ($JK^{-1}m^{-2}$)
C_k	Thermal capacity up to the kth layer ($JK^{-1}m^{-2}$)
c_{pw}	Specific heat capacity of water ($Jkg^{-1}K^{-1}$)
C_w	Thermal capacity of emitter water (JK^{-1})
C_m	Thermal capacity of emitter material (JK^{-1})
C_i	Thermal capacity of the ith room element (JK^{-1})
c_{pl}	Specific heat capacity of the lth layer ($Jkg^{-1}K^{-1}$)
D	Feasible domain region
d_i	Tube internal diameter (m)
f'	Vectorised coefficients of x
f_{cl}	Ratio of body's surface area when fully clothed to body's surface area when nude
f_k	Reduced model resistance rations ($k = 1, 2, 3$)
G_{inh}	Inherent valve characteristic
G_{ins}	Installed valve characteristic
G_o	Valve let-by
g	Moisture content of air (kg/kg)
g_{ss}	Moisture content of air at saturation (kg/kg)
g_l	Reduced model capacitance rations ($l = 1, 2$)
h_e	Air side heat emitter heat transfer coefficient ($Wm^{-2}K^{-1}$)
h_{cw}	Water-side heat emitter convection coefficient ($Wm^{-2}K^{-1}$)
h	Specific enthalpy of water vapour (kJ/kg)
H_r	Internal air enthalpy (kJ/kg)
H_o	Outdoor air enthalpy (kJ/kg)
I_{cl}	Thermal resistance of the clothing (Clo)

J	Inequality constraints of the general feasible domain, D
K	equality constraints of the general feasible domain, D
k_w	Thermal conductivity of water ($(Wm^{-1}K^{-1})$)
k_l	Thermal conductivity of l^{th} layer $(Wm^{-1}K^{-1})$
L_{bound}	lower bound on the optimised function, x
m_w	Emitter water flow rate (kgs^{-1})
Met	Human metabolic rate (W/m^2)
M	Mass of air in a room (kg)
m_o	Input ventilation mass flow rate (kg/s)
n	Heat emission index
N	Valve authority
Nu_d	Nusselt number (with respect to tube diameter)
n	Number of construction element layers
Pr	Prandtl number
Pw_{sat}	Partial pressure of saturated water-vapour at a given temperature (N/m^2)
pv	Relative air velocity (m/s)
Q_s	Solar intensity (W)
Q_p	Plant heat output (W)
Q_r	Radiant heat input to space (W)
Q_g	Casual heat gains to space (W)
Q_l	Latent heat gain (kJ)
Q	Heat flux at surface element (W)
Q_w	Heat transfer from water (W)
Re_d	Reynolds number (with respect to tube diameter)
R_{total}	Area-integrated overall thermal resistance (KW^{-1}).
R_{ins}	Area-integrated inner region thermal resistance (KW^{-1}).
R_{out}	Area-integrated outer region thermal resistance (KW^{-1}).
R_k	Thermal resistance of the k^{th} layer (m^2KW^{-1}).
R_k^*	Equivalent area-integrated thermal resistance up to the k^{th} layer (m^2KW^{-1})
r_{si}	Inside surface thermal resistance (m^2KW^{-1}).
r_{so}	Outside surface thermal resistance (m^2KW^{-1}).

r_a	Air gap thermal resistance (m^2KW^{-1}).
S	Percentage saturation
T_{wo}	Emitter outlet water temperature (°C)
T_{wi}	Emitter inlet water temperature (°C)
T_m	Emitter material temperature (°C)
T_g	Earth temperature (°C)
T_o	Outdoor (external) air temperature (°C)
T_i	Internal (room) air temperature (°C)
T_j	Surface temperature of the j^{th} construction element (°C)
T_{mrt}	Mean radiant temperature (°C)
T_{cl}	Surface temperature of clothing (°C)
U_{bound}	Upper bound on the optimised function, x
U_i	Overall thermal transmittance of the i^{th} room element ($Wm^{-2}K^{-1}$)
x	Optimised function
x_l	Thickness of l^{th} layer (m)
α	Accessibility factor
λ_i	Lagrange multiplier
ϕ_i	Internal relative humidity (%)
ϕ_{ext}	Outdoor air relative humidity (%)
ρ_l	Density of l^{th} layer (kgm^{-3})
ρ_w	Density of water (kgm^{-3})
v_w	Mean velocity of water (ms^{-1})
μ_w	Dynamic viscosity of water ($kgm^{-1}s^{-1}$)

List of Figures

Chapter 1

Introduction, Research Aims and Thesis Organisation

Chapter 1

Introduction, Research Aims and Thesis Organisation

1.1. Introduction

In most European countries, buildings account for approximately 40% of the total energy use. Energy use is increasing, despite the fact that improved technologies and stricter building codes are making buildings more energy efficient. Furthermore, their total number is increasing; they use more equipment, and have higher comfort requirements than ever.

Research and development on energy efficiency and the use of renewable energy in buildings has until recently primarily focused on small scale, residential buildings. In

most European climates, high-energy prices and strict building codes have resulted in residential buildings that use very little energy for space heating.

Significant progress has also been made on maximising passive solar heating loads through the careful selection of glassing, orientation and internal mass. Control of space heating in buildings of this type has become a complex problem and it is this area that has been addressed in this thesis.

Key issues in the control of heating in low energy buildings with passive solar features are as follows:

1. Frequent instances of reduced output operation (stability, tracking and minimising energy use).
2. Ability to deal with a range of room space thermal capacity (robust, stability and tracking).
3. Ability to respond to solar inputs likely to be received at a later part of the day (need for adaptability).

Additionally, and in common with most building control applications, there is a need to develop a control solution that permit simple and transparent set up and commissioning procedures.

1.2. Research aims and objectives

The aims of this thesis are to develop and test an adaptive control method for space heating in buildings with significant solar input. The intention is to establish a control strategy that enjoys at least the same stability and tracking properties as "well tuned" conventional control is adaptive to change in adventitious heat gain (solar and other sources). Also, it should display good robustness properties for light load control and operation in both high and low thermal capacity space, and enjoys simple and intuitive commissioning. Thus, the proposed control strategy should have the following properties:

1. Consideration of solar radiation in the control strategy.

2. Self-adaptation of the controller to building and climate parameter changes.
3. Robust, i.e. wide applicability of the controller to the characteristics of the buildings space and plant capacity.
4. Reduced commissioning over the conventional controller.

Many of the above points can be addressed through the use of adaptive fuzzy systems. It is therefore intended that a fuzzy framework will form the brains of the control strategy to be developed. Fuzzy logic has the advantages of being able to model imprecise conditions whilst not requiring an exact mathematical model of the control process, and is capable of decision-making as well as dealing with multi-variant problems.

The objectives of the research are therefore as follows:

1. A simulation model of the thermal performance of a building with space heating plant and control will be developed as a test bed for analysing control strategies.
2. Design of a single-input single-output fuzzy logic controller, as an internal air temperature regulator, and benchmarking with a conventional proportional-integral-derivative (PID) controller.
3. Design of a thermal comfort based fuzzy logic controller to provide an acceptable range of thermal comfort for the occupants as a refinement of the above.
4. Development of a predictor to estimate internal comfort conditions with a moving time horizon as a basis for control system adaptability. Initially, the use of an artificial neural network (ANN) is expected to be promising in this role.
5. Design of a mechanism for the adaptiveness to changing climate variables (in particular solar heating) of the comfort –based fuzzy logic controller.
6. Real-time implementation and evaluation of the proposed controller.

1.3. Organisation of the Thesis

A brief description of the thesis organisation is given below.

Chapter 2: Literature review

This chapter reviews the previous research with reference to heating system control. The aim of the review was to establish the various types of controllers have

been used in the past in this application, together with their successes and failures. An area of emphasis is the review of previous application of fuzzy logic to the control of heating, ventilating and air-conditioning (HVAC) plant.

Chapter 3: Building modelling for control investigation

This chapter describes the development of a simulation model of a building space to assess the performance of different control strategies developed in later chapters of the thesis. A lumped parameter model based on an optimisation technique has been proposed and validated and it is shown that this model gives an improvement over the widely used first order lumped parameter model based on Lorenz & Masy [1]. Development and implementation of solar data processor is also discussed.

Chapter 4: Heating system modelling

In this chapter, a detailed model of a hot water heating systems and related control devices is developed and evaluated for the specific purpose of control simulation.

Chapter 5: Static fuzzy logic and PID controllers

This chapter presents the architecture and the principles in the design of the static fuzzy logic controller (FLC) developed for the control of the internal air temperature. A PI-based fuzzy logic controller and conventional PID controller are developed in which the error and change of error between the internal air temperature and the user set point temperature are used as the controller inputs. The output of the controller is applied to the heating system to bring the internal air temperature to the setpoint temperature. The parameters of the controllers are set to values that result in the best performance under likely disturbances and changes in setpoint.

Chapter 6: Thermal comfort based fuzzy logic control

In this chapter, the predicted mean vote (PMV) is used to control the indoor temperature of a space by setting it at a point where the PMV index becomes zero and the predicted percentage of persons dissatisfied (PPD) achieves a maximum threshold of 5%. This is achieved through the use of a fuzzy logic controller that takes into account a range of human comfort criteria in the formulation of the control action that

should be applied to the heating system to bring the space to comfort conditions. The resulting controller is free of the set up and tuning problems that hinder conventional HVAC controllers. The PMV-based fuzzy logic controller investigated in this chapter starts with the evaluation of the predicted mean vote level and compares this with the required comfort range in order to arrive at a linguistic definition of the comfort sensation. The controller then adjusts the air temperature set point in order to satisfy the required comfort level, given the prevailing values of the other comfort variables contributing to the comfort sensation. A comparison is then made between the developed control strategy and the conventional method of building space-heating control.

Chapter 7: Adaptive fuzzy logic control

In this chapter a new adaptive controller has been proposed. The development of a proposed quasi-adaptive fuzzy logic controller is developed in two steps. A feedforward neural network is used to predict the internal air temperature, in which a singular value decomposition (SVD) algorithm is used to remove the highly correlated data from the inputs of the neural network to reduce the network structure. Then, the fuzzy controller has two inputs: the first input is the error between the setpoint temperature and the internal air temperature and the second input is the predicted future internal air temperature. The controller is shown to give good tracking to the setpoint temperature, reduced the energy consumption for the heating and improve thermal comfort for the occupants by reducing solar overheating.

Chapter 8: Controller testing

In this chapter, the proposed controller is tested in a real time test cell using an oil-filled electric radiator, temperature and solar sensors. The experiment was carried at a remote test facility at Cranfield University. Hardware consisted of a filter circuit for the internal and external air temperature, an amplifier and filter for solar radiation, a pulse width modulation circuit and semiconductor relay as a power circuit for the oil-filled electric radiator. A comparison is carried out between the proposed controller and a conventional PID controller.

Chapter 9: Conclusions and recommendations for further work

This final chapter considers the findings of the research project and presents the main conclusions. Recommendations are made with regard to areas of the research that are worthy of further investigation.

1.4. Contribution of this Thesis

The contributions from this research work are summarised as follows:

1. A new approach to building space modelling is described and implemented, based on a parameter-optimised second order description of each building envelope element.
2. Subsystem models of HVAC plant and control are also developed making use of an existing component library where possible. The result is a detailed dynamic model of a building space with HVAC plant and control which enjoys flexibility, transparency and computational efficiency, essential for the specialist case of investigating control system response over low time scales.
3. A new thermal comfort based fuzzy logic controller has been developed based on the using of predictive mean vote (PMV) as a control criterion but using air temperature as a proxy for comfort.
4. A new application of a feedforward neural network with singular value decomposition (SVD) to predict the internal air temperature of the building space based on the external climate and internal behaviour of the heating system and the building space has been demonstrated.
5. A new combination between a fuzzy logic control and neural network to produce a quasi-adaptive fuzzy controller has been developed. This controller is designed and tested to compensate for afternoon solar heating received by the building space.

The contributions of this work are supported by various publications:

1. *Gouda MM, S Danaher, and C P Underwood* "Modelling the Heating of A Building Space Using MATLAB-SIMULINK", 3rd Mathematical and Modelling Conference (3rd MATHMOD), Vienna University, Vienna, Austria, 2000.

2. *Gouda MM, S Danaher, and C P Underwood* "Fuzzy Logic Control versus Conventional PID for Controlling Indoor Temperature of a Building's Space", Computer Aided Control System Design (CACSD2000) Conference, Salford University, Salford, UK, 2000.
3. *Gouda MM, S Danaher, and C P Underwood* "Low Order Model for the Simulation of a Building and Its Heating System", Building Services Engineering Research and Technology, 2000.
4. *Gouda MM, S Danaher, and C P Underwood* "Thermal Comfort based Fuzzy Logic control", Building Services Engineering Research and Technology, 2001.
5. *Gouda MM, S Danaher, and C P Underwood* "Building Thermal Model Reduction by Non-linear Constrained Optimisation", Building and Environment, 2001.
6. *Gouda MM, S Danaher, and C P Underwood* "Development of an artificial neural network predictor for indoor temperature of a solar building", IASTED Conference of Intelligent System and Control (ISO2001), Tampa, Florida, USA, 2001.
7. *Gouda MM, S Danaher, and C P Underwood* "Application of an artificial neural network for modelling the thermal dynamics of a building's space and its heating system", Mathematical and Computer Modelling of Dynamic Systems, 2002.

Chapter 2

Literature Review

Chapter 2

Literature Review

2.1 Introduction

It is now frequently acknowledged that heating systems present one of the most challenging situations to deal with from the point of view of control. Swings in day to day, week to week and season to season energy demand, together with an infinitely complex combination of user needs at the human interface, contribute to highly non-stationary "environment" within which control takes place. It is little wonder then that much of heating system control is about compromise; a compromise that usually amounts to reasonable comfort at minimum energy use and cost.

Heating system control, in common with all process system control, requires the governance of two distinct actions: those of "switching" or "enabling" and "regulating" or "adjustment". Switching in the majority of applications amounts to ensuring that the plant is available at certain times of the day (generally clock based, occupancy sensor based or indeed based on some other logical two state conditions such as an alarm state). Regulation, which is what this thesis essence is about, amounts to ensuring that the plant capacity is matched to the demands placed upon the system. The HVAC or heating system controller can be classified according to its system and/or according to its action.

This chapter aims to give the reader an overview of the research previously carried out into the use of different control strategies and more specifically fuzzy control for controlling the heating system and HVAC applications. Also, it gives the previous work, carried out in the area of building modelling techniques.

2.2. Energy crises and solar buildings design

In the mid-1970s, when the so-called energy crisis first made all the world aware of the finite nature of fossil fuels, architects and urban planners, who are in the part responsible for a field that account for more than half our energy consumption, were unable to find an immediate answer to this problem. For far too long, energy had been available in unlimited quantities and at a reasonable price, and there had seemed to be no vital need to reduce its consumption. Although there was a great sense of insecurity at the time, the challenge that this new situation presented was at least recognised: the primary function of buildings-the provision of shelter and comfort for man and his belongings-had to be reinterpreted.

The careful husbanding of energy and its more effective use in ecologically sustainable forms (in particular solar energy) came to assume a central role in the work of buildings design. This new approach was a pragmatic response to the situation and was not based just on fashionable trends. Now, three decades later, one can point to a number of outstanding structures that reveal an ambitious architectural concept as well as completely new interpretations and intense applications of

environmental energy-for heating, cooling, natural ventilation, lighting and the generation of electricity. The buildings in which solar energy has become a factor of the design and has been used in aesthetically effective form include schools, universities, housing schemes of all kinds and sizes, offices, museums, galleries and many other structures.

Concepts for new urban districts are now being developed in which structures using solar energy are no longer exotic, isolated examples. Today, the many potential uses of solar energy are seen in conjunction with the structures of urban and building developments, public open spaces and the infrastructure as forming an integral whole. As a result, it has been possible to achieve a considerable reduction in the consumption of energy from fossil fuels for the complex system that the city represents [2]. There are two benefits found from decreasing the energy consumption:

1. From cost point of view, energy consumption has become an important issue for policy makers on a global scale. This is due to additional strain on the environment due to the expected vast increase in world energy demand over the next 30 years [3]. In addition to the global concern, escalation in energy costs has made energy savings for building owners a viable option.
2. From environmental point of view, the energy saving reduce the production of greenhouse gases and/or other harmful waste products.

Good examples of solar buildings are the Doxford solar office in Sunderland, and the BP institute, University of Cambridge [4]. Passive solar building can contribute to reduce energy consumption in two ways: by increasing useful solar gains in buildings and thus offsetting the demand on the building's heating system. Also, by controlling heat gain in non-domestic buildings and allowing solar heated air to assist natural circulation and ventilation, a reduction of the need for mechanical ventilation and cooling is achieved. Unfortunately, this high level of uncontrolled solar gain can lead to uncomfortable overheating periods, even during the heating season. An adaptive heating control strategy should take both concerns into account in order to minimize occupant discomfort while keeping the energy consumption as low as possible.

There is a need for this type of controller (adaptive heating controller) not only for building spaces with high insulation and variable thermal mass but to adapt to adventitious heat gains received by the space under control. Instantaneous heat gains (i.e. arising from internal casual gains) can easily be dealt with by direct feedback but the lagging source due to solar radiation is much less responsive and requires the controller to take on an adaptive role.

2.3. Space heating control

Many electronic HVAC controller traditionally have fixed tuning which can not be adjusted on-site, often leaving the maintenance team with the problem of making the best out of a bad job in situation where the controller is not suited to an application.

Thus, development of current and future generation of HVAC control has begun to focus on in-built intelligence at the controller, in particular, adaptive control. Many of the ideas presently being explored are not new. John & Dexter [5] first discussed the potential for intelligence in building services control in 1989, identify progress and ongoing work in fields such as self-tuning, adaptive and rule base control. Zaheer-uddin [6] also reviews progress in adaptive and optimal control and gives illustrative examples of their applications in the HVAC field. Dexter & Haves [7] who discuss implementation issues of self tuning control with reference to HVAC applications.

Self-tuning and adaptive control are similar, representing control systems capable of adjusting themselves to changes in their operational domain as well as hanging requirements. Self tuning control systems make these adjustments in search of optimality over an initial period, and then freeze the parameters, whilst the adaptive controller continues to make adjustments throughout the life of the system. A general consensus is that with self-tuning controllers it is assumed that the process under control has initially unknown but constant parameters which can be estimated on-line, whilst no such assumptions about parametric constancy can be made with adaptive control. The early heating optimisers are examples of self-tuning systems in so far as a finite adjustment timespan is concerned, and considerable work has been done on these over the years [8-11].

Jota & Dexter [12] have developed general minimum variance (GMV) and general predictive control (GPC) algorithms for the heating and cooling coils of an air handling system. These have been applied directly to valve actuators and also "cascaded" in which the algorithm modifies the set point of a conventional fixed parameter PI controller. Direct application was found to produce unacceptable oscillation whilst the cascaded method gave a substantial improvement.

Brandt [13] developed a pole cancellation algorithm with "bracketing software" and applied it to two (small or large) VAV (variable air volume) systems with the bracketing software applied to the large test case only. The algorithm was applied to cooling coil and mixing damper control in each system. Brandt concluded that self-tuning control can work as well as a well tuned PID fixed parameter control without the need for lengthy and repetitive tuning of the latter, but the bracketing software proved essential for robustness. Other work on HVAC adaptive controllers using the pole placement method are reported by MacArthur et al. [14], Zaheer uddin [6] and Wellenborg [15].

Robust design offers the potential to deal with situations in which several aspects of the plant behaviour are uncertain in the presence of disturbances and measurement noise. Despite this, little work has been done to apply the robust methods the HVAC case. Though Attia & Rezeka [16] develop a state observer method to obtain robust multivariable control of temperature and humidity in the hot arid climates. Their results, based on simulations demonstrate improved stability and response times over conventional control, subject to a significant room space participating in the control loops.

Currently, fuzzy control is by far the most successful application of fuzzy logic to practical problems. Fuzzy controllers are expert control systems that smoothly interpolate between hard–boundary crisp rules. Rules fire simultaneously to a continuous degree or strengths and the multiple resultant actions are combined into an interpolated result. Processing of uncertain information and saving of energy using common sense rules and natural language statements are the basis for fuzzy control. The use of sensor data in practical control systems involves several tasks that are usually done by a human in the decision loop. All such tasks must be performed

based on the evaluation of data according to a set of rules in which the human expert has learned from experience or training.

Dexter & Trewhella [17] were among the first to apply fuzzy logic methods to HVAC plant. They developed five fuzzy inputs sets for the performance assessment of a hot water fan coil unit under PI control. The fuzzy input sets cover performance, energy use, control error, valve travel and occupant dissatisfaction. Two fuzzy output sets are generated, reflecting occupant response and plant performance. The rule base was developed with some advice from practitioners. The results revealed that fuzzy approach can give a plausible assessment of plant performance though a careful interpretation of the results was found to be essential.

For an unusual application in the holistic treatment of FLC, Dounis et al. [18] consider the thermal and visual environment resulting in a fuzzy controller which controls heating, cooling and window opening, shading and lighting.

Huang & Nelson [19] combine a PID controller with FLC and apply it to a general second order plant model. Fuzzy input sets are developed for control error, integral error and derivative error and an output set for the control signal. Results obtained using computer simulation show that the combined controller can virtually eliminate all of the damped oscillation common with tuned conventional PID control as well as achieving faster response.

Huang and Nelson [20] present a rule based fuzzy logic controller, which considered the error and rate of change of error as inputs to the controller. The paper discusses three important elements that have a critical influence on the behaviour of such controllers. These are the rule base, the membership functions and the scale factors (or tuning parameters). In a companion paper Huang and Nelson [21] described an experiment using the developed rule based fuzzy logic controller to control an HVAC system. Experimental results indicated that the fuzzy logic controller performed better than a conventional PID controller. The design of the fuzzy logic controller is similar to that reported by So et al. [22].

Willey [23] considered the use of fuzzy logic to model occupant actions and hence their control of the internal environment. The study suggests that fuzzy logic is better suited to estimating the imprecise actions an occupant may take to control their environment, e.g. window opening, than conventional algorithms.

Geng and Dexter [24] examine the use of fuzzy gain scheduling methods to deal with the non-linearities of HVAC plant. The paper considers the fuzzy gain scheduling of the control loops of a conventional proportional integral controller and a self-tuning predictive controller. The paper shows that the fuzzy gain scheduling schemes used in the control loop improved the overall performance of the system.

Ling et al. [25] examined the development of fuzzy rule-based supervisors for a self-tuning controller based on the Generalised Predictive Control Algorithm [26,27]. A fuzzy rule based fuzzy gain scheduler is first used to make use of the qualitative prior knowledge about changes in the plant gain, over the entire operating region. A simple fuzzy rule based fuzzy supervisor is then used to adjust the tuning parameters of the controller according to expert opinion based on qualitative descriptions of application dependent performance criteria, so improving the control loop performance gradually. The research suggests that the fuzzy gain scheduling provides a means of incorporating the uncertain prior knowledge about the process and improves the stability and or performance of the controller.

Dounis et al. [28] describe the use of a fuzzy reasoning process to provide visual comfort within buildings. A fuzzy logic controller is used to control lighting levels and glare by the use of window blinds and the turning on and off of artificial lights within the space. It shows that fuzzy control in this case is better than no control but does not prove any improvements over conventional control techniques. However, the research does bring out the ease with which fuzzy logic can be implemented without the availability of a mathematical model by incorporating human knowledge in the form of natural language.

MacConnell and Owens [29] used a fuzzy supervisor to ensure user comfort is maximised. The commissioning costs of the controller were minimised, the fuel economy was maximised by efficient use of the plant, maintenance costs were

reduced by eliminating stop-start cycles and allowing adaptation to unscheduled disturbances. The theory could also be implemented using low cost chip technology for real-applications.

Dounis et al. [30] investigated the impact of natural ventilation on the thermal comfort index assuming the implementation of fuzzy reasoning control for visual thermal comfort as described by Dounis et al. [28]. Controlling the window openings provided thermal comfort, and hence ventilation flows, by conventional controllers responding to the difference between the outside and zone temperatures. Free cooling was made available using this approach. The paper claims that the fuzzy visual comfort reasoning machine was capable of exploiting natural ventilation to control thermal comfort.

Early work applying ANNs to HVAC problems mostly concerned identification and modelling problems. Miller & Seem [31] use a three layers feedforward ANN, trained using back-propagation, to predict the start up time for heating during set back – in effect "optimal start control". They compare the results of ANN prediction with a conventional recursive least squares method, concluding that there was no significant advantage for the ANN in performance terms. However, the ANN required less data for training than the RLS and the ANN proved to be more robust. Anstett & Kreider [32] apply an ANN to the prediction of energy use in a large institutional building and, like Miller & Seem [31] they compare this approach with a conventional approach to energy management.

Curtiss et al. [33] use a backpropagated feed forward ANN with two hidden layers, each of 10 neurons, for energy management in central plant, concluding that ANNs can be successfully used to model energy use as well as to carry out energy management tasks, such as set point resetting. Huang & Nelson [34] train an ANN to determine delay times in HVAC plant. Besides successfully predicting delay time, the ANN was found to be capable of tolerating different levels of input measurement noise.

Curtiss et al. [35] and So et al. [36] develop ANN based predictive controllers as alternatives to conventional PID control. Curtiss and co workers develop a "look

ahead" adaptive ANN in which plant error is backpropagated through the ANN in a Hopfield-like fashion and the network used to predict future plant behaviour (i.e. future error) as a basis for control action. The resulting controller was found to be at least as good as well-tuned PID control but this crucially depended on the choice of network learning rate. In later work, Curtiss [37] goes on to demonstrate the implementation of a network assisted PID controller on a laboratory scale heating coil control loop. So et al. [36] develop a combined identifier/controller for MISO application in which control of an entire air handling plant is considered using an ANN. They compare this with well tuned PID and a fuzzy logic controller concluding that the response rate of ANN based method was inferior to the fuzzy logic controller and the steady state accuracy was slightly inferior to well tuned PID. However, the ANN training data were relatively easily obtained, the controller required nor tuning, no did it require any expert knowledge (as did the fuzzy logic controller).

Krideer and Wang [38] have applied ANNs to predict energy use in commercial buildings. In particular the authors have applied the method as part of their work on the application of expert systems to HVAC diagnostics in commercial buildings. They have used ANNs to determine with good accuracy the energy use of the chillers by using hourly averaged data collected from the system.

Curtiss et al. [39], demonstrated how ANNs can be used to optimise the energy consumption in a commercial scale HVAC system. For this study information from the actual system has been used to train a network in an attempt to optimise the energy consumption without sacrificing comfort and by considering all the physical limitations of the system.

Ling and Dexter [40] use a fuzzy rule based supervisor to evaluate control performance and adjust the temperature set point of an air-conditioning system within a given comfort band. The overall control objective aims to use free cooling, by altering the amount of fresh air entering a zone in a constant volume system, to maintain the zone temperature close to the upper limit of the comfort band. When free cooling is not capable of achieving this, plant cooling is used.

von Altrock [41] describes the use of a fuzzy controller to create an adaptive controller for use with a home heating system. The controller ensures optimal adaptation to customer heating demands while using one sensor less than a conventional control system. The findings of this paper are also given in Ross [42].

Dounis et al. [43] investigated the performance of a fuzzy reasoning machine for the control of indoor air quality in naturally ventilated buildings. Simulations were carried out using an airflow and pollutant transport model that used CO_2 concentrations as an index for indoor air quality. The aim of the fuzzy controller was to maintain the CO_2 concentration within certain limits while ensuring good stability of the window opening area. Using conventional control techniques to adjust actuators for the window opening would cause continuous window movement and would bother the occupants.

SO et al. [44] applied FLC to the control of air handling plant VAV systems. Using triangular FISs for error and error rate, FLC signals are generated for the air handling plant, fresh air damped fan control, cooling coil, humidifier and reheat coil. Results are compared with tuned and detuned PID control, using computer simulation. The results show that the FLC compares well with tuned PID control but was more robust and the FLC was superior to detuned PID control. In later work, they develop a self-learning FLC using an artificial neural network (ANN) based on the same air handling control problem as their earlier work [45]. The ANN is used to monitor the plant and update the parameters of the FLC, which permits robustness in spite of changes in operating conditions and non-linearities.

Egilegor et al. [46] described the results of simulations using a neuro fuzzy controller to adjust the airflow rate through fan coils for three zones of a dwelling to improve thermal comfort. The input variables of zone temperature and humidity are used to calculate the value of Fanger's PMV thermal comfort index, which is then used as a comfort variable. Fuzzy proportional derivative control is used to provide the desired zone conditions while a neural network is trained to tune the fuzzy controller to optimise the fuzzy tuning parameters and improve the control performance for different situations. Simulations carried out for the neuro fuzzy

controller indicate an improvement in the PMV compared to the benchmark simulations using thermostatic control.

2.4. Conclusions

This chapter introduced the reader to a brief history about energy crises, solar building design, space heating control and thermal modelling of the building. The review showed that, spurred by the energy crises, building designers produced passive solar buildings. However, this type of building can carry a high overheating risk due to large solar gain.

The review showed that, each controller provides only one or two benefits such as: good tracking, robustness, consideration of the solar radiation in the control strategy, self-adaptation of the controller to building and climate parameter changes, or reduced commissioning over the conventional controller.

Also, the review of previous applications of fuzzy logic to the control of building services components suggests that fuzzy logic is capable of providing control techniques which are often simpler to implement than conventional control systems and sometimes capable of providing superior control. Where a lack of knowledge regarding system behaviour exists, a solution using fuzzy logic may be possible where conventional control techniques are not suitable.

The research project described by this thesis aims to develop and test an adaptive control method for space heating in buildings with significant solar input. The literature review carried out into fuzzy logic and neural network suggested that an adaptive controller based upon a fuzzy control system combined with a neural network would be capable of dealing with such control aims.

Chapter 3

Building Modelling for Control Investigation

Chapter 3

Building Modelling for Control Investigation

3.1. Introduction

The short-time horizon modelling of building thermal response is of relevance in situations where Heating, Ventilating and Air Conditioning (HVAC) plant and control system analyses are of interest. In the precise area of building thermal modelling, issues of model accuracy and computational efficiency become important. Significant progress has been made in recent years on the development of modular and generic simulation programs for investigating the thermal behaviour of buildings and associated HVAC plant and controls. A large variety of building codes suitable for the evaluation of the energy consumption of building are available today. These codes use energy parameters [46], physical laws [48-52], and performance data [53-

56] to predict building energy consumption. The physical models use three basic methods [50]: numeric [48], harmonic [51], and response factors [49,52]. Building thermal models are used for calculation of energy consumption in a variety of buildings: single and multiple zone, thermally light and heavy, low rise and high rise [47,57], and residential and office [47,58]. Some building models also have integrated models of heating ventilation and air condition (HVAC) systems [51,55], of airflow in buildings [59], and passive solar, photovoltaic and combined heat and power system [60]. These models use either simulation or sensitivity analysis to design new buildings, and for retrofit applications to evaluate their heating and cooling performance [58,61,62]. These models can be either simple to apply and use, such as the low-cost, one zone model called BRE-ADMIT [63], or more laborious and time consuming to set-up and run such as DOE-2 [61,64], BLAST [65], TRNSYS [66], BUNYIP [67], and ESP [60]. These latter examples are also more expensive.

Such programs have found widespread acceptance as tools for energy analysis or thermal design of large commercial buildings. Also, many simplified programs are merely computer implementations of handbook methods [68]. Usually, these models cannot be changed, thereby reducing the flexibility of design. Thus a major disadvantage of such software is that they are often used for conditions for which they are not valid, or their results are misinterpreted due to poor understanding of the mathematical models on which they are based. Many of these programs are furthermore inflexible for the specific analysis of HVAC plant and control systems due to combinations of the following [69,70]:

1. Most established thermal modelling programs are not suited to short-time scale investigations (minutes or hours), having been developed with computational efficiency in mind for long-time-scale applications (e.g. seasonal energy use),
2. The use of steady-state plant component models in some instances makes them prone to numerical instability when high-frequency input excitations are applied and the dynamical design of controller is not possible with such model formulations, and
3. Programs using finite-differences for building dynamics tend to be computationally inefficient (though this is becoming less important with advances in computer technology).

In response to these shortcomings, a simple modelling method is needed which is numerically stable, when dealing with a wide spectrum of plant input excitations, and yet is computationally efficient. For the time horizons of interest in controller design, it is necessary and sufficient for such a modelling method to yield accurate results over several hours or a few days (i.e. as opposed to weeks or months as in the case of the "traditional" programs mentioned in earlier). The aim therefore is to develop and validate a flexible "lumped parameter" thermal model of a building, where many control strategies may be applied tested and "tuned" dynamically in order to investigate their behaviour under realistic plant operating conditions.

Lumped parameter (or lumped capacitance) approach have been used for some time to satisfy the dual needs of computational efficiency, whilst reconstructing the main dynamic features of interest among the various state variables. However the earlier, coarser, lumping strategies are known to have weaknesses and a method is proposed here which seeks to address this.

For the treatment of plant dynamics in buildings, the building response model requires not being only sufficiently accurate for the purpose but also computational efficient, since the faster-acting plant dynamics will tend to govern the choice of the time interval used for the solution of the equations. Relatively low order linear systems can capture the essential elements of observed behaviour. Simplified, or reduced order lumped parameter thermal models are therefore of interest. Potential advantages of simplified thermal models include reduced computing overheads, shorter coding, analytical solution of the state equations and easier verification.

Lorenz and Masy [1] made the first serious attempt at low-order thermal response modelling based on the proposals of Laret [71]. This work in turn formed the basis of analytical parameter estimation for the 5-parameter 2nd order model of Crabb et al. [72] in which a room air capacitance and a single lumped construction capacitance was linked with an instantaneous conduction path through a network of three resistances. Though good agreement with a limited set of observed data was demonstrated with reference to dominant inputs (i.e. ventilation rate and zone heat

inputs), the impact of model structure on this was not discussed, especially at lower timescales when plant dynamics tend to dominate.

Dewson et al. [73] developed the model of Crabb et al. [72] further by proposing a method for identifying the values of the required five parameters of the model from observed data for possible application to online system identification.

Tindale [74] recognised that the 2nd order prescriptions used by the previous workers broke down when applied to buildings with very high thermal capacity (i.e. involving one or more high-mass construction elements). He added a further node to the basic 2nd order model and separated the convective and radiant heat transfer paths that had previously been treated as a lumped air equivalent point. The further node was connected as a fictitious path and a method was developed for the calculation of its parameters.

The model gave improvements over the simpler 2nd-order model but there remained uncertainty regarding the adequacy of treatment of heat transfer through massive construction elements.

Variations on the above have been reported based on extending the two or three-node problem to one in which a capacity node is used to treat each opaque construction element resulting in 5th/6th order representations (one node each for floor; ceiling/roof; external wall (two external walls for a corner room); partitions and room air) [74-76]. These models tend to move away from analytical solutions to the low order problem to computationally efficient state-space methods for these higher-order cases.

In this chapter, two models are developed based on the lumped parameter method. In the first method, each construction element is described using a single lumped capacitance and a method proposed by Lorenz & Masy method [1] is used to find its parameters. The second model describes each construction element as a second order element and uses an optimisation technique based on nonlinear constrained optimisation to find its parameters. Both modelling methods are completed using

first-order air capacitance and both are applied to low and high thermal capacity buildings for comparison.

3.2. Building thermal model input variables

There are many factors that influence the energy balance on a building space, such as follows (figure (3.1)):

1. Microclimate; external air temperature, wind effects and solar heat gains.
2. Casual heat gains.
3. The heating system.

Most solar heat gain to a building space is by direct radiation through windows. The heat gain in a building by radiation from the sun depends upon site-specific factors and dynamic factors. The former consists of the surface area and angle of tilt of the glass, the composition of the glass, the geographic location of the site, the orientation of the building on the site and any local shading factors. The dynamic factors consisting of the season of the year, prevailing cloud conditions and the existence of any adjustable shading mechanisms (e.g. moveable external louvres or internal blinds).

The maximum gain through vertical south-facing windows in the northern hemisphere tends to occur in spring and autumn when the prevalent lower sun-angles cause radiation to fall more directly onto the window surfaces. Similarly, where roof lights are used, the maximum gain will be in peak summer when the sun's altitude is at a maximum. Clearly with careful window and shading element design, the solar gain can assist winter heating whilst giving minimum nuisance overheating in summer–the objective of passive solar design of building spaces.

The fabric solar heat gains through walls and roofs may be considered negligible for most old buildings. Little solar heat reaches the interior of the building because the high thermal capacity of "heavy" constructions tends to delay transmission of the heat until its direction of flow is reversed with the arrival of evening. Low thermal capacity construction on the other hand tends to be well insulated ensuring that solar heat transmission is minimised.

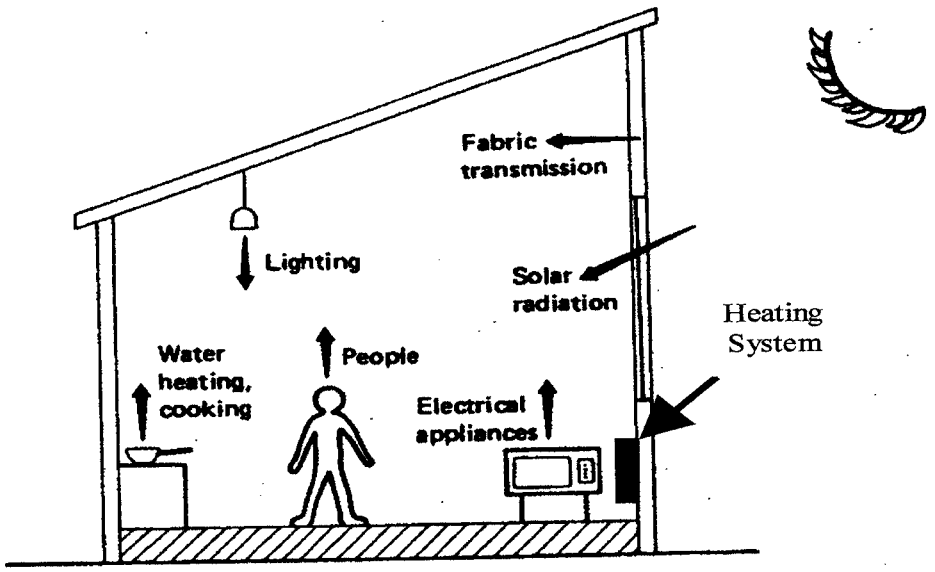

Figure (3.1): Building energy balance.

Casual heat gains take account of the heat given off by various activities and equipment, the major sources being people, lighting, cooking and electrical appliances. Casual heat gain is useful in winter and, as buildings become better insulated, can form a high proportion of the total heat needed in certain types of building. Since the heating system in intermittently-used buildings is sized for early morning preheating when casual sources and solar radiation are unavailable, the availability of these sources after preheating ensures that the heating is heavily oversized during normal operation, making control at light load especially crucial.

Figure (3.2) illustrates the relationship between the various energy transfer paths in a building space.

From a control system perspective, the zone temperature (T_i) is defined as a process output that has to be controlled. This temperature is the result of controllable and uncontrollable energy inputs, as shown in figure (3.3).

The primary heat input is the controllable input through the radiators (electric or hot water radiator). The secondary heat input is the uncontrollable input represented by solar radiation, outdoor air temperature and internal casual gains. Though the solar

input is at least partly controllable in practice (e.g. through the use of moveable louvres and blinds) it is assumed for the purpose of this study that it is uncontrollable.

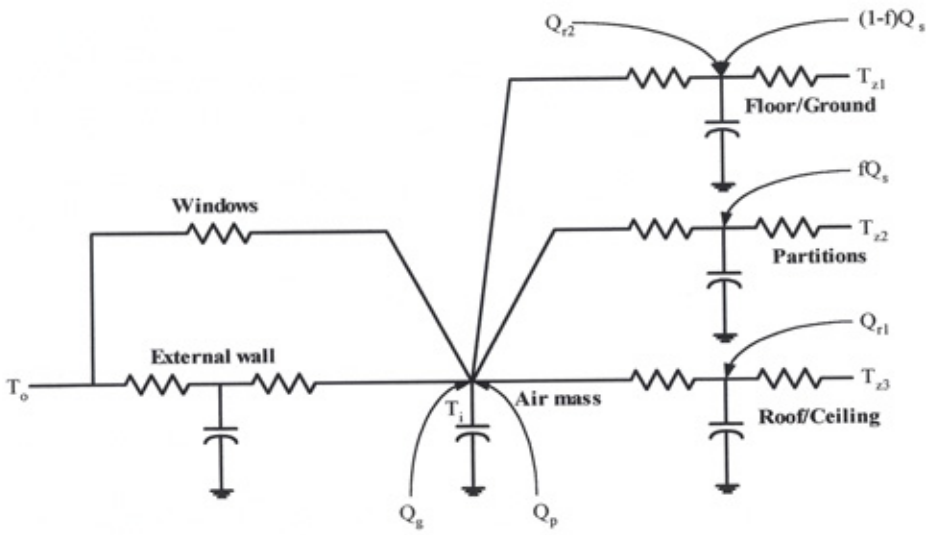

Figure (3.2): Simplified building energy transfer paths.

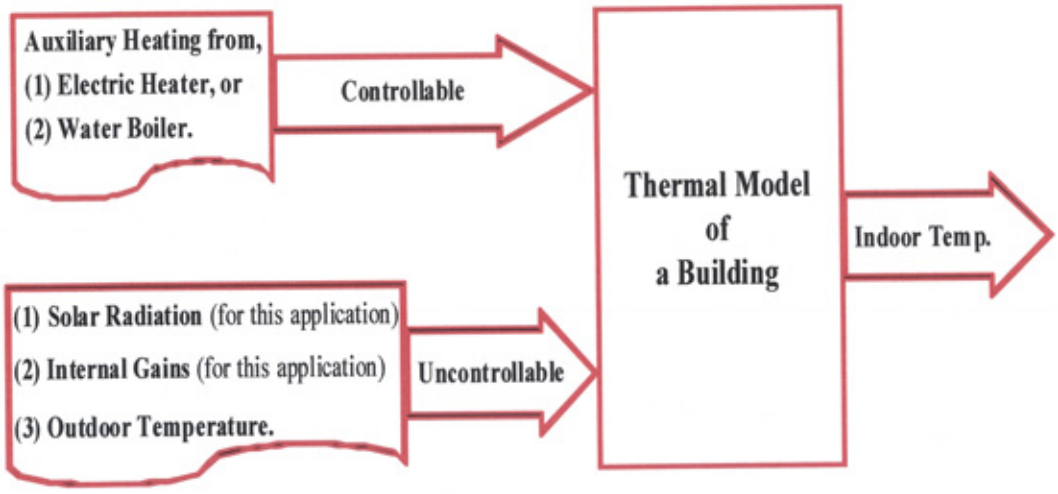

Figure (3.3): Classification of variables.

Therefore the controllable influence over zone air temperature (T_i) lies in one or more heating system parameters e.g. hot water flow rate or temperature (and, conceivably, both).

3.3. Basic application of the lumped parameter method

The following is based on the prescription of Lorenz and Masy [1] and has been applied by a number of previous workers as discussed above. The method has been included here as a basis for comparison with the reduced-order method developed later.

A construction element consists of several layers of different materials, each layer defined by its thickness, thermal conductivity, specific heat capacity and density as shown in figure (3.4). With this method, an element consisting of n layers of material can be combined to form two "lumped" thermal resistances (R_{ins}, R_{out}), and one thermal capacity (C_{total}), as illustrated in figure (3.5).

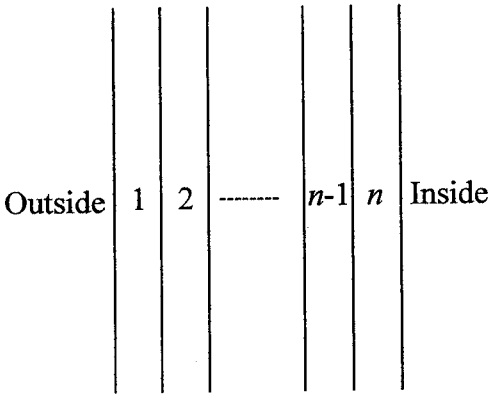

Figure (3.4): Construction element layers.

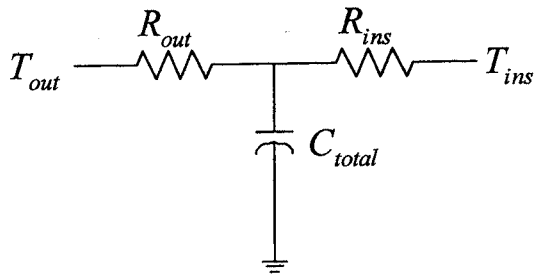

Figure (3.5):"Lumped Parameters" construction element.

The total thermal resistance and the total thermal capacitance can be calculated by following equations:

$$R_{\text{total}} = (r_{\text{si}} + r_{\text{so}} + r_{\text{a}} + \sum_{l=1}^{l=n} \frac{x_l}{k_l}) / A \tag{3.1}$$

$$C_{total} = A \times (\sum_{l=1}^{l=n} x_l \times \rho_l \times C_{pl}) \tag{3.2}$$

R_{ins} and R_{out} can be calculated by the following equations (Lorenz and Masy [1]):

$$R_{\text{ins}} = \alpha \times R_{\text{total}} \tag{3.3}$$

$$R_{\text{out}} = (1-\alpha) \times R_{\text{total}} \tag{3.4}$$

α, the "accessibility factor", can be calculated for the external construction elements using the following equations:

$$\alpha = 1 - \left(\frac{\sum_{k=1}^{k=n} R_{\text{k}}^{*} \times C_{\text{k}}}{R_{\text{total}} \times C_{\text{total}}} \right) \tag{3.5}$$

where:

$$R_{\text{k}}^{*} = \sum_{i=1}^{i=n-1} R_{\text{i}} + \frac{R_{\text{k}}}{2} \tag{3.6}$$

3.4. Proposed method

The coarse lumped parameter approach involving Lorenz and Masy [1] parameter evaluation is known to break down when dealing with high thermal capacity elements or elements involving a mix of materials with differing thermal properties. There are also difficulties when dealing with surface (i.e. radiant) heat flux because the method can not represent the behaviour between transmission and storage adequately. A higher order description will overcome these difficulties but with an associated high computational cost. Thus in this section, a very high order description is "reduced" to a low order description in an attempt to satisfy both modelling objectives.

The purpose of model order reduction is to derive a low order model of an intrinsically high order system to achieve an advantage in terms of computational effort required preserving as much of the dominant dynamic description possessed by the original high order system as possible. Any model reduction approach should

include appropriate methods for the selection of key parameters and their optimisation in relation to some specified criteria. Various authors (e.g. [77]) have pointed out that there can be no universal model reduction algorithm due to the diversity of plant characteristics and applications. Indeed no general model reduction approach has been developed though, from a theoretical viewpoint, such a possibility should not be excluded. Model reduction techniques can be grouped into three categories:

1. Polynomial reduction methods.
2. Optimisation approaches.
3. State-space transformation based techniques.

Polynomial reduction methods are generally applied in the frequency domain and usually are not computationally intensive. They are used to find low-order transfer functions whose coefficients are chosen to satisfy various criteria, so that the output of the reduced order model matches, as much as possible, the output of higher-order system. Some of the available methods are based on matching moments and Markov parameters between the original and reduced order models. The Padé approximation (coupled with various procedures to preserve the stability of the approximate model) is also popular and effective, as is the method of continued fraction expansion. Approaches following the Routh method, which retains stability properties and preserves a contribution in the energy sense of the impulse response in the low-order model, are also available [78].

Optimisation approaches form the second class of the model reduction techniques. In general, they are based on sequential parametric optimisation procedures aimed at the minimisation of some index, which measures an error between the original and the reduced order models. If the reduced order model has fixed eigenvalues, a model can usually be obtained analytically. Otherwise optimal reduced order models must be obtained numerically by an iterative solution of linear matrix equations leading to high computational effort that may be prohibitive if the original model order is high. The optimal projection approach can also be used in solving such problems. These methods, often applied in the time domain, are dependent on and limited by the choice of the error index [78].

The third class of model reduction method includes procedures that involve the transformation of an original state-space model representation. The approach is based on the evaluation of the stability of different state coordinate selections in the full order model and on the selection of a reduced order model maintaining, as much as possible, the original model properties (time response, observability, controllability, closed loop performance).

The value and potential accuracy of first order simplified construction element thermal models have been established and shortcomings of these simple models have been identified in terms of application to high time resolution problems involving plant and control simulations, and applications involving "massive" construction elements. The following describes some straightforward modifications that can significantly improve the accuracy of these models without seriously compromising simplicity or speed of computation. These modifications involve describing each construction element with a 2nd order description and "tuning" the parameters of these descriptions with reference to a high order model description for which the calculation errors may be assumed to be negligible [78].

3.4.1. Optimisation method

Optimisation in engineering refers to the process of finding the 'best' possible values for a set of variables for a system while satisfying various constraints. The term 'best' indicates that there are one or more design objectives that require being optimised by either minimising or maximising. In an optimisation process, variables are selected to describe the system (e.g. size, shape, material type, and operational characteristics). An objective refers to a quantity that the decision-maker wants to be made as high (a maximum) or as low (a minimum) as possible. A constraint refers to a quantity that indicates a restriction or limitation on an aspect of the system's technological capabilities. Generally, an optimisation problem that involves minimising one or more objective functions subject to some constraints is stated as:

$$\text{minmize}_{x \in D}\{f_1(x), f_2(x), \ldots\ldots, f_m(x)\} \tag{3.7}$$

where f_i, $i = 1,.....m$, is a scalar objective function that maps a variable vector x into the objective space. The n-dimensional design variable vector x is constrained to lie in a region D, called the feasible domain. Constraints to the above problem are included in the specification of the feasible domain. In general, the feasible domain is constrained by J-inequality and/or K-equality constraints as:

$$D = \{x: g_j(x) \le 0, h_k(x) = 0, j = 1,...,J, k = 1,...K\} \tag{3.8}$$

An optimisation problem in which the objective and constraint functions are linear functions of their variables is referred to as a linear programming (LP) problem. On the other hand, if at least one of the objective or constraint functions is nonlinear, then it is referred to as a non-linear programming (NLP) problem. An LP problem can be stated as fellows:

$$\begin{aligned} &\text{minmize } f^{'}(x) \\ &\text{subject to: } Ax \le b \\ &\qquad A_{eq}x = b_{eq} \\ &\qquad L_{bound} \le x \le U_{bound} \end{aligned} \tag{3.9}$$

where $f^{'}$, b, and b_{eq} are vectors and A and A_{eq} are matrices. The quantity x is a vector of design variables, and the apostrophe indicates the transpose. The matrix A and the vector b are the coefficients of the linear inequality constraints, and A_{eq} and b_{eq} are the coefficients of the equality constraints.

NLP problems may be divided into two classes: unconstrained methods and constrained methods. The latter method is in most cases preferable because of the discipline it places on problem solving.

Constrained non-linear optimisation methods find the minimum of a constrained function as formulated by Eqs (3.7) and (3.8) for the case of a single objective function, i.e. $m = 1$. This can involve a constrained single-variable method or

constrained multi-variable method. The constrained single-variable method finds the minimum of a function of one variable on a fixed interval as follows:

$$\text{minimize}_x f(x) \text{ subject to } a_1 \le x \le a_2 \tag{3.10}$$

In constrained multivariable optimisation, the method finds the minimum of a non-linear multivariable constrained optimisation problem. Both equality and inequality constraints can be considered. Also, both the objective and/or the constraint functions can be non-linear. A non-linear multivariable constrained optimisation problem can be stated as:

$$\begin{aligned}
&\text{minimize}_x f(x) \\
&\text{subject to: } Ax \le b \text{ (linear inequality constraints)} \\
&\qquad A_{eq}x = b_{eq} \text{ (linear equality constraints)} \\
&\qquad C(x) \le 0 \text{ (nonlinear inequality constraints)} \\
&\qquad C_{eq}(\mathrm{x}) = 0 \text{ (nonlinear equality constraints)} \\
&\qquad L_{bound} \le x \le U_{bound}
\end{aligned} \tag{3.11}$$

The general aim is to transform the problem into an easier sub-problem that can then be solved and used as the basis of an iterative process. A characteristic of a large class of early methods is the translation of the constrained problem to a basic unconstrained problem by using a penalty function for constraints, which are near or beyond the constraint boundary. In this way the constrained problem is solved using a sequence of parameterised unconstrained optimisations, which in the limit (of the sequence) converge to the constrained problem. These methods are now considered relatively inefficient and have been replaced by methods that have focused on the solution of the Kuhn-Tucker (KT) equations. The KT equations are necessary conditions for optimality for a constrained optimisation problem. If the problem is so called convex programming problem, that is, $f(x)$ and $g_i(x)$, $i = 1,....,m$, are convex functions, then the KT equations are both necessary and sufficient for a global solution point. Referring to equation (3.11), the Kuhn-Tucker equation [79] can be stated as:

$$
\begin{aligned}
& f(x^*) + \sum_{i=1}^{m} \lambda_i^* . \nabla g_i(x^*) = 0 \\
& \nabla g_i(x^*) = 0 \qquad i = 1,.....m \\
& \lambda_i^* \geq 0 \qquad\quad i = 1,.....,m
\end{aligned}
\tag{3.12}
$$

The first equation describes a cancelling of the gradients between the objective function and the active constraints at the solution point. For the gradients to be cancelled, Lagrange Multipliers (λ_i, $i = 1,.....m$) [80] are necessary to balance the deviations in the magnitude of the objective function and constraint gradients. Since only active constraints are included in this cancelling operation, constraints that are not active must be included in the operation and so are given Lagrange Multipliers equal zero. This is stated implicitly in the last two equations of equation (3.12).

The solution of the KT equations forms the basis of many non-linear programming algorithms. These algorithms attempt to compute directly the Lagrange Multipliers. Many algorithms are available to compute the Lagrange Multipliers directly. Constrained quasi-Newton methods guarantee super-linear convergence by accumulating second order information regarding the KT equations using a quasi-Newton updating procedure.

These methods are commonly referred as Sequential Quadratic Programming (SQP) methods since a quadratic programming sub-problem is solved at each major iteration. SQP methods represent state of the art in non-linear programming methods. Schittowski [81] for example has implemented and tested a version that out-performs every other method in terms of efficiency, accuracy, and percentage of successful solutions over a large number of the test problems. The work of Biggs [82], Han [83], and Powell [84,85] allows Newton's method for constrained optimisation to be closely emulated just as is done for unconstrained optimisation such that at each major iteration an approximation is made of the Hessian of the Lagrangian function using a quasi-Newton updating method. This is then used to guarantee a quadratic programming sub-problem whose solution is used to form a search direction for a line search procedure. For an overview of SQP methods see Fletcher [86], Gill *et al* [87], Powell [88], and Hock and Schittowski [89].

3.5. Application of the optimisation method

As a basis for comparison, the optimisation method is implemented along with the coarse lumped parameter method of Lorenz and Masy [1]. The two methods were applied to a high thermal capacity example space in a campus building at the University of Northumbria. This building has been the subject of extensive research into photovoltaic cladding [90] as shown in figure (3.6). The selected space is a south facing corner space and it has a floor area of 63 m^2 and volume of 179.5 m^3. It has two external walls, an internal floor, internal ceiling and two partitions, and the internal elements were treated as adiabatic. Details of the room model with construction elements defined according to the Lorenz and Masy prescription can be found in Gouda *et al* [91] and the properties of the various construction elements are given in appendix A.

Figure (3.6): Northumberland building, south facing.

Figure (3.7) shows that, increasing the order level resolution of a monolithic construction element (i.e. up to 300 layers for example) had little impact on the results of the internal air temperature responses to a step change in external air temperature above about 20 layers (i.e. produced "rapid convergence" of the step response with model order). The thickness of each layer throughout the element domain was taken to be the same. As an accuracy benchmark, each construction element of the space was split into 20 layers as shown in figure (3.8). It is argued that this would yield a sufficiently accurate outcome at least from a modelling point of view.

In figure (3.8), (R_1,.....,R_{21}) are the values of the layer thermal resistances and (C_1,.....,C_{20}) are the values of the layer thermal capacities.

For the simplified case, the values of the thermal resistances (R_{ins}, R_{out}), and one thermal capacity (C_{total}), for the first order lumped parameter model of the construction element can be calculated using the equations (3-5).

Following a preliminary trial-and-error approach, it was noted that a 2nd order model with parameters "tuned" from the 20th order benchmark case using the optimisation method described above gave results which were very close to the high-order model but differed considerably from a 1st order description. Thus parameters of a 2nd order model template were set as the optimisation objective functions.

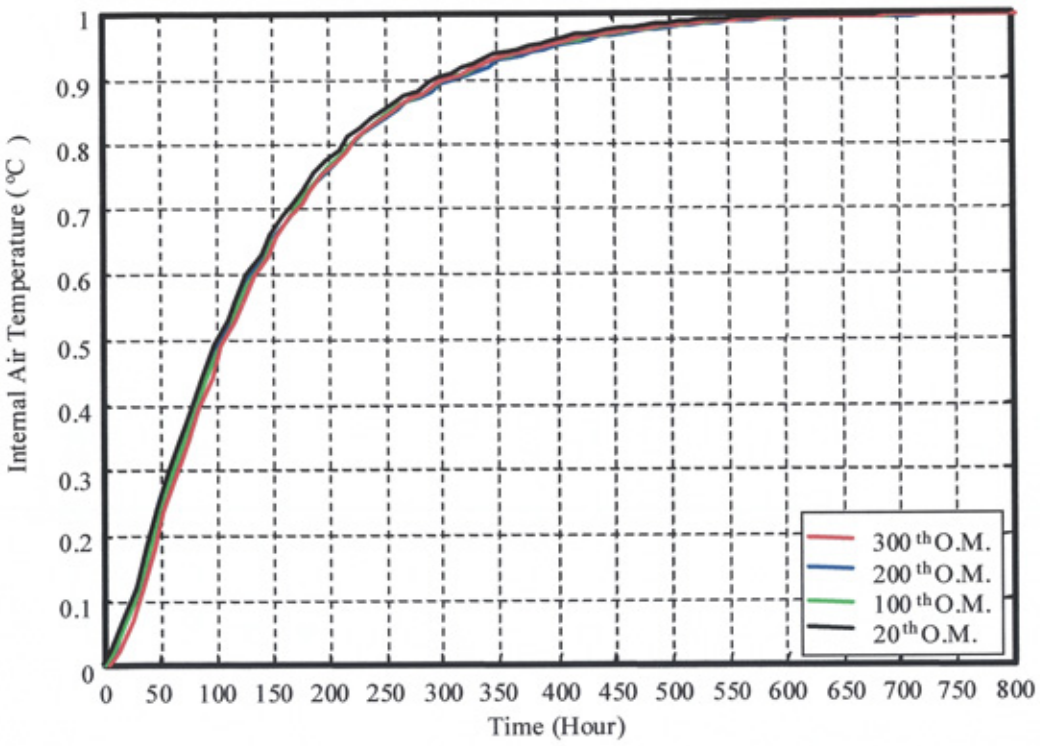

Figure (3.7): Step response of the same construction element with different number of layers.

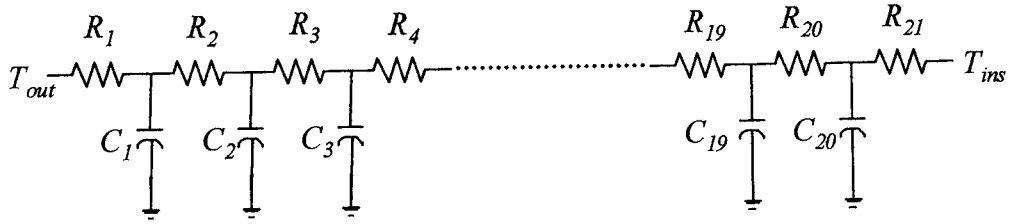

Figure (3.8): 20th order lumped parameter "benchmark".

The values of the 2nd order model parameters (C_1, C_2, R_1, R_2, R_3), as shown in figure (3.9), were arbitrarily initiated using the following two sets of lower and upper boundary conditions respectively, and naturally the equality constraints given in set 3 and set 4:

$$\text{Set1 (lower): } C_1, C_2 = C_{total}/100; R_1, R_2, R_3 = R_{total}/100$$

$$\text{Set2 (upper): } C_1, C_2 = 0.99C_{total}; R_1, R_2, R_3 = 0.99R_{total}$$

$$\text{Set3 (equality): } C_1 + C_2 = C_{total}$$

$$\text{Set4 (equality): } R_1 + R_2 + R_3 = R_{total}$$

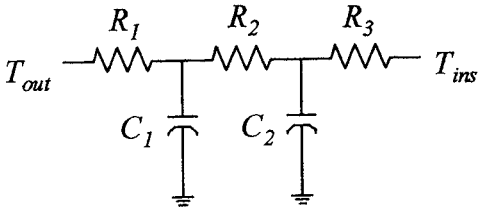

Figure (3.9): 2nd order lumped parameter template.

The optimisation method described by Eqs (3.11,3.12) was applied to minimise the square root of the sum-squared-error (SSE) between the step responses of the 20th order benchmark model and the 2nd order template model by varying the 5 parameters of the template model. Optimisations were carried out on individual construction elements (external walls, internal partition, floor construction and ceiling construction) for unit step disturbances in two excitation variable types: the external temperature (T_{out} -step 1K); and internal surface heat transfer (Q–step 1W).

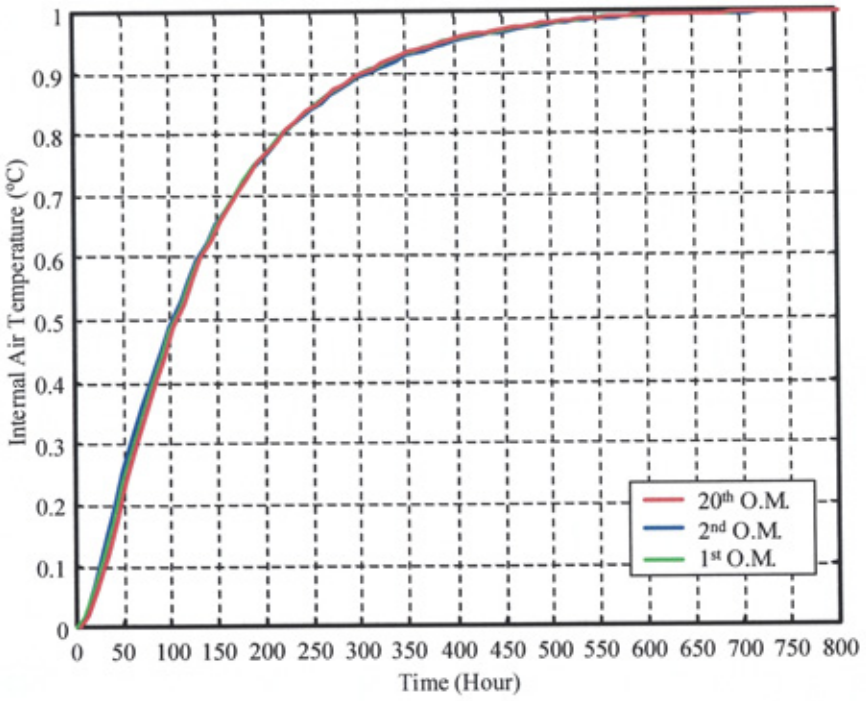

Figure (3.10): Unit step response of the high-order "benchmark", tuned 2nd order and simple 1st order lumped parameter models for outdoor temperature excitation (external construction element).

Results of the internal temperature (T_i) responses to a step change in external temperature (T_{out}) for the case of one of the external wall elements (appendix A) are shown in figure (3.10).

Tests were then conducted based on a step response to surface heat flux in which simplified representations of the various model networks can be seen in figures (3.11 (a)-3.11(c)), and results shown in figure (3.12). Note that both figures represent unit step responses thus the response of figure (3.12) is for 1 W excitation and, consequently, the temperature response scale is very small (the response indicated can be scaled to any input step magnitude desired).

An excellent agreement between all three-model types is evident for an external temperature excitation. However, an excitation in heat flux at the surface of all construction elements, whilst giving an excellent association between the benchmark

and tuned 2nd order model case, gives a poor agreement in the case of the simple 1st order model.

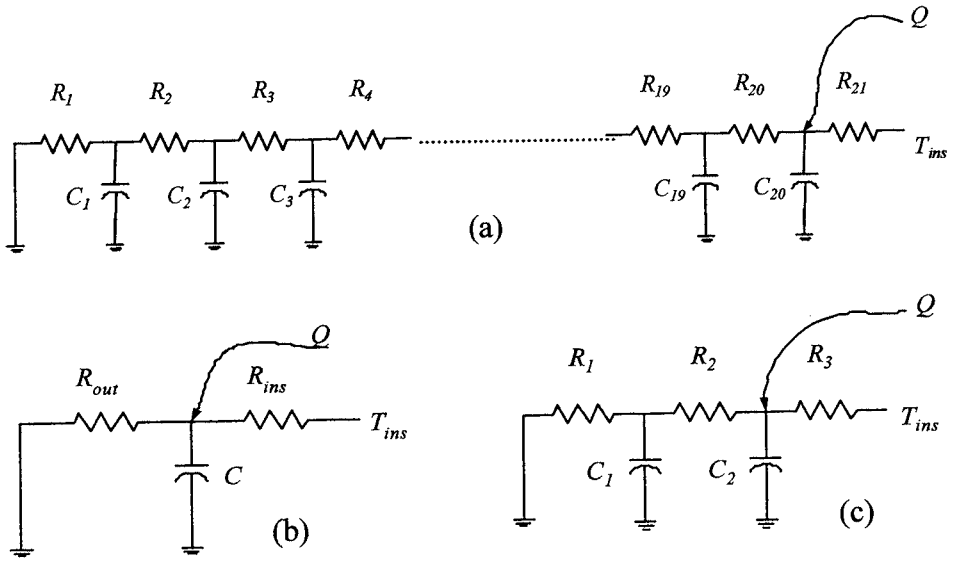

Figure (3.11): Simplified network representations for surface heat flow excitation ((a): high-order "benchmark"; (b) 1st order; (c) 2nd order)

Evidently, for surface flux, the 1st order model capacitance charges slowly resulting in a restricted build-up of construction element temperature and, consequentially, limited surface convection back to the space (to T_i). The quicker charging of the inner capacitance, C_1, for the 2nd order model on the other hand results in a rapid rise in inner material temperature with increased convection and radiation back to the space (hence a better tracking of T_i). This has significant implications when using low-order building models of this type in applications involving radiant (i.e. surface) exchanges.

3.5.1. Room modelling high thermal capacity

A model was developed for the entire space of the essentially high thermal capacity room described briefly earlier (and in detail in Gouda *et al* [70]). Each of the construction elements of the room were represented using 2nd order descriptions with parameters determined using the method applied above and, for comparison, simple 1st order prescriptions were also applied. Thus 6th order (figure (3.13)) and 11th order (figure (3.14)) room models were arrived at based on two external wall elements, an

internal partition element and internal floor and ceiling elements with the air capacity (treated as a 1st order entity) completing both model descriptions. The room has two inputs; outdoor temperature and solar radiation and the problem was thus treated as a "free float" case without any internal user/plant inputs. The solar radiation was applied to the floor surface.

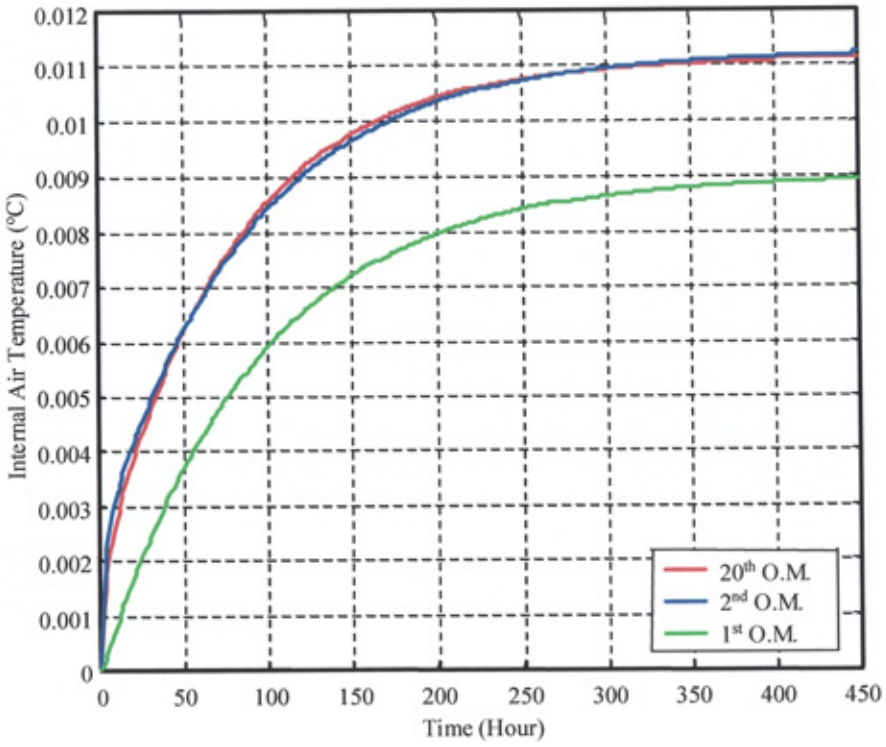

Figure (3.12): Unit step response of the high-order "benchmark", tuned 2nd order and simple 1st order lumped parameter models for surface heat flow excitation (external construction element)

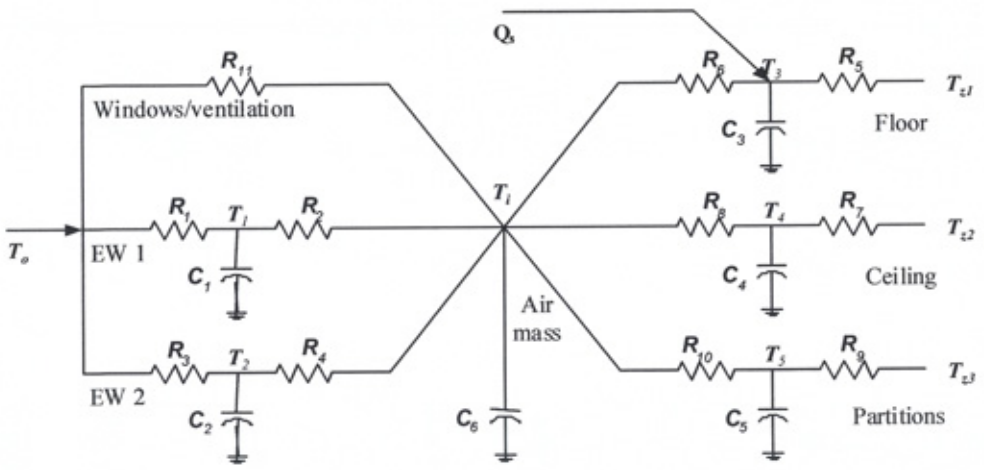

Figure (3.13): 6th order model realisation for the selected example space

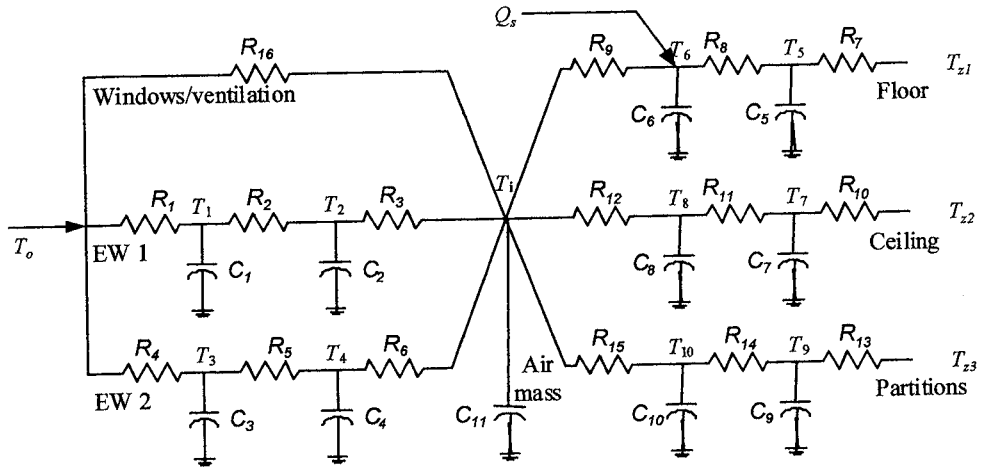

Figure (3.14): 11th order model realisation for the selected example space

The state equations for the 6th order thermal model of the selected example space, can be written as follows:

$$C_1 \dot{T}_1 = (T_o - T_1)/R_1 + (T_i - T_1)/R_2 \tag{3.18}$$

$$C_2 \dot{T}_2 = (T_o - T_2)/R_3 + (T_i - T_2)/R_4 \tag{3.19}$$

$$C_3 \dot{T}_3 = (Tz1 - T_3)/R_5 + (T_i - T_3)/R_6 + Qs \tag{3.20}$$

$$C_4 \dot{T}_4 = (Tz2 - T_4)/R_7 + (T_i - T_4)/R_8 \tag{3.21}$$

$$C_5 \dot{T}_5 = (Tz5 - T_5)/R_9 + (T_i - T_5)/R_{10} \tag{3.22}$$

$$C_6 \dot{T}_i = (T_1 - T_i)/R_2 + (T_2 - T_i)/R_4 + (T_3 - T_i)/R_6 + (T_4 - T_i)/R_8 + (T_5 - T_i)/R_{10} + (T_o - T_i)/R_{11} \tag{3.23}$$

Because all zones air temperature are equal to the internal air temperature of the space of interest (adiabatic case), so the state space model of the selected example space can be written as following:

$$\dot{\mathbf{X}} = \mathbf{AX} + \mathbf{BU}$$
$$\mathbf{Y} = \mathbf{CX} + \mathbf{DU} \tag{3.24}$$

Where $\mathbf{X}$ is the state vector $[T_1\ T_2\ T_3\ T_4\ T_5\ T_i]^T$, $\mathbf{U}$ is the input vector $[T_o\ Qs]^T$, $\mathbf{Y}$ is the output vector (i.e. in this case the internal air temperature, T_i).

The parameters ($R_1 \cdots\cdots R_{10}$, and $C_1 \cdots\cdots C_5$) of the 6th order thermal model are calculated using the Lorenz & Masy method (equations 3.1 to 3.6). The internal air mass C_6 is calculated as:

$$C_6 = \text{Volume of the room} \times \text{Density of the air} \times \text{Specific heat capcitance of the air} \tag{3.25}$$

and the thermal resistance of the windows R_{11} can be calculated as:

$$R_{11} = 1/(\text{total area of the windows} \times \text{Thermal transmittance of the glass}) \tag{3.26}$$

The state equations for the 11th order thermal model of the selected example space, can be written as follow:

$$C_1 \dot{T}_1 = (T_o - T_1)/R_1 + (T_2 - T_1)/R_2 \tag{3.27}$$

$$C_2 \dot{T}_2 = (T_1 - T_2)/R_2 + (T_i - T_2)/R_3 \tag{3.28}$$

$$C_3 \dot{T}_3 = (T_o - T_3)/R_4 + (T_4 - T_3)/R_5 \tag{3.29}$$

$$C_4 \dot{T}_4 = (T_3 - T_4)/R_5 + (T_i - T_4)/R_6 \tag{3.30}$$

$$C_5 \dot{T}_5 = (Tz1 - T_5)/R_7 + (T_6 - T_5)/R_8 \tag{3.31}$$

$$C_6 \dot{T}_6 = (T_5 - T_6)/R_8 + (T_i - T_6)/R_9 + Qs \tag{3.32}$$

$$C_7 \dot{T}_7 = (Tz2 - T_7)/R_{10} + (T_8 - T_7)/R_{11} \tag{3.33}$$

$$C_8 \dot{T}_8 = (T_7 - T_8)/R_{11} + (T_i - T_8)/R_{12} \tag{3.34}$$

$$C_9 \dot{T}_9 = (Tz3 - T_9)/R_{13} + (T_{10} - T_9)/R_{14} \tag{3.35}$$

$$C_{10} \dot{T}_{10} = (T_9 - T_{10})/R_{14} + (T_i - T_{10})/R_{15} \tag{3.36}$$

$$C_{11} \dot{T}_i = (T_2 - T_i)/R_3 + (T_4 - T_i)/R_6 + (T_6 - T_i)/R_9 + (T_8 - T_i)/R_{12} + (T_{10} - T_i)/R_{15} + (T_o - T_i)/R_{16} \tag{3.37}$$

And the state vector $\mathbf{X}$ in this case will be $[T_1\ T_2\ T_3\ T_4\ T_5\ T_6\ T_7\ T_8\ T_9\ T_{10}\ T_i]^T$. Results of the construction element parameter optimisations are given in Table (3.1) based on

the following resistance and capacitance rationing for the k^{th} resistor ($k = 1,2,3$; 1 = outermost) and l^{th} ($l = 1,2,3$; 1 = outermost) capacitance in an element:

$$R_k = f_k R_{total} \tag{3.38}$$

$$C_l = g_l C_{total} \tag{3.39}$$

Note that in the case of the identical internal floor and ceiling constructions, values of the element model parameters for the ceiling construction can be taken from the corresponding values for the internal floor construction with the values f_1, f_2, f_3 and g_1, g_2 interchanged.

Elements	f_1	f_2	f_3	g_1	g_2
External Wall 1	0.3884	0.5059	0.1107	0.8138	0.1862
External Wall 2	0.4224	0.5593	0.0183	0.9186	0.0814
Internal Partitions	0.4696	0.4238	0.1066	0.9096	0.0904
Internal Floor	0.6463	0.2668	0.0869	0.8736	0.1264

Table (3.1): Results of the optimised 2nd order element parameters

Both the internal air mass C_{11} and the thermal resistance of the windows R_{16} are calculated using equation (3.25) and equation (3.26) respectively.

A preliminary model was implemented using the realisation shown in figure (3.15). The building space model, which was expressed as a state-space block (either equation (3.27) or equation (3.37)), was solved using a variable step Runga-Kutta scheme selected from within the solver library of the MATLAB-SIMULINK software package.

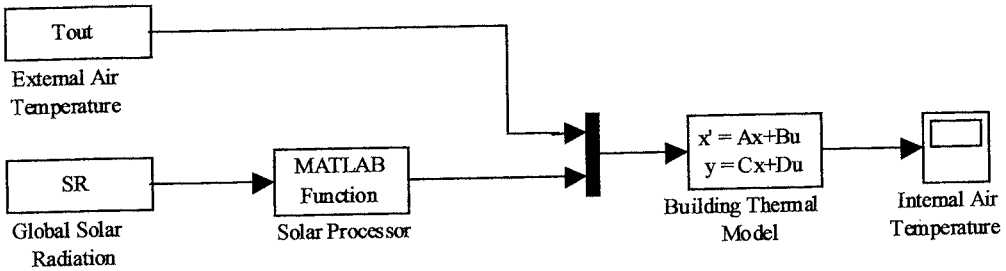

Figure (3.15): Overall model for the building space using MATLAB-SIMULINK packages.

Measurements of free float internal air temperatures for the room were available for a 30-day period during a time when the space was unoccupied and corresponding time series measurements of (15-minute) solar irradiances and external air temperatures were also available as driving inputs (figure (3.16a) and (3.16b)). The model was initially run for several days using the first time row values of the measured input data until all element temperatures converged to steady values, prior to submitting to full 30 day simulation.

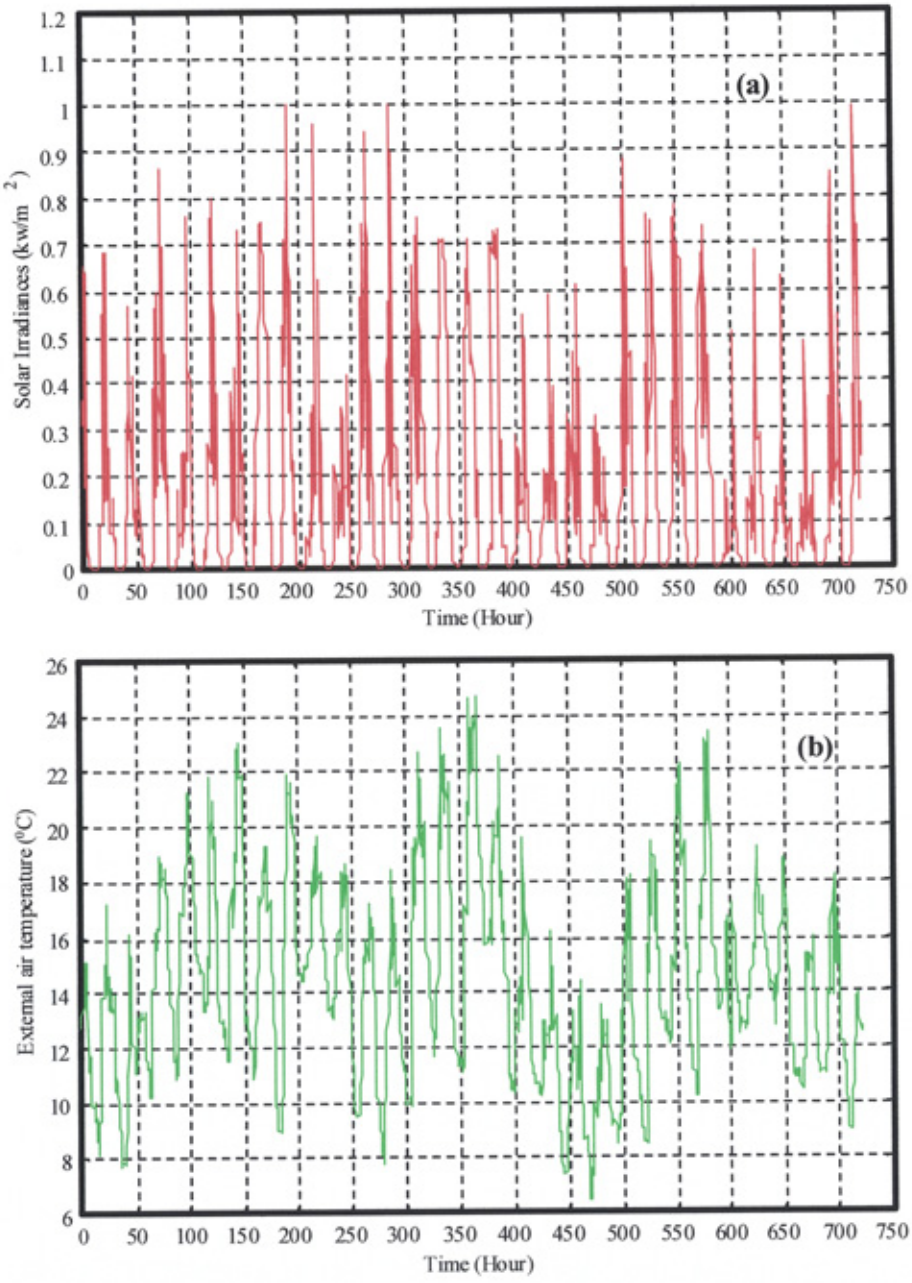

Figure (3.16): Measured climate data

(a): Solar irradiances (b): External air temperature

Results of measured and simulated internal air temperatures for a four-week period are shown in figure (3.17a). A one-week period from this is also shown in figure (3.17b) at higher resolution.

The tracking performance of both models in relation to measured data is good but both models underpredict the internal temperature consistently. In the case of the simple model based on Lorenz & Masy's prescription [1] the degree of underprediction is significant at 1-2K.

In the case of the higher order model based on "tuned" second order element modelling as proposed in this study the degree of underprediction is much less significant at typically less than 1K. Thus the model formulation proposed in this study represents a significant improvement over the simple low order room modelling method.

It is evident that the key uncertain variable in both models in the rate of external ventilation air. Since the modelling problem explored here has concerned itself with an unoccupied space, external ventilation is due solely to leakage infiltration. The rate of external air assumed for modelling purposes was 0.5 air changes per hour. Clearly, during free float conditions in mild weather with solar radiation, the internal temperature will be higher than the external temperature at all times. Thus it is likely that the infiltration rate will actually have been lower than the latter value. To test for this, a further modelling run was implemented but with the air change rate set at $0.25h^{-1}$.

Results have been included in the one-week graph of figure (3.17b). It is clear from this that the degree of underprediction of the "tuned" model is now negligible and certainly within the typically uncertainty of measurement of the internal air temperature (±0.2K). Though further study needs to be done on a satisfactory method of representing ventilation air rates in this improved model, it is clear that the rate of ventilation of external air is the dominant uncertain variable in the problem presented here. Thus the improvement offered by the modelling approach recommended here could be concluded with some confidence.

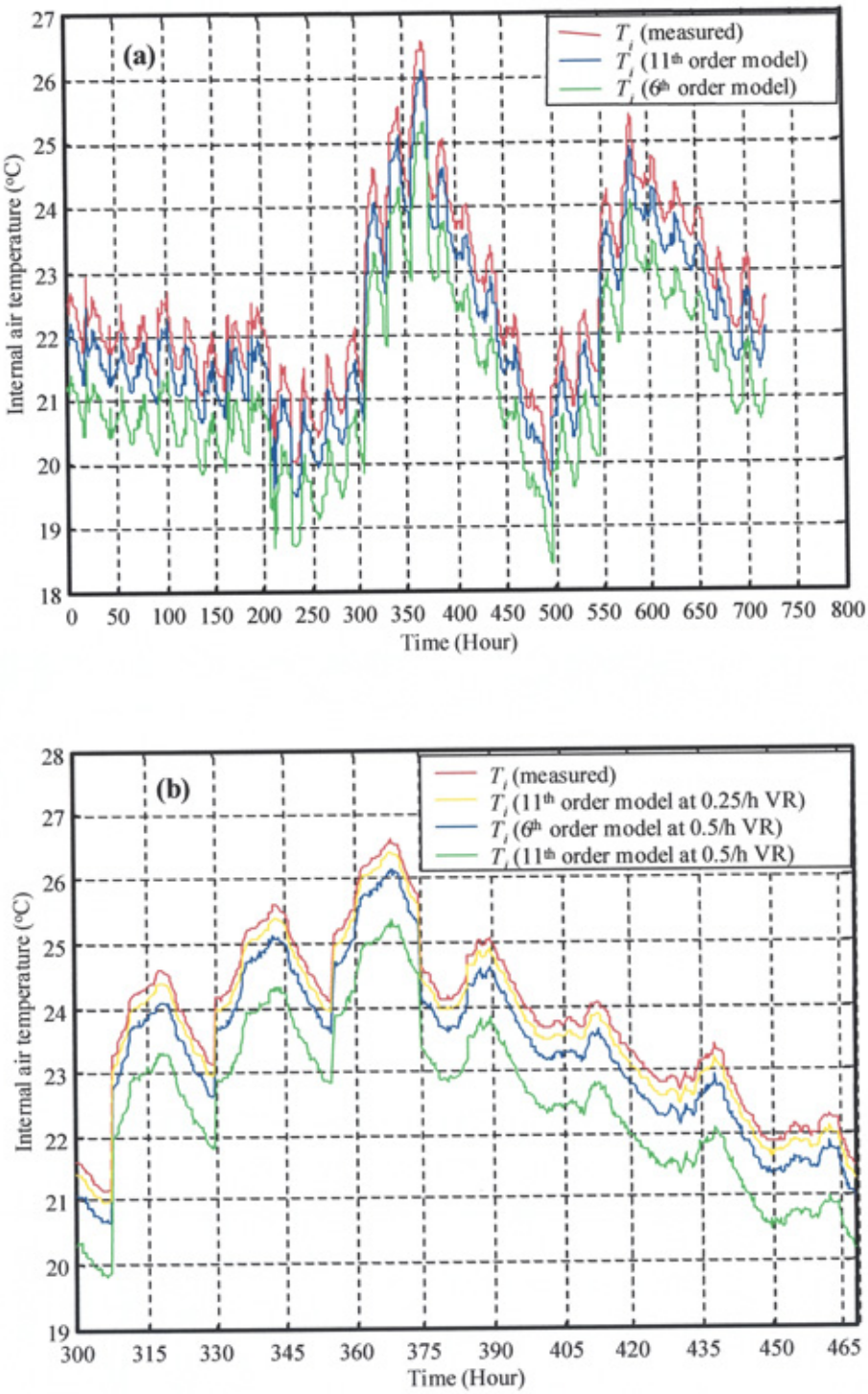

Figure (3.17): Measured and simulated internal air temperatures

(a): Four-weeks period (b): One-week period

In terms of computational effort, the 20th order "benchmark" description of a typical element required 3.986s of computer time whereas the proposed model required 0.211s and the Lorenz & Masy [1] based model required 0.19s. These results

were based on a computer equipped with a Pentium 650MHz processor. Thus the increase in computational effort required by the proposed model is negligible when compared with existing 1st order model descriptions.

3.5.2. Application to a low thermal capacity room

The building space considered above can be characterised as one of typically high thermal capacity, with an indicative time constant (i.e. the time constant arising from a step disturbance in external air temperature) of approximately 220 hours. To investigate the impact of the element model fitting method applied to a building with low thermal capacity characteristics, the previous room was adopted but all construction elements were replaced using combinations of material choices with low capacity.

The choices, though arbitrary, were based on typical constructions that might be found in a "lightweight" building in practice in order to retain a degree of realism. To ensure that the transmittances were identical (i.e. only the thermal capacitances were allowed to vary) the thickness of the certain layers (i.e. insulating and finish layers) were adjusted in order to ensure equivalent overall resistances of each element between the high and low thermal capacity cases. Thus the indicative time constant in this case is approximately 25 hours. Construction details are given appendix B.

Calculations of the optimised 2nd order element model parameters were carried out using the method described in section (3.4.1) and section (3.6) and results for these new constructions are given in Table (3.2).

Elements	f_1	f_2	f_3	g_1	g_2
External Wall 1	0.5985	0.3795	0.0220	0.8120	0.1880
External Wall 2	0.7416	0.2401	0.0183	0.9389	0.0611
Internal Partitions	0.4127	0.4767	0.1106	0.8016	0.1984
Internal Floor	0.4181	0.4818	0.1001	0.7893	0.2107

Table (3.2): Results of the optimised 2nd order element parameters

Simulation results using the same input data set as was used for the previous construction types is given in figure (3.18) based on the original air infiltration rate (i.e. $0.5h^{-1}$). Again the level of disagreement between the two modelling methods is clear with the simple low order model underpredicting the model proposed in the present study by typically 1-2K.

It is not possible to generalise the pattern of results neither between construction element types, nor between the two cases considered above in terms of the rationing of element resistances and capacitances. Nevertheless, there is a rough consistency between the two sets of results. Specifically, the mean inner resistance share of the overall value is under 10% whereas the average middle resistance share is about 40% and the outer value 50%. As to capacitance rationing, an inner capacitance share of about 15% and an outer share of 85% would appear to cover many applications.

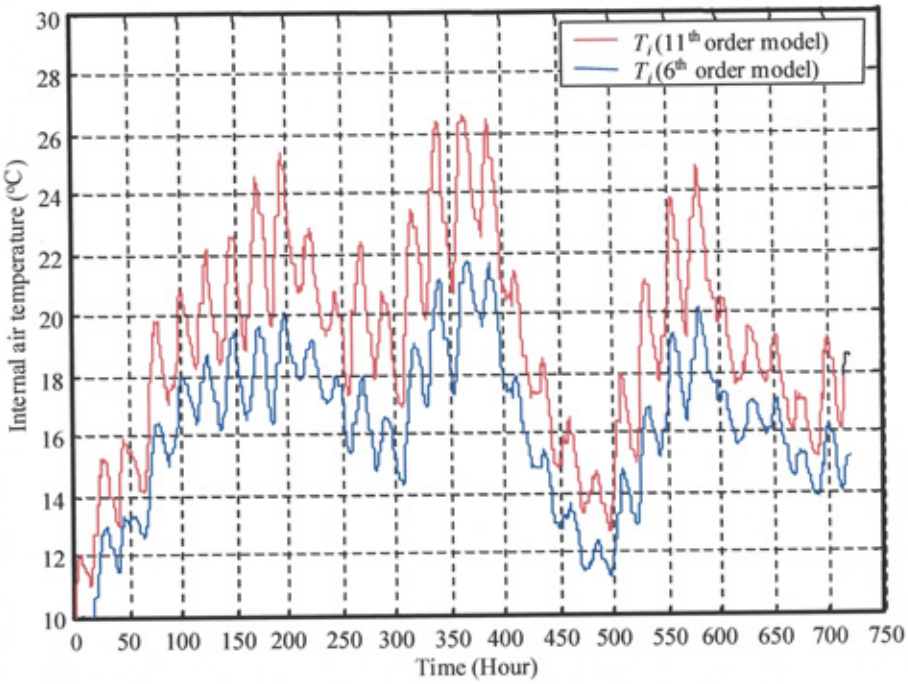

Figure (3.18): Simulated internal temperatures (low thermal capacity space)

3.6. Solar processing

In simulation modelling, weather data is based on measured data from weather stations usually presented as *typical meteorological year* (TMY) data. The solar measurements from such stations tend to be global horizontal values (i.e. the sum of direct and diffuse radiation measured on the horizontal plane at the site in question).

To estimate the incident solar irradiance on a surface at any orientation, estimations of the diffuse and direct fractions of incident radiation on the horizontal plane are required. From these values, an estimate of incident radiation on a tilted surface may be made. The diffuse and direct components may either be modelled or based on a measurement of the total horizontal (global) radiation.

A combination of two algorithms was used for this purpose. The first algorithm presented by Skartveit and Olseth (S&O) [91] was used to estimate the diffuse and direct fraction from the measured global value. The second model, by Lui and Jordan [92] used the estimated results of the S&O algorithm to determine the radiation incident on a (potentially tilted) building surface [93].

A MATLAB function has been developed, which given the site longitude, latitude, the surface azimuth; and elevation will give the effective incident radiation.

3.7. Conclusions

In this chapter an approach is described for the optimisation of reduced-order lumped capacity modelling of the dynamic thermal behaviour of building spaces. The method is appropriate for simplified and computationally efficient building envelope model descriptions of the type needed for short-term analysis of energy and environment in buildings, such as plant and control system simulations.

The method described is based on "tuning" the parameters of 2^{nd} order construction element model descriptions using nonlinear constrained optimisation adopting the Kuhn-Tucker equations. The reference point for these optimisations is an equivalent 20^{th}–order "benchmark" description. Results of these optimisations lead to an 11^{th} order lumped parameter building model. The proposed method results in three resistances and two capacitances for each construction element making up the building space. The values of these resistances and capacitances are fractions of the overall calculated resistance and capacitance values.

Whilst it is not possible to derive general rules for the values of these fractions due to the infinite range of construction element types likely in practice, the analysis of

several construction types of mixed materials suggests that the innermost-to-outermost resistance fractions to be typically 0.1; 0.4 and 0.5 respectively. The corresponding innermost and outermost capacitance fractions are typically 0.15 and 0.85 respectively.

A solar algorithm has been included to estimate the incident solar irradiance on the windows from the measurement of horizontal (global) solar irradiance. For whole space simulations compared with measured data, the 11^{th} order model developed in this study was compared with a simpler 6^{th} order model based on the prescriptions of Lorenz & Masy [25] as has been used extensively in the past. Though both models were found to consistently underpredict the measured trend of internal temperature over a 30-day "free float" period of simulation, the 11^{th} order model was found to give substantial improvement over the simpler model. It was noted that the major inadequacy with the simple model lies in its inability to adequately track the transient effects of heat transfer received at internal building surfaces (i.e. radiation).

The main uncertain variable in all these model types was the rates of ventilation of external air (i.e. the air change rate) which was an assumed value and taken to be constant. Reducing this uncertain value improved the performance of the 11^{th} order model such that its agreement with measured data was consistently within the uncertainty of measurement.

The computer time needed to solve a typical element simulation using the proposed 2^{nd} order element modelling method was only 11% higher than that required by the simpler 1^{st} order element model. Both methods required considerably lower computer time than a 20^{th} order "benchmark" test case (both requiring under 6% of the computer time needed by the latter). Thus the method proposed in this study gives a substantial improvement in modelling performance for a negligible increase in computer effort.

In order to develop a control system for solar buildings, naturally the heating system also has to be modelled. This is done in the next chapter.

Chapter 4

Heating System Modelling

Chapter 4
Heating System Modelling

4.1. Introduction

The control of heating, ventilation, and air conditioning (HVAC) systems is difficult due to the nonlinear nature of its components, the wide range of operating conditions under which they must operate, and the many interactions between them. While many models already exist, their accuracy under closed loop control and varied external parameters is often limited, compared with open loop accuracy, due to more variables changing during a closed loop test.

The reasons for intensified research in improved control for heat, ventilation and air conditioning (HVAC) systems are increased energy costs together with higher demands upon the indoor climate and air quality. Due to the fast progress in computerised control, and also because research into control theory has resulted in new advanced controllers coming onto the market, the use for more advanced controllers in this fields has become possible.

To improve the performance of controllers and to benefit from the use of advanced control algorithms the dynamics of the process have to be fairly well known. The best and easiest way to acquire such knowledge is through the dynamic simulation of the actual process. Many HVAC mathematical models exist which are very complex and with a large number of parameters in the area of building design. In general, these are not easy to use, in order to check the behaviour of control strategies, due to the many parameters that are necessary to take into account [94].

Developments in HVAC simulation program have addressed problem-specificity; the two most promising developments are TRNSYS [95] and HVACSIM$^+$ [96]. Underwood [97], for instance, has developed HVAC control component models for TRNSYS that have general applicability, while HVACSIM$^+$ has been used extensively for investigating a wide range of HVAC control problems [98,99]. One restriction with these programs is that many of the plant component models are steady state or quasi-steady-state, making them suitable (and computationally efficient) for low frequency dynamic analysis, but unsuitable for high frequency disturbances, which are important in many instances for control design.

It is therefore argued that a modelling environment is needed, in which developed models have a high degree of transportability and transparency, and the model itself requires to be spectrally inclusive for wide applicability in control synthesis and design. A modelling environment that has the potential to meet these needs in MATLAB-SIMULINK [100], which has the added advantage of convenient access to a very wide range of control system analysis and design tools. Hence this method has been used in the present work.

One component in particular, the hot-water radiator, is very nonlinear in practice and attempts are often made to linearise these components using nonlinear control valves and thus force a more linear control system response overall.

In this chapter, a detailed model of a hot water heating systems and related control devices is developed and evaluated for the specific purpose of control simulation.

4.2. Heating system model

For certain types of problems such as long term energy usage, it is possible to treat the plant as a *quasi-steady-state* problem. Conventional steady-state theory is applicable, and the central assumption is that the plant variables assume steady-state trajectories within the integration time interval of relevance, to the simulation of the building envelope and room air energy balance.

For problems involving control system design, a *quasi-steady-state* approach fails to capture all of the fast and slow dynamics that describe the coupled room space and plant problem and the plant needs also to be described dynamically. The simplest approach is the *stirred tank* methodology, which is, in effect, a lumped parameter method for plant. Here, the plant is broken down into a series of inter-connected components such that the properties of each component part can be assumed to be entirely uniform. For example, in a hot water radiator, it would be assumed that the water temperature is perfectly mixed and, thus, equal to the outlet water temperature (i.e. system return temperature). This is an acceptable approximation so long as the radiator or emitter is broken down into a number of smaller sub-systems.

The heat emitter is coupled to the space thermal environment through the space air temperature and, if the emission is in part radiant, through the various space surface temperatures.

The mathematical description of the hot water heating system is divided into two parts. The first part is the description of the heat exchanger and its water connections,

and the second part is a description of the control valve, also the temperature sensor will be described as a part of the heating system. There are three possible control strategies to control the heating emitted from the hot-water heating systems:

1. Variable flow-rate constant temperature (VFCT): In this case, the heat emitted from the heating system is controlled via the hot water-flow rate, with constant water flow temperature.
2. Constant flow-rate variable temperature (CFVT): In this case, the heat emitted from the heating system is controlled via the temperature of the hot water, with constant hot water flow rate.
3. Variable flow-rate variable temperature (VFVT): In this case, the heating emitted from the heating system is controlled by a combination of water flow rate and flow water temperature.

4.2.1. Hot water radiator

Other than in special industrial applications, the type of hot water heat emitter most commonly used in current practice will provide natural convection or some combination of natural convection and radiation.

Figures (4.1) and (4.2) depict the extremes of this range–the convector-radiator (figure (4.1)) and the encased natural convector (figure (4.2)).

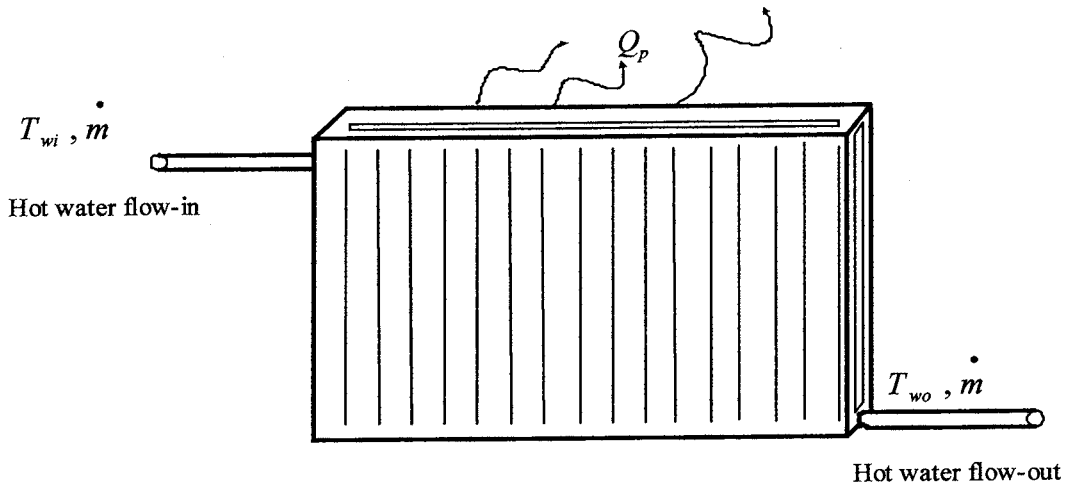

Figure (4.1): Convector radiator

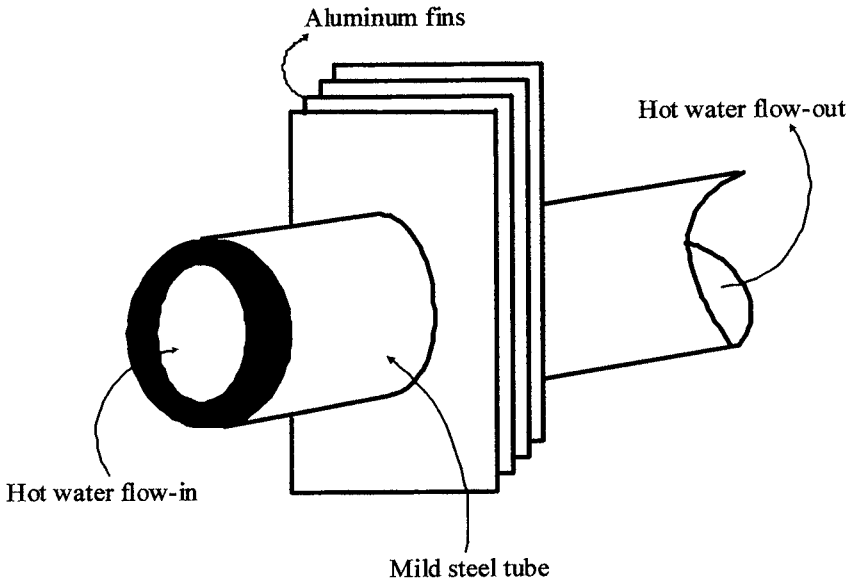

Figure (4.2): Finned-tube convector

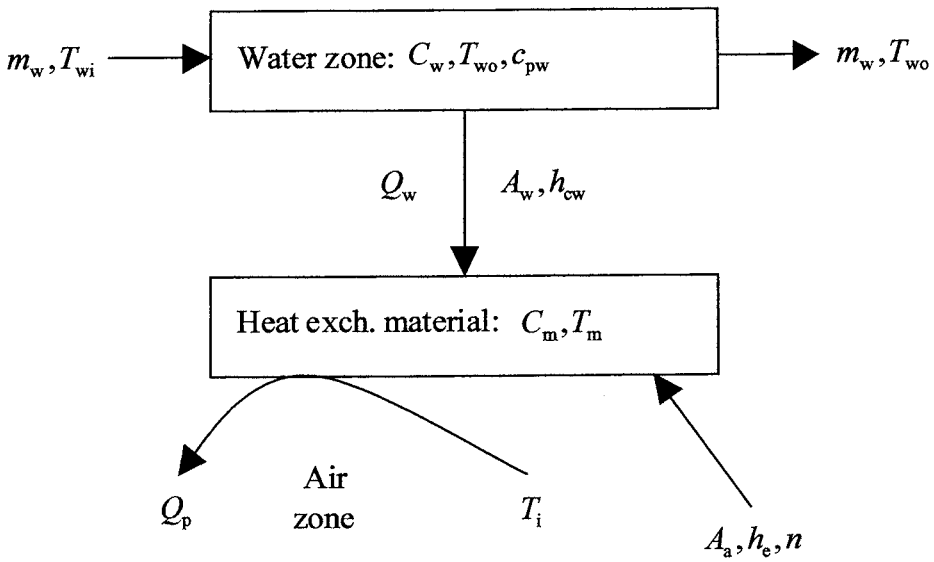

Figure (4.3): Heat emitter model zoning

Referring to figure (4.3), an energy balance on the waterside gives:

$$C_w \dot{T}_{wo} = m_w c_{pw}(T_{wi} - T_{wo}) - Q_w \tag{4.1}$$

$$Q_w = h_{cw} A_w (T_{wo} - T_m) \tag{4.2}$$

An energy balance about the heat emitter material gives:

$$C_m \dot{T}_m = Q_w - Q_p \tag{4.3}$$

In which the heat emitted from the convector is assumed instantaneous and given by:

$$Q_p = h_c A_a (T_m - T_i)^n \tag{4.4}$$

n is typically in the range 1.3→1.7

In the above, it has been assumed that heat emission by convection and radiation may be "lumped" as one which is acceptable so long as the space air temperature, T_i, and mean room surface temperatures are in reasonably close agreement.

Whilst the combined airside emission coefficient h_e, may be assumed constant, the waterside convection coefficient h_{cw}, may not. The water flow conditions in the emitter will, at certain positions of the control valve under VFCT or VFVT control strategies be laminar. When the control valve is operating nearer full capacity, flow conditions may be laminar or turbulent depending on the type of emitter. Thus h_{cw} will depend on whether the prevailing flow condition is laminar or turbulent.

For flow in tubes, the transition from laminar to turbulent flow occurs at [101]

$$\mathrm{Re_d} = \frac{\rho_w v_w d_i}{\mu_w} \tag{4.5}$$

(in which $\mathrm{Re_d}$ is the Reynolds number with respect to flow in tubes).

In practice, the transition is not quite so abrupt as implied by equation (4.5) and a range of Reynolds numbers for transition may be observed. Depending on the pipe roughness and smoothness of the flow, the generally accepted range for transition is [101]:

$$2000 < \mathrm{Re_d} < 4000 \tag{4.6}$$

By continuity:

$$m_w = \rho_w v_w A_{tcross} \tag{4.7}$$

So that the Reynolds number may also be written as:

$$\mathrm{Re_d} = \frac{m d_i}{A_{tcross} \mu_w} \tag{4.8}$$

Under turbulent flow conditions, the following empirical expression may be used to obtain the waterside convection heat transfer coefficient [101]:

$$\mathrm{Nu_d} = \frac{h_{cw} d_i}{k_w} = 0.023\,\mathrm{Re_d^{0.8}}\,\mathrm{Pr^{0.33}} \tag{4.9}$$

(in which $\mathrm{Nu_d}$ is the Nusselt number for flow in tubes).

For laminar flow ($\mathrm{Re_d} < 2000$) the Nusselt number can be shown to be a constant value which for tubes is approximately 4.36, i.e.,

$$\mathrm{Nu_d} = \frac{h_{cw} d_i}{k_w} \cong 4.36 \tag{4.10}$$

In the transition region ($2000 < \mathrm{Re_d} < 4000$) the Nusselt number (and, hence h_{cw}) is obtained using a polynomial curve fitting with reference to the extremes defined by equations (4.9) and (4.10), i.e.,

$$4.36 \leq \frac{h_{cw} d_i}{k_w} \leq 0.023\,\mathrm{Re_d^{0.8}}\,\mathrm{Pr^{0.33}} \tag{4.11}$$

4.2.2. Control valve

Valves in a heating system are provided for two purposes: one is to enable parts of the system to be isolated, and the second, to enable regulation to be carried out. These two purposes are quite separate and distinct, and it is indeed a fact that a good isolating valve usually makes a very poor regulating valve. For control applications, control valves are used to regulate heat transfer through flow rather than to regulate flow as such.

There are two types of control valves, two port valves and three port valves. Two port valves are increasing in popularity especially in large networks where there is a large number of zone control valves [102]. Three port valves are used extensively in HVAC application. Mostly, these valves are designed as mixing valves having two inlet ports and one outlet such that, with correct connection arrangements, variable-flow constant-temperature or variable-temperature constant-flow control can be realised with respect to emission [103].

Mathematical models of control valves for liquids are generally based on expressing the relationship between the flow rate passed by the valve and the position of the valve stem; the valve characteristic [104]. Thus the valve can be expressed by an "inherent characteristic", G_{inh} (with the absence of connected system effects), leading to an "installed characteristic", G_{ins} (including connected system effects). Usually G_o referred to as the "let by" of the valve. This is the closure flow rate arising from the need to maintain a small clearance between plug and port thereby preventing the plug from "sticking" to its seat and requiring an inordinate force by the positioning device to fit it. The "let by" for most control valves, though dependent on valve differential pressure, is very low (usually less than 1% of the design rated flow rate), and it may be obtained from the manufacturer.

There are two cases, to express the inherent characteristic, one is linear case, and the other is equal-percentage case. For the linear case, it is thus clear that the inherent characteristic can expressed as:

$$G_{inh} = G_o + u(1 - G_o) \tag{4.12}$$

For the equal-percentage case, equal increments of valve position will be produce equal ratios of flow, and can be expressed as:

$$G_{inh} = G_o^{(1-u)} \tag{4.13}$$

In practice, the very action of the valve in controlling flow results in pressure changes in the controlled circuit so that the inherent characteristic is not physically realisable and an installed characteristic which includes system effects becomes applicable.

An installed characteristic can be derived from the inherent characteristic based on the valve authority $N = \Delta P_v / (\Delta P_v + \Delta P_s)$, where ΔP_v and ΔP_s are respectively, the pressure drop across the fully open valve and controlled circuit at design condition. The installed characteristic of the valve in terms of its inherent characteristic and the valve authority can be written as follows:

$$G_{ins} = [1 + N(1/G_{inh}^2 - 1)]^{-1/2} \tag{4.14}$$

As matters of good design practice the valve authority N, can be assumed to lie in the range $0.5 \le N \le 0.7$.

Thus the non-linear characteristic of the valve (e.g. figure (4.4)) attempts to compensate for the non-linear heat emission characteristic.

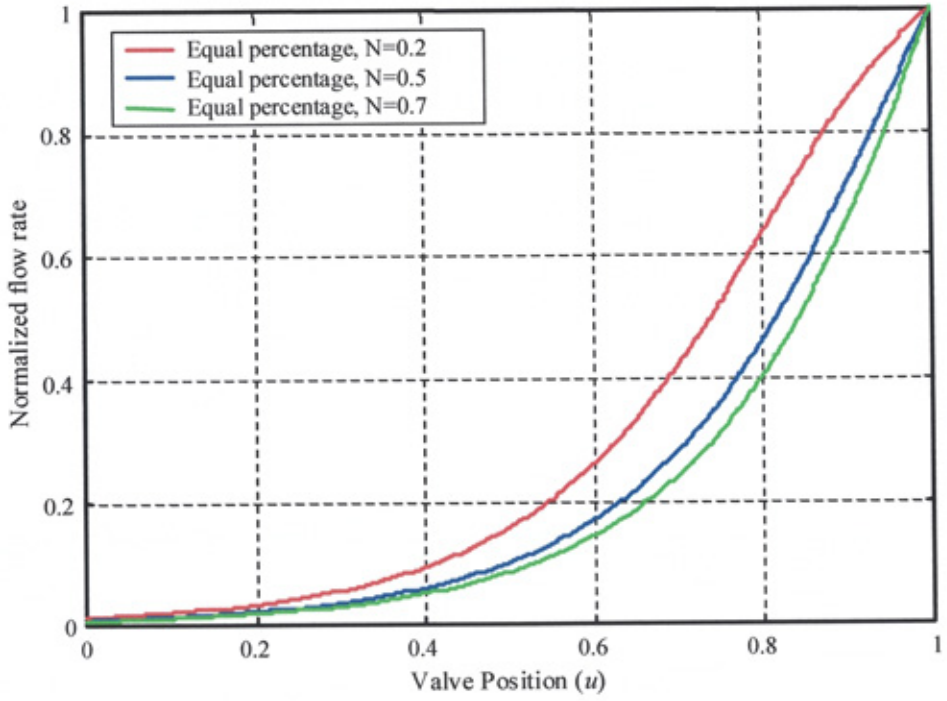

Figure (4.4): Non-linear valve characteristic

The equal-percentage valve gives a good match with the required flow characteristic at $0.5 \leq N \leq 0.7$, though the higher value of N will result in a high valve pressure drop requirement. In practice, $N = 0.5$ gives a good compromise between characteristic and pressure drop. Clearly therefore besides ensuring an appropriate valve characteristic, a control valve must have a significant pressure drop in relation to the controlled circuit if it is do its job correctly.

4.2.3. Temperature sensor model

In this work, the room air temperature sensor is relevant. In most applications involving heating control, resistance temperature detectors (RTDs) are used. Currently, these use thin film technology and so are precise and responsive.

Measuring instruments (e.g. temperature detectors, pressure and flow detectors, heat meters, power meters) usually take from a few seconds to a few minutes to register and process the data they measure. For example, sensors mounted in fast-moving liquid streams in pipes will tend to respond quickly (a fraction of one second to a few seconds). On the other hand a sensor mounted on a room wall measuring air-dry bulb temperature in relatively still air will respond more slowly (a fraction of one minute to a few minutes).

It is common for such components to respond exponentially such that a first-order lag characterised by a *time constant* is generally a good description. Thus for the room air temperature detector:

$$t_{\mathrm{d}} \frac{\mathrm{d}T_{\mathrm{i}}'}{\mathrm{d}t} = T_{\mathrm{i}} - T_{\mathrm{i}}' \tag{4.15}$$

In which $T_{\mathrm{i}}', t_{\mathrm{d}}$ are the temperature signal from the detector and detector time constant respectively. Figure (4.5) shows a simple block–just a function block and an integrator:

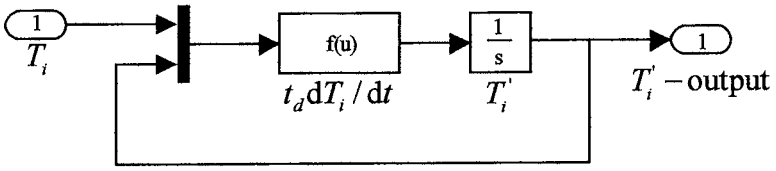

Figure (4.5): Measuring instrument SIMULINK block

4.3. Heating system model synthesis

The heating system model is summarised as shown in figure (4.6) in which a hot water supply from central boiler is delivered at constant temperature T_{wi} (i.e. the heat emitted from the heating system is controlled via the hot water-flow rate, with constant water flow temperature). The valve controls the water flow-rate, which is applied to the radiator to produce the heating. The simulation model was

implemented using MATLAB-SIMULINK. A block diagram representation of the heating system is shown in figure (4.7).

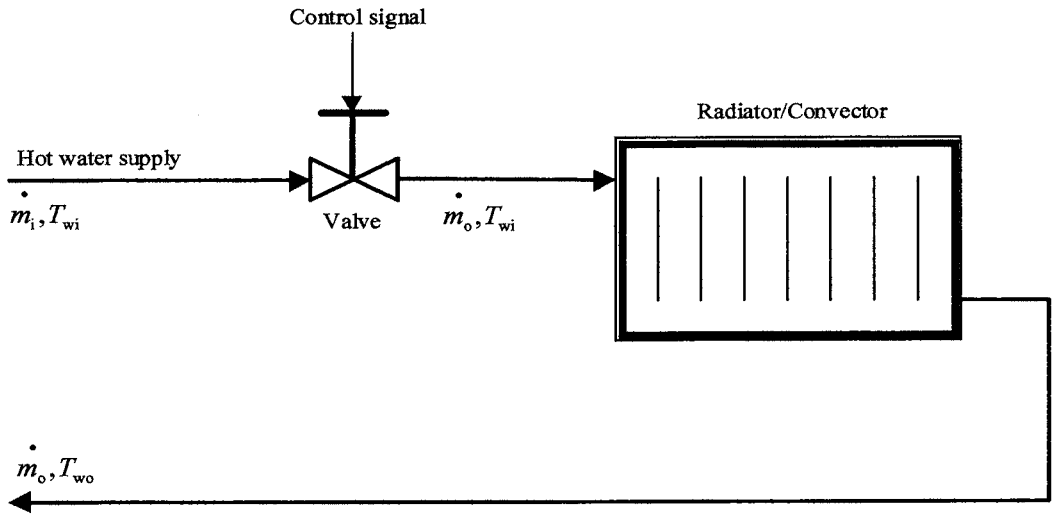

Figure (4.6): Heating system

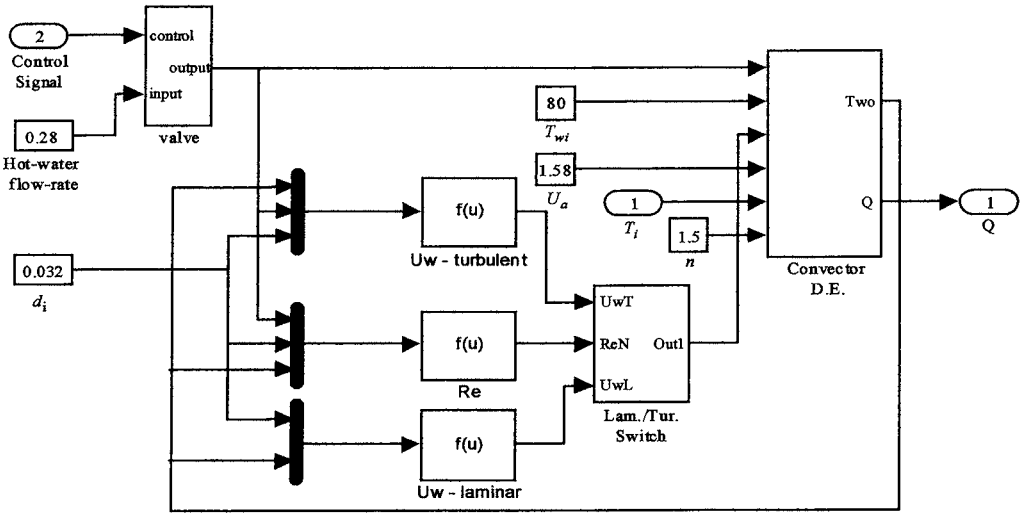

Figure (4.7): Model realisation of the hot water heating system

In summary, the heating system model has 10 input parameters: C_w, c_{pw}, C_m, A_w, A_a, n, d_i, m_w, h_e, N and G_o (appendix C). There are 2 boundary variables: control signal u, and inlet water temperature T_{wi}, and 2 state variables: T_{wo}, T_m.

The heating system response due to unit step applied as a control signal to the valve is shown in figure (4.8), obviously from the graph, the nominal time constant of the given heating system is within one minute (c.f. appendix C).

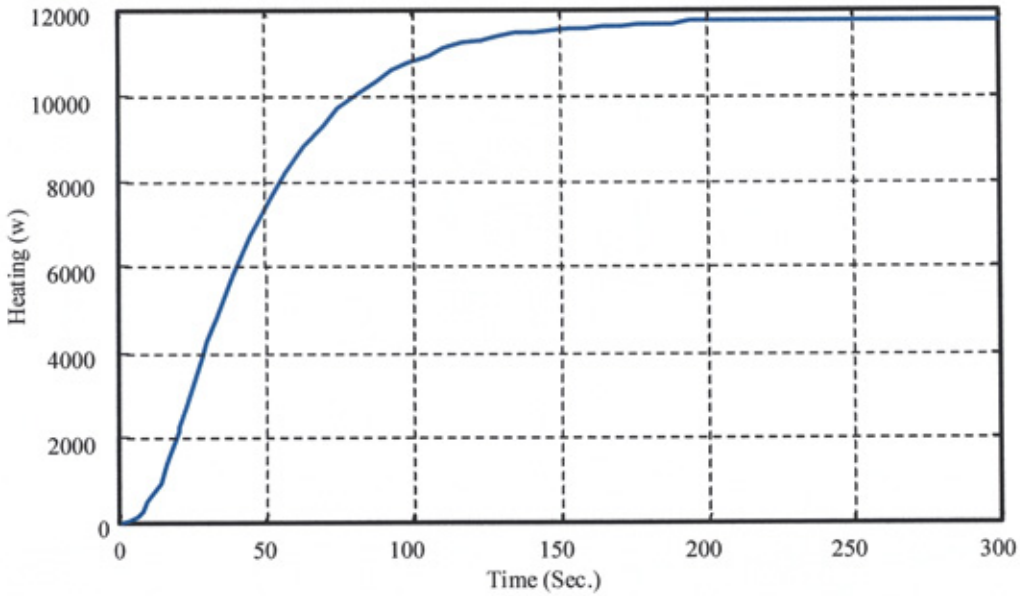

Figure (4.8): Step response of the heating system

Figure (4.9): Northumberland building, north facing

4.4. Model application

The combined building model (described in chapter 3), and heating system model was applied to an example space in a campus building at the University of

Northumbria. This building, as shown in figure (4.9), has been the subject of extensive research into photovoltaic cladding [90].

The selected space is north facing with a floor area of 63 m^2 and volume of 179.5 m^3. It has two external walls, an internal floor, internal ceiling and two partitions and the internal elements were treated as adiabatic, the model realisation of the selected example space shown in figure (4.10), in which the model parameters optimised using the technique outlined in section (3.4) in chapter 3.

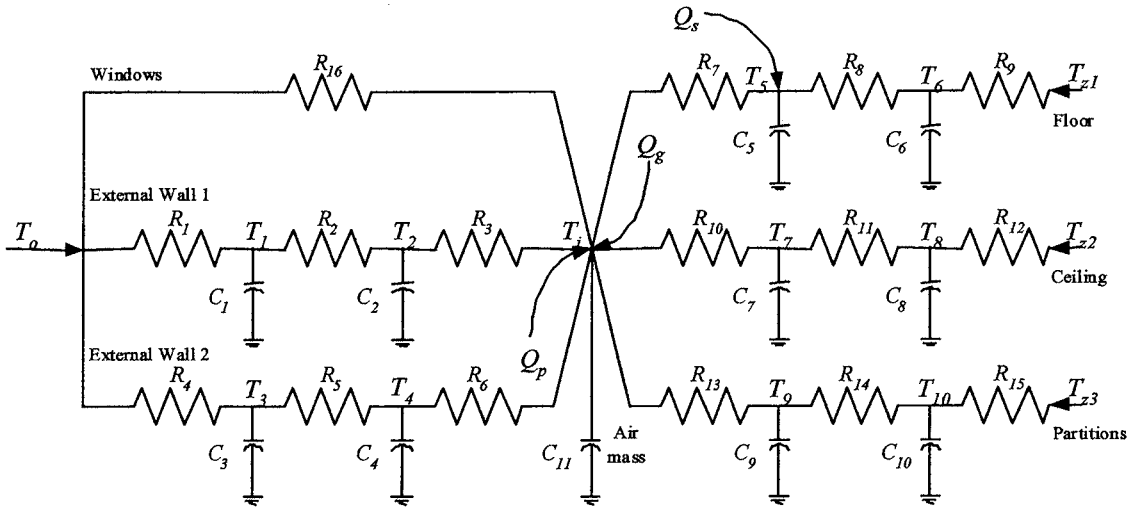

Figure (4.10): Model realisation for the selected example space

This north-facing room (i.e. the diffuse component of solar radiation is very small and neglected) was selected at a period in which the room was known to be heated but not in use, and it is selected to study the behaviour of the effect of the heating system and the outdoor temperature only. This enabled a simpler validation test scenario than would have been the case had casual heat gains and direct solar radiation been active. The heating system consists of an encased finned natural convector which is controlled from a room temperature sensor and a three-port diverting valve which seeks to vary the hot water flow rate in response to room temperature (i.e. a VFCT control strategy is in use), as shown in figure (4.11).

The state equations for the 11th order thermal model of the selected example space, including the hot water heating system can be written as follows:

$$C_1 \dot{T}_1 = (T_o - T_1)/R_1 + (T_2 - T_1)/R_2 \quad (4.18)$$

$$C_2 \dot{T}_2 = (T_1 - T_2)/R_2 + (T_i - T_2)/R_3 \quad (4.19)$$

$$C_3 \dot{T}_3 = (T_o - T_3)/R_4 + (T_4 - T_3)/R_5 \quad (4.20)$$

$$C_4 \dot{T}_4 = (T_3 - T_4)/R_5 + (T_i - T_4)/R_6 \quad (4.21)$$

$$C_5 \dot{T}_5 = (Tz1 - T_5)/R_7 + (T_6 - T_5)/R_8 \quad (4.22)$$

$$C_6 \dot{T}_6 = (T_5 - T_6)/R_8 + (T_i - T_6)/R_9 + Qs \quad (4.23)$$

$$C_7 \dot{T}_7 = (Tz2 - T_7)/R_{10} + (T_8 - T_7)/R_{11} \quad (4.24)$$

$$C_8 \dot{T}_8 = (T_7 - T_8)/R_{11} + (T_i - T_8)/R_{12} \quad (4.25)$$

$$C_9 \dot{T}_9 = (Tz3 - T_9)/R_{13} + (T_{10} - T_9)/R_{14} \quad (4.26)$$

$$C_{10} \dot{T}_{10} = (T_9 - T_{10})/R_{14} + (T_i - T_{10})/R_{15} \quad (4.27)$$

$$C_{11} \dot{T}_i = (T_2 - T_i)/R_3 + (T_4 - T_i)/R_6 + (T_6 - T_i)/R_9 + (T_8 - T_i)/R_{12} + (T_{10} - T_i)/R_{15} + (T_o - T_i)/R_{16} + Qg + Qp \quad (4.28)$$

Figure (4.11): Finned-tube hot water heating system, room 302, NBB

Because adjacent zone temperature (T_{z1}, T_{z2}, T_{z3}) are taken to be equal the internal air temperature of the space under test (adiabatic case), the state space model of the selected example space can be written as follows:

$$\dot{\mathbf{X}} = \mathbf{AX} + \mathbf{BU}$$
$$\mathbf{Y} = \mathbf{CX} + \mathbf{DU} \tag{4.29}$$

where $\mathbf{X}$ is the state vector $[T_1\ T_2\ T_3\ T_4\ T_5\ T_6\ T_7\ T_8\ T_9\ T_{10}\ T_i]^T$, $\mathbf{U}$ is the input vector $[T_o\ Q_s\ Q_p\ Q_g\ T_{z1}\ T_{z2}\ T_{z3}]^T$, $\mathbf{Y}$ is the output vector (i.e. in this case the internal air temperature, T_i).

4.5. Model implementation and validation

Validation is essential for the improvement in the quality of a model [105], since it increases confidence in the predicted result. Bowman & Lomas identify three-validation methods [106]:

1. Analytical verification.
2. Inter-model comparison.
3. Empirical validation.

In analytical verification, the model predictions are compared with known exact solutions. Within a limited scope of application, this technique is useful for investigating errors in algorithms but generating exact solutions is highly problematical.

In inter-model comparison, results from an identical problem are generated using two or more programs and the results are compared. However, favourable comparisons of results do not necessarily mean that these results are correct. Hence this method's usefulness is restricted to checking the consistency of predictive algorithms.

Empirical validation on the other hand compares a program's predictions with experimental data usually based on field measurements. In principle, this method

gives "real world" results, restricted only by the reliability and comprehensiveness of the measurements.

The empirical method has been applied here based on a data sample for a period of several consecutive days from the (north-facing) example space when the heating was active but the room known to be unoccupied. This eliminated the following input excitations which are not of particular interest for the present study, thus simplifying the validation process:

1. Direct solar radiation, (in this case the model only needs the diffuse part of solar irradiance, because the selected space is north-facing).
2. Casual heat gains due to lighting, people and computer equipment.
3. Natural ventilation due to open windows.

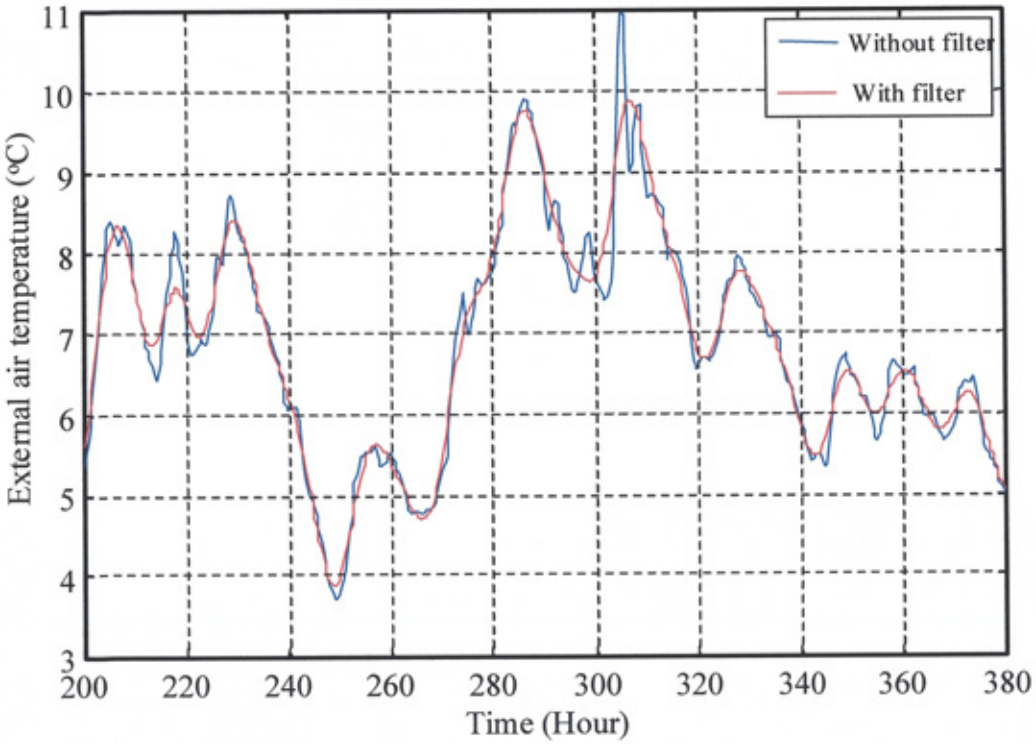

Figure (4.12): External air temperature with and without Butterworth lowpass filter

The measured data sample consisted of a one-week (approximate) time series at 15-minute intervals of space dry bulb temperatures and heating control valve signals. The external temperature time-series was applied directly, and then filtered using a third-order Butterworth lowpass filter with 11 mHz cut-off frequency in order to

smooth out some unacceptable noise spikes. The external temperature with and without filter is shown in figure (4.12).

The final model was implemented using the realisation shown in figure (4.13) in which the model of the temperature sensor was included for the data comparison purpose. The building space model, which was expressed as a state-space block, was solved with the essentially nonlinear differential equations forming the heating system model using a variable step Runge-Kutta scheme selected from within the solver library of the software used.

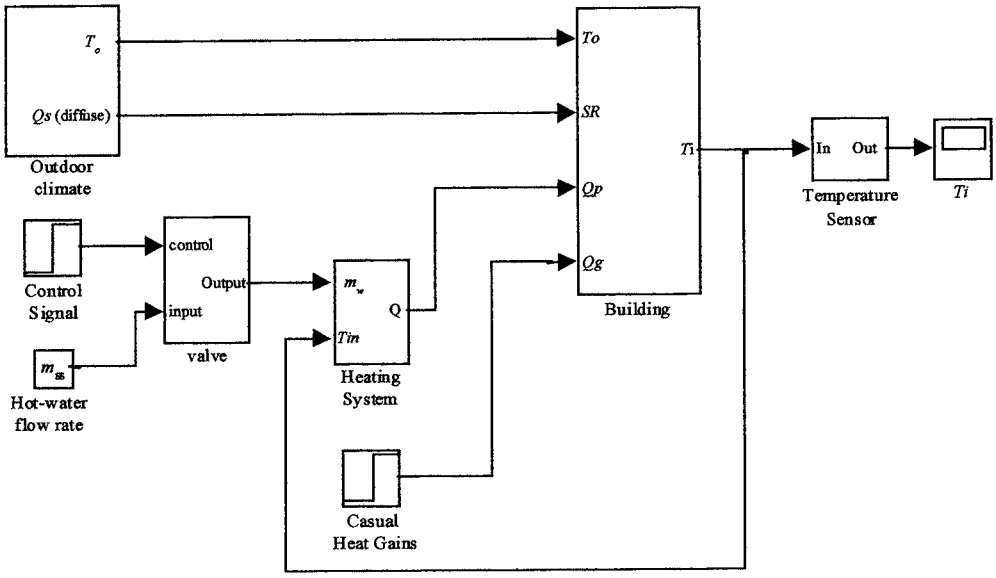

Figure (4.13): Overall model for the building space and its heating system

In figure (4.14), the response to several cycles of heating is compared with field measurement data. The initial period represents a weekend whilst the 5 cycles of heating and cooling represent Monday-Friday. Results based on the model and field-measurements compare very favourably after the external temperature time series had been filtered to remove noise from the data.

Figure (4.15) shows the error between the model predictions and field measurements, the overall root-mean-square error being approximately 0.1K. Though the 2nd-order heating system model is simple, it seems clear from figure (4.12) that it captures the essential dynamics of the problem as far as control system analysis is concerned.

For long-term investigations, the building envelope mass clearly dominates whereas for short-term investigations the room air mass dominates. The dynamics of the room air mass are much closer to the heating system dynamics than to building envelope mass.

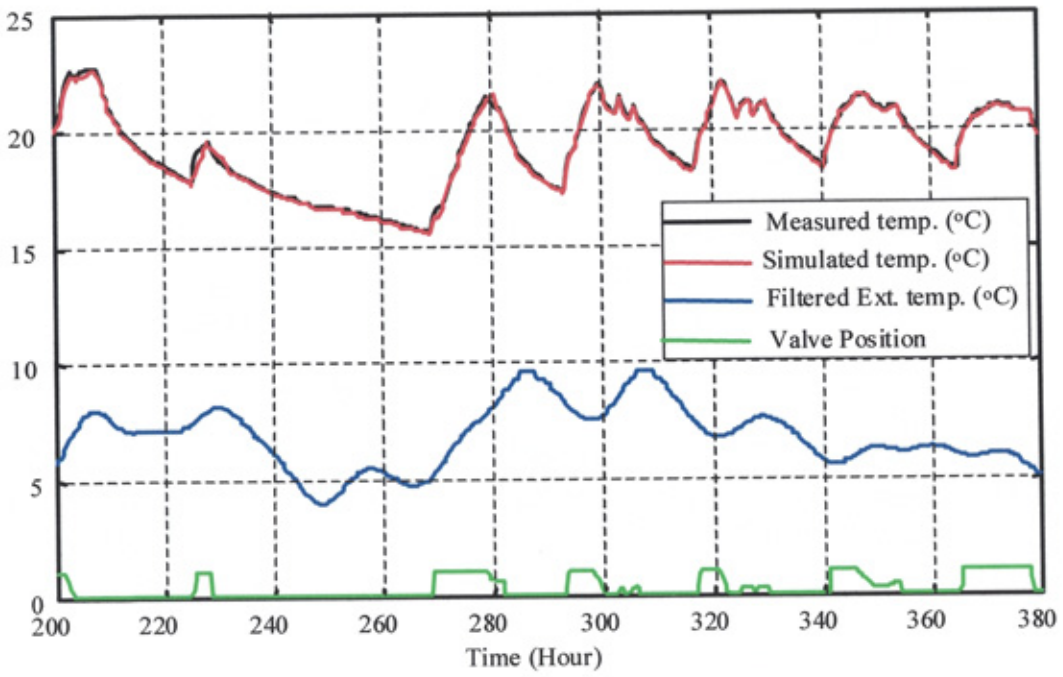

Figure (4.14): Comparison between model and field measurement data

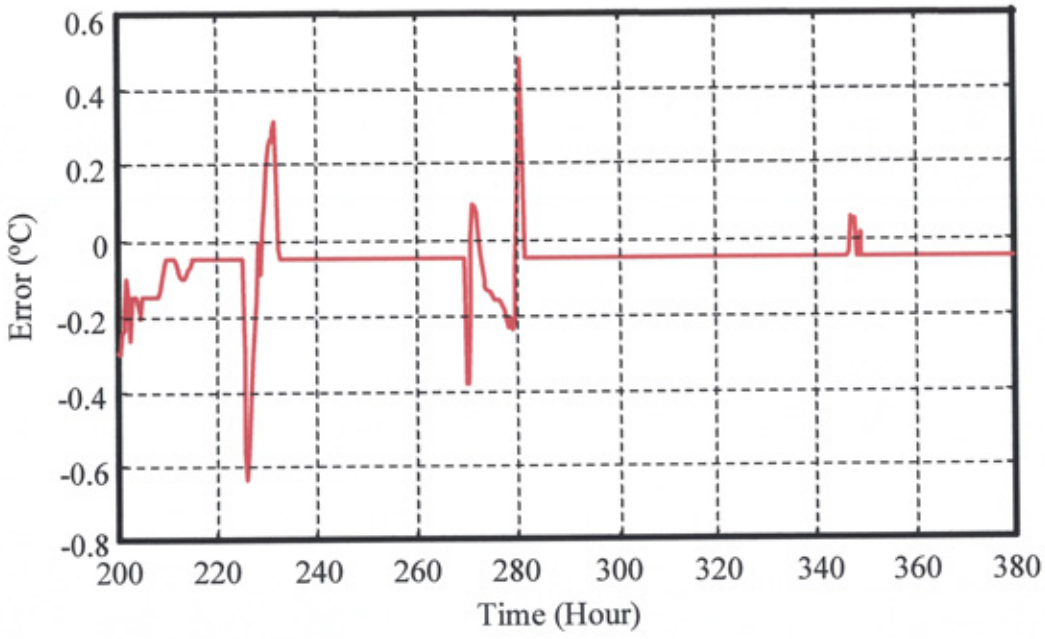

Figure (4.15): Error between model predictions and field measurements

Hence it is argued that a simple heating system model which captures the key low frequency dynamics (i.e. neglects such high frequency effects as measurement noise) is in harmony with the dominant air thermal capacity effect of the space.

4.6. Conclusions

The goal of this chapter was to develop a suitable model of a hot water heating system which, when couple to the room space model of chapter 3, could facilitate the study of nonlinear control laws.

The model developed in this chapter represents a lumped-parameter non-linear heating system description. Excellent agreement has been found between the model and results from field monitoring of a building. However, these results apply to a building with a high thermal capacity facing north (with, consequently, low solar radiation). Nevertheless, it may be concluded that the model is simple, computationally efficient and sufficiently accurate to have potential for applications to short time-scale simulations appropriate to control system analysis.

Using the building space model developed in chapter 3 and the heating system model developed in this chapter, as a test bed for analysing strategies, the next chapter will demonstrate the comparison between fuzzy logic control and a benchmarking PID controller.

Chapter 5

Static Fuzzy Logic and PID Controllers

Chapter 5

Static Fuzzy Logic and PID Controllers

5.1. Introduction

There are many different controllers for heating systems. The type of control action may classify controllers or the variable used for the control signal. Control techniques applied to heating systems may be two position (On/Off), in which the controller output is either "on" or "off", modulating (utilising proportional, integral and differential modes or some combination of these) [107] or more advanced techniques such as predictive control [108].

Presently, most of the controllers used in industry are based on PID control. It is often very difficult to obtain an exact mathematical model of a nonlinear dynamical process. Therefore, the fact that PID controllers utilise the error, the integral and the derivative of the error, rather than an explicit model of the process, has made them quite popular. However, the proportional, integral and derivative gain constants determined by tuning the controller heavily depend on system parameters. Changes in these parameters require retuning of the controller.

An alternative to conventional control is fuzzy logic control (FLC). Fuzzy logic control is based on the fact that an experienced human operator can control a process without knowledge of its dynamics [109]. Developing FLC is usually easier and cheaper than PID controller and FLCs are more robust in that they can cover a wider operation range.

FLCs are becoming increasingly popular [110-117] because of their ability to deal with processes which are ill defined, do not lend themselves to mathematical modelling, and hence difficult to control by conventional methods. The power of FLCs for dynamical systems is based on the ease of design of control rules, the understandable nature of the resulting control signal, non-dependency on accurate process model, and their ability to deal with nonlinear systems. Today the success of fuzzy logic controllers can be found in diverse areas such as consumer electronics [110,118], home appliances [119-121], industrial process [122-124], financial systems [125] and transportation systems [126,127].

In this chapter, PI-based fuzzy logic controller and conventional PID (proportional, integral and derivative) controllers were developed in which the error between the internal air temperature and the user set point temperature was used as the controller input. The output of the controller was applied to the heating system to bring the internal air temperature to the user setpoint temperature. The controller's parameters were set to values that result in the best performance under likely disturbances and changes in set point.

This chapter presents the architecture and the principles in the design of the static FLC developed for the control of the internal air temperature. The chapter starts with the basic structure of a simple fuzzy logic controller in section 5.2. The design details of each of the principal components of a fuzzy logic controller are discussed in general in section 5.3. A closed loop system based alternately on PID and FLC are developed in section 5.4 and a comparison between the performance of the two controllers is given in section 5.5.

5.2. Basic structure of a fuzzy logic controller

The basic structure of a simple FLC is shown in figure (5.1). There are four principal components: a fuzzification interface, a knowledge base, decision-making logic, and a defuzzification interface [114].

A) Fuzzification interface: performs the following functions:

(1) Measure the values of input variables, which are the outputs of the system to be controlled,

(2) Scale mapping that transfers the range of values of input variables on to a corresponding universe of discourse, and

(3) Fuzzification that converts input data into suitable linguistic values, which may be viewed as labels of fuzzy sets.

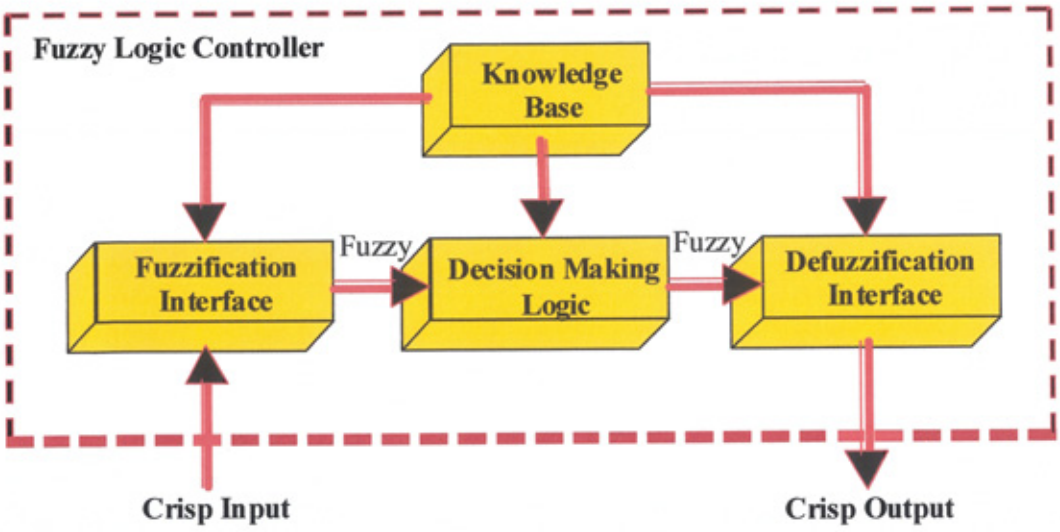

Figure (5.1): Block diagram of the basic fuzzy logic controller

B) Knowledge base: comprises a knowledge of the application domain and the desired control goals. It consists of a data base and a linguistic (fuzzy) control rule base or simply a rule base.

(1) The data base provides the necessary definitions, which are used to define linguistic control rules and fuzzy data manipulation, and

(2) The rule base characterises the control goals and control policy of the domain experts by means of a set of linguistic control rules.

C) Decision making logic: this is the kernel of a fuzzy logic controller. It has the capability of simulating human decision-making based on fuzzy concepts and of inferring fuzzy control actions employing fuzzy implication with rules of inference.

D) Defuzzification interface: Defuzzification is a mapping from a space of fuzzy control actions defined over an output universe of discourse into a space of non-fuzzy (crisp) control actions.

A detailed description and the design of each of these components is given in the following sections.

5.3. Design issues of fuzzy logic controllers

5.3.1. Methodology

In this section, a detailed description of the methodology used in the design of fuzzy logic controllers is presented. Before going into the design details, it is appropriate to mention the five basic assumptions, which are commonly made. They are listed below [128]:

(1) The plant is observable and controllable: State, input and output variables are usually available for observation and measurement or computation.

(2) There exists a body of knowledge comprised individually, or combination of, a set of expert production linguistic rules, engineering common sense, intuition, a

set of input/output measurement data, or an analytical model that can be fuzzified and from which rules can be extracted.

(3) A solution exists.

(4) The control engineer is looking for an acceptable solution, not necessarily the optimum one.

(5) The controller is designed to the best of available knowledge and within an acceptable range of precision.

With the awareness of the above assumptions, the design methodology of a fuzzy logic controller can be divided into the following stages [114]:

1. Design of the fuzzification process,
2. Design of the data base, involving:
   - Discretization of the universe of discourse,
   - Fuzzy partition of the input and output spaces, and
   - Choice of the membership function linguistic terms.
3. Design of the rule base, using either: expert experience and control engineering knowledge, model of an operator's control actions, a fuzzy model, or learning or self-organising process.
4. Design of decision making logic, using either: Mamdani's method, Larsen's method, Tsuhamoto's method, or Sugeno's (or TSK) method.
5. Design of defuzzification process, using either: height method, centroid method, weighted average method, mean of maximum method, or centre of sum method.

5.3.2. Specification of the fuzzification process

Fuzzification is related to the vagueness and imprecision in a natural language and is defined as a mapping from an observed input space to fuzzy sets in a certain input universe of discourse. In fuzzy control applications, the observed data are usually crisp data. Since the data manipulation in a fuzzy logic controller is based on fuzzy set theory, fuzzification is necessary during an earlier stage. Fuzzification is dealt with by a fuzzification operator, which is defined as follows.

A fuzzification operator has the effect of transforming crisp data into fuzzy sets. Symbolically,

$$x = fuzzifier(x_o) \tag{5.1}$$

where x_o is a crisp input value from a process; x is a fuzzy set; and *fuzzifier* represents a fuzzification operator. A fuzzification operator conceptually converts a crisp value into a fuzzy singleton within a certain universe of discourse (UOD). This strategy has been widely used in fuzzy control applications, as it is natural and easy to implement. Other ways of fuzzification can be found in [129-131].

5.3.3. Design of the data base

The knowledge base of a fuzzy logic controller comprises of two components; a data base and a rule base. The data base is used to characterise fuzzy data manipulation and its design includes the following stages:

- Discretization of UOD: Discretization of a UOD is frequently reffered to as quantisation. In effect, quantisation discretises a universe into a certain number of segments (quantisation levels). Each element is labelled as a generic element and forms a discrete universe. A fuzzy set is then defined by assigning grades of membership values to each generic element of the new discrete universe. For the purpose of discretisation, a scale mapping is needed which will serve to transform measured variables into values in the discretised universe. The mapping can be uniform (linear), nonuniform (nonlinear), or both. The choice of quantisation levels reflects some a priori knowledge. For example, course resolution could be used for large errors and fine resolution for small errors. Thus, in a three input one output fuzzy system, the control rule may be of the form:

  "R_i: If error (e) is A, sum of errors (se) is B and change of error (de) is C Then output is D"

- Fuzzy partition of input and output spaces: A linguistic variable in the antecedent of a fuzzy control rule forms a fuzzy output space. In general, a linguistic variable

is associated with a term set, with each term defined on the same UOD. A fuzzy partition then determines how many terms should exist in a term set. A typical example is shown in figure (5.2a and 5.2b), depicting two fuzzy partitions of the same universe [-1, +1]. It should be noted that the fuzzy partition of the fuzzy input/output space is not deterministic and has no unique solution. A heuristic trial and error procedure is usually employed to find the optimal fuzzy partition and expert experience plays an important role in this process.

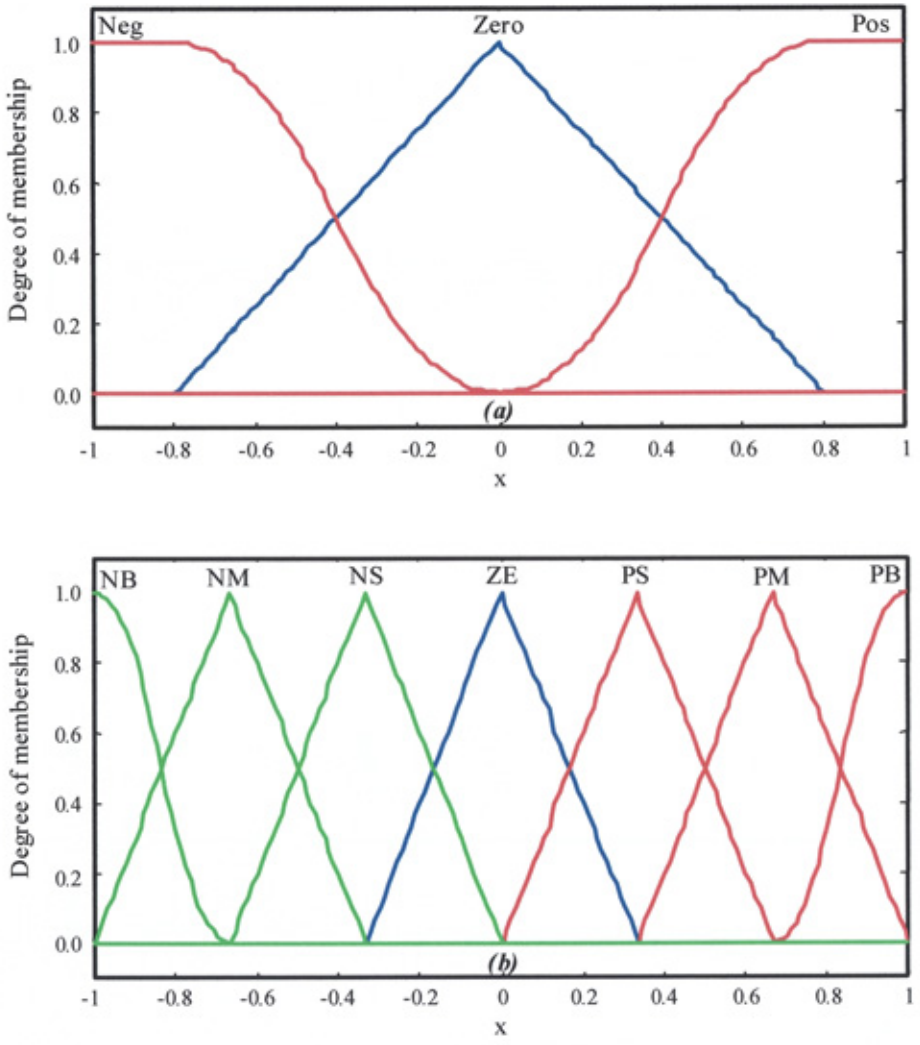

Figure (5.2): Diagrammatic representation of fuzzy partitioning: Three terms, *(b)* Seven terms

- Membership function of a linguistic term: The membership function (MF) of a fuzzy set is usually represented in the form of a function. Some popular MFs

include, a triangular–shaped function, a bell-shaped function, a trapezoid-shape function, etc, and a characteristic equation for some of these can be written as follows. A triangular membership function is specified by three parameters $\{a,b,c\}$ as follows:

$$triangle(x,a,b,c) = \begin{cases} 0 & x < a \\ \dfrac{x-a}{b-a} & a \le x \le b \\ \dfrac{c-x}{c-b} & b \le x \le c \\ 0 & c \le x \end{cases} \tag{5.2}$$

By using min max, we have an alternative expression for the preceeding equation

$$triangle(x,a,b,c) = \max(\min(\frac{x-a}{b-a}, \frac{c-x}{c-b}),0) \tag{5.3}$$

The parameters $\{a,b,c\}$ (with $a < b < c$) determine the x co-ordinates of the three corners of the underlying triangular membership function. Similarly a trapezoidal membership function is specified by four parameters $\{a,b,c,d\}$ as follows:

$$trapeziod(x,a,b,c,d) = \max(\min(\frac{x-a}{b-a}, 1, \frac{d-x}{d-c}),0) \tag{5.4}$$

The parameters $\{a,b,c,d\}$ (with $a < b < c < d$) determine the x co-ordinates of the four corners of the underlying trapezoidal membership function. Based on these equations, the membership values or grades of membership are based on the subjective criteria of the decision. One important criterion for the selection of MFs, is that they should be sufficiently wide to reduce the sensitivity to noise. This raises the issue of the fuzziness or, more accurately, the specificity of a membership function, which in turn affects the robustness of a fuzzy logic controller.

5.3.4. Design of the rule base

A fuzzy system is characterised by a set of linguistic statements based on expert knowledge. The expert knowledge is usually in the form of if-then rules, which are easily implemented by fuzzy conditional statements in fuzzy logic. A collection of fuzzy control rules that are expressed as fuzzy conditional statements forms the rule

base or rule set of a fuzzy logic controller. The issues related to the design of the rule base are discussed below.

Fuzzy control rule generation plays an important role in the design of a fuzzy logic controller. There are four methods for the generation of fuzzy control rules [132, 114, 133] and these methods are not mutually exclusive. A combination of them may be necessary to construct an effective method for the derivation of fuzzy control rules.

1. Expert experience and control engineering knowledge: In this method the fuzzy control rules are designed by verbalisation of a human operator's and/or a control engineer's knowledge in controlling the process/plant. This type of formalisation of fuzzy control rules can be achieved by means of two heuristic approaches. The most common one involves an introspective verbalisation of human expertise. A typical example of such verbalisation in case of a cement kiln [134] is as follows:

   "if the air flow is increased then the temperature in the smoke chamber will increase, while the kiln drive load and the oxygen percentage will decrease".

   From this verbal statement, the following fuzzy control rule can be derived.

   "If drive load gradient is normal, AND drive load is slightly high AND smoke chamber temperature is low THEN change percentage is positive AND change airflow is positive".

Another approach involves interrogating of experienced experts or operators using a carefully organised questionnaire. Using this approach, prototypical of fuzzy control rules can be formed. Finally, a heuristic cut-and-try procedure is used to fine tune the rules.

This method is the least structured of the four methods, and yet it is the most widely used one. The disadvantages are that (i) an operator may not be able to verbalise his or her knowledge, and (ii) it may be difficult for a control engineer to write down control rules because the process is too complex.

2. Modelling an operator's control actions: The operator's skilled actions or control behaviour can be modelled in terms of fuzzy implication using the input-output

data and the obtained input-output model can be used as a fuzzy controller. The idea behind this mode of derivation is that it is easier to model an operator's actions than to model a process since the input variables of the model are likely found by analysing the control actions. A typical example is Sugeno's fuzzy car [135]. This model car has successfully followed a crank-shaped track and parked itself in a garage. The training process involves a skilled operator guiding the fuzzy model car under different driving conditions. The control policy incorporated is represented by a set of state-evaluation fuzzy control rules of the following form:

$$\text{"}R_i\text{; If } x \text{ is } A \text{ and....and } y \text{ is } B\text{, Then } z = a_0 + a_1 x + \ldots\ldots + a_n y\text{"} \quad (5.5)$$

where $x, \ldots, y$ are linguistic variables representing the distance and orientation in relation to the boundaries of the track, z is the next steering angle decided by the i^{th} control rules, and $a_0, \ldots, a_n$ are the parameters entering in the identification process of skilled driver's actions. Besides modelling an operator's action, this method is also used to model (identify) controlled processes according to their input-output data, which involves parameter learning as well as structure learning [136]. These are called linguistic control rule approaches to fuzzy modelling or identification.

The design of a fuzzy logic controller based on the derived fuzzy model is called a model based fuzzy logic controller design and is representative of the third method of design described next.

3. Based on a fuzzy model or behaviour analysis of a controlled process: In this method, fuzzy control rules are derived or justified based on either the fuzzy model or the behaviour analysis of a controlled process. In this context, fuzzy modelling means the representation of the dynamic characteristics of the process by a set of fuzzy implications with inputs, state variables, and outputs.

4. Based on learning (or self-organising): Many fuzzy logic controllers have been built to emulate human-decision making behaviour. Currently, many research efforts are focused on emulating human learning, that is, the ability to create fuzzy control rules and to modify them based on experiences. Procyk and Mamdani [137] proposed the first self-organising controller (SOC).

5.3.5. Design of the decision making logic

This is the kernel of the fuzzy logic controller in modelling human decision making within the conceptual framework of fuzzy logic and approximate reasoning. In on line processes, the states of a control system play an essential role in control actions. The inputs to the controller are measured by sensors and are crisp. These inputs are fuzzified using the techniques discussed in section (5.3.2). Then the necessary data-base and rule-base are derived for desired control action using the methods discussed in sections (5.3.3) and (5.3.4). Then using the rule base, the conclusion or the appropriate control actions have to be derived depending on the input conditions or states. This process of computing a result or conclusion from a set of fuzzy rules is called fuzzy inference. Approximate reasoning or fuzzy reasoning is such an inference procedure. In general, there are four types of fuzzy reasoning currently employed in fuzzy control applications, as mentioned in section (5.3.1). For explanatory purposes, assume a two input single output fuzzy system with fuzzy control rules R_1 and R_2 as follows:

Input: x *is* A *and* y *is* B

Output: z *is* C

R_1: *if* x *is* A_1 *and* y *is* B_1 *then* z *is* C_1

R_2: *if* x *is* A_2 *and* y *is* B_2 *then* z *is* C_2

z *is* C

where A_i, B_i and C_i are linguistic values of the linguistic variables x, y and z in the UODs U, V, and W respectively, with $i = 1,2,.....,n$; and C is the consequence. Then the fuzzy control rule *"if* (x *is* A_1 *and* y *is* B_1) *then* (z *is* C_1)*"* is implemented as a fuzzy implication (relation) R and is defined as

$$\mu_{R_i} = [\mu_{A_i}(u) \text{ and } \mu_{B_i}(v)] \longrightarrow \mu_{C_i}(w) \tag{5.6}$$

where A_i and B_i are fuzzy sets $A_i \times B_i$ in $U \times V$; R=(A_i and B_i)$\rightarrow C_i$ is a fuzzy implication (relation) in $U \times V \times W$; and $\rightarrow$ denotes a fuzzy implication function. If the firing strengths of the first and second rules are α_1 and α_2 then:

$$\alpha_1 = \mu_{A_1}(x_0) \wedge \mu_{B_1}(y_0)$$
$$\alpha_2 = \mu_{A_2}(x_0) \wedge \mu_{B_2}(y_0) \tag{5.7}$$

where $\mu_{A_1}(x_0)$ and $\mu_{B_1}(y_0)$ play the role of the degree of partial match between the user-supplied data and the data in the rule-base and "$\wedge$" represents min operation. Because it is computationally very efficient and saves a lot of memory, the method used in this work (Mamdani's method), can be described as follows.

Fuzzy reasoning of first type- Mamdani's minimum operation rule, R_c as a fuzzy implication function: In this method of reasoning, the i^{th} rule leads to the control decision as given below.

$$\mu_{c_1}(w) = \alpha_1 \wedge \mu_{c_1}(w) \tag{5.8}$$

the final inferred consequence C is given by:

$$\mu_C(w) = \mu_{c_1} \vee \mu_{c_2} = [\alpha_1 \wedge \mu_{c_1}(w)] \vee [\alpha_2 \wedge \mu_{c_2}(w)] \tag{5.9}$$

To obtain a deterministic control action, a defuzzification strategy is required, as will be discussed in section 5.3.6. This fuzzy reasoning process is illustrated in figure (5.3).

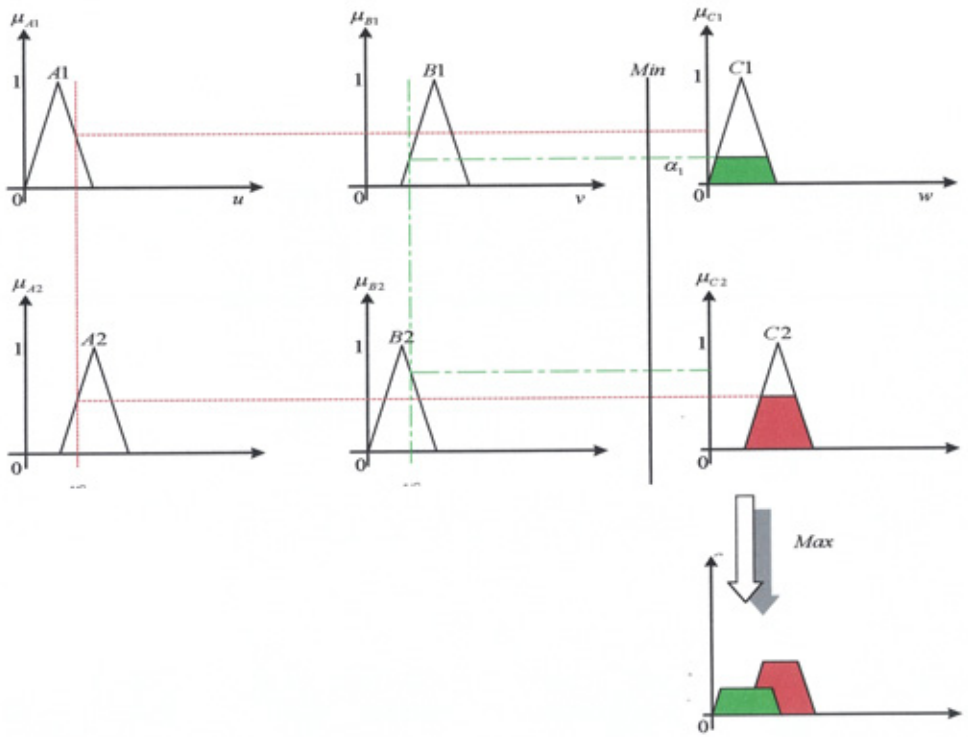

Figure (5.3): Diagrammatic representation of fuzzy reasoning (Mamdani)

5.3.6. Defuzzification Design

Defuzzification is defined as a mapping from a space of fuzzy control actions defined over an output UOD into a space of non-fuzzy (crisp) control actions. A defuzzification strategy is aimed at producing a non-fuzzy control action that best represents the possibility distribution of an inferred fuzzy control action. Though, there is no systematic procedure for choosing a defuzzification strategy, some of the established methods can be found in [123, 114, 138, 139], the defuzzification method used in this work is discussed below.

Centroid, Centre of Area (COA) or Centre of Gravity (COG) method: This procedure is the most prevalent and physically appealing of all the defuzzification methods. In the case of a continuous UOD, it is given by the following expression:

$$z_0 = \frac{\int_{-\infty}^{\infty} \mu_c(w) w dw}{\int_{-\infty}^{\infty} \mu_c(w) dw} \tag{5.15}$$

This method is shown graphically in Figure (5.4).

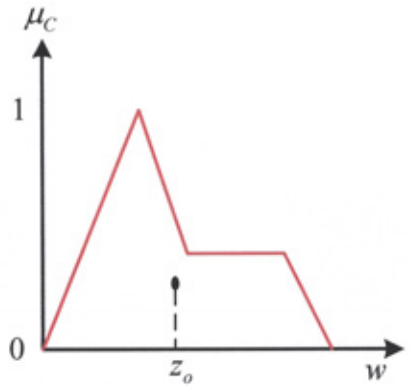

Figure (5.4): Centroid defuzzification method

The whole process of designing a fuzzy logic controller can be summarised [123] into the following steps:

- Identify the variables (inputs, states and outputs) of the plant.
- Partition the UOD or the interval spanned by each variables into a number of fuzzy subsets, assigning each a linguistic label,
- Assign or determine a membership function for each fuzzy subset,

- Assign the fuzzy relationships between the input fuzzy subsets and output fuzzy subsets, thus forming the required rule base,
- Choose appropriate scaling factors for the input and the output variables in order to normalise the variables to the [0,1] or [-1,1] interval,
- Fuzzify the inputs to the controller,
- Use appropriate inference mechanism to aggregate the fuzzy outputs recommended by each rule, and
- Apply appropriate defuzzification to form a crisp output.

So far, the construction of fuzzy logic controllers and the principles involved have been discussed in general. Now, the following sections will discuss how these principles have been applied in designing a PI-based fuzzy logic controller for solar buildings, and comparison with a conventional PID controller.

5.4. Closed loop results

A controller and feedback path were added in order to close the open loop system (i.e. the building and its heating system) described in chapter 3 and chapter 4. The controlled variable (T_i) is compared with the user reference temperature and the resulting temperature error is applied to the controller. Outdoor temperature, solar radiation and casual heat gains act as disturbances, as shown in figure (5.5).

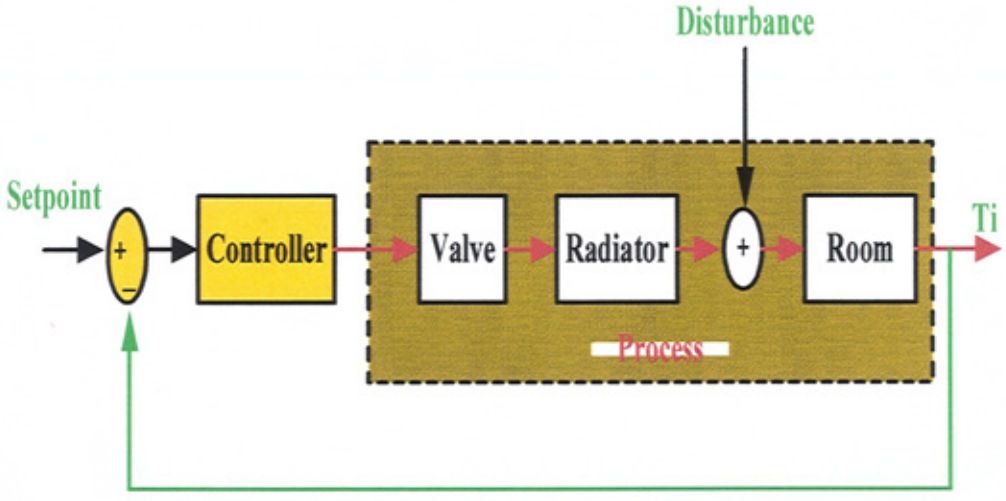

Figure (5.5): Closed loop system

5.4.1. PID Controller

PID control is commonly used in heating systems [107,140]. Although a PID controller is reliable and efficient, its parameters require precise adjustment to obtain optimal performance, and they are heavily dependent on system parameters. The output of a PID is given by:

$$u(t) = k_p e(t) + k_i \int_0^t e(t)dt + k_d \frac{de(t)}{dt} \tag{5.19}$$

in which e, k_p, k_i, and k_d are the error, proportional gain, integral gain and derivative gain for the controller respectively. The three gain values are *tunable control parameters* (i.e. are adjusted in practice to give "good" control – usually amounting to a stable response with favourable set-point tracking criteria).

The control error, $e = T_r - T_i$, where T_r is in this case the reference value or *set point* in room temperature.

When a PID controller experiences an input error signal which is both large and sustained the integral term gradually accumulates a very large output value. This will occur for example during early morning preheating when the error is large to start with but it also takes some time (sometimes a few hours) for the heating operating at full capacity to bring the control error to within its proportional band. By the end of the preheat period therefore, the integral term will have forced the control signal to a very large value causing *actuator saturation* (i.e. the valve actuator is stuck at the fully open position even when the error has reduced to zero or near-zero). The control variable then overshoots causing the sign of the error to change. This sign change then ensures that the integral signal de-accumulates but it takes time for the signal value to come down sufficiently for the actuator to de-saturate. This "stickiness" problem is called *integral wind-up* and an anti-wind-up mechanism is needed on most PID controllers likely to experience such periods of operation in order to prevent this from happening.

There are a few anti-wind-up strategies but they are all based on the same idea – that of retarding the integral term in some way when the actuator reaches saturation.

The simplest thing to do is to saturate the integral term to the upper and lower limits of the control signal that correspond to actuator saturation (i.e. 1 and 0 in this case). This can easily be done in SIMULINK because the integrator block has a "limit output" facility that allows us to fix upper and lower saturation limits on integration.

Also a saturation block should be added on the overall control signal output value leaving the controller and limit the signal to 0 (minimum); 1 (maximum). This is because the valve model equations are based on a control signal in the fractional range 0→1. Thus any value outside this range is likely to lead to a mass flow rate from the control valve subsystem which is outside the design range hence we adopt a fractional control signal convention accordingly.

The PID controller described by equation (5.19) was applied to the system. The actual parameters of the controller in the sample building space (k_p, k_i, k_d) are $0.1K^{-1}$, $0.01K^{-1}s^{-1}$, and $0.5sK^{-1}$ respectively and these were initially applied. This produced a reasonable response but with overshoot (figure (5.9)), leading to more energy consumption and thermal discomfort for the occupants.

A tuning algorithm was adopted to adjust the controller parameters in order to eliminate this overshoot. In practice, Ziegler Nichols rules [141] or similar tuning rules are used for predicting PID controller settings. These are based on achieving favourable response criteria of a hypothetical linear low-order system and, thus, have limited utility other than in the precise region of plant operation in which the tuning was carried out.

It is possible to obtain optimum PID settings using norminal values as a starting point by minimising a cost function attached to the target variables T_i. This process is more or less equivalent to using an automated self-tuner on site. In practice, tuning will normally take place in the off-design phase when the plant is operating around the required set point but with higher entering air temperatures, simply because it will rarely be convenient to wait for design conditions to prevail before commissioning is carried out. The optimisation was therefore carried out using a nonlinear control design (NCD) blockset available from within the extended program library used at

arbitrarily chosen mid-session conditions corresponding to an entering air temperature [142].

The NCD block works as follows. A constraint envelope is defined that defines upper and lower bounds of the controlled variable, together with one or more tunable variables. A cost function is generated consisting of a weighted maximum constraint violation. At each iteration, each tunable variable is perturbed in turn and the resulting constraint values and cost function are evaluated. A gradient search direction is determined from these results and a line search along the gradient is performed in order to minimise the cost function while simultaneously satisfying the constraint envelop criteria.

Hence the NCD block setup involved the following:

- A constraint envelope was defined for the controlled variable T_i. This consisted of an arbitrary but "desirable" response to a step change in the setpoint from "0 °C " to "20 °C ".
- The controllers' parameters were set as tunable variables. The initial values used were the actual values of the manufacturers' settings.

To give initial estimates of the controller parameters, an error mapping method was used as shown in figures (5.6, 5.7, 5.8). In which, the simulation model of the building, heating system and PID controller was running with fixed one of the controller parameters and varied the other two parameters to get a minimum a performance index. The square root of the sum-squared-error (normalised error) between reference temperature and the internal air temperature is used as a system performance index. Using the initial mapped values to initiate the tuning algorithm, tuned controller parameters of $1.527K^{-1}$, $0.005K^{-1}s^{-1}$, and $0.050sK^{-1}$ respectively were obtained for k_p, k_i, k_d. The response of the system under tuned PID controller is shown in figure (5.9).

The tuned PID controller gives good results at the precise conditions for which it has been designed. However, as will be seen later, when these conditions change performance is less favourable unless the controller is re-tuned.

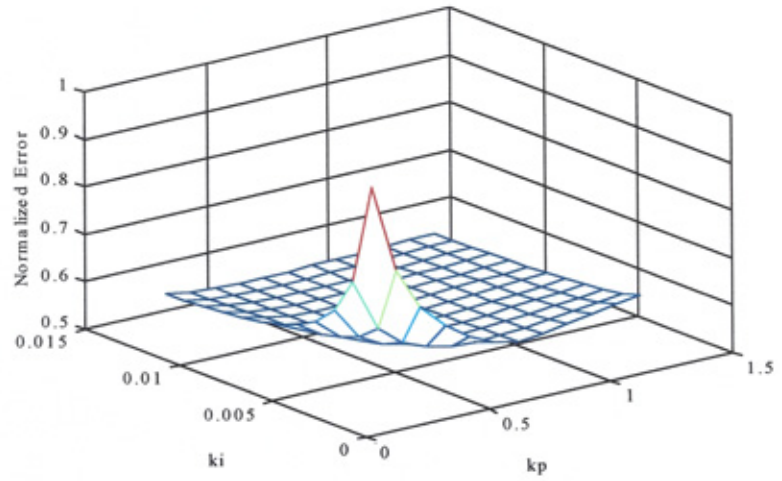

Figure (5.6): Normalised error vs k_p, k_i

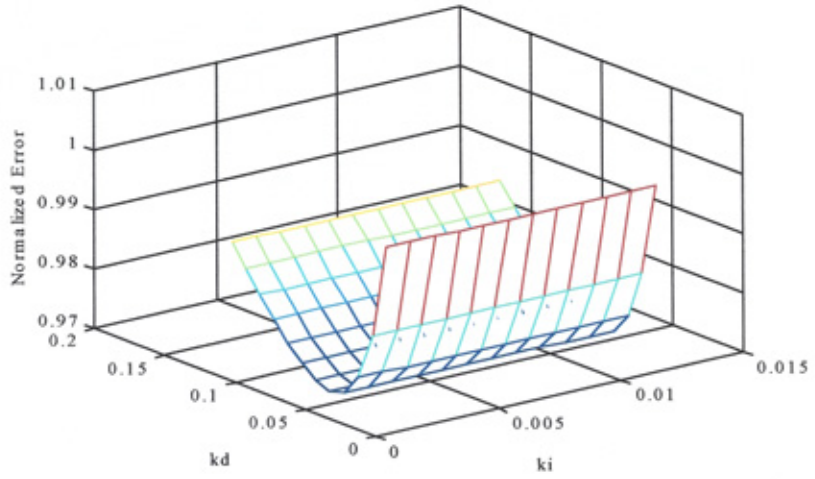

Figure (5.7): Normalised error vs k_d, k_i

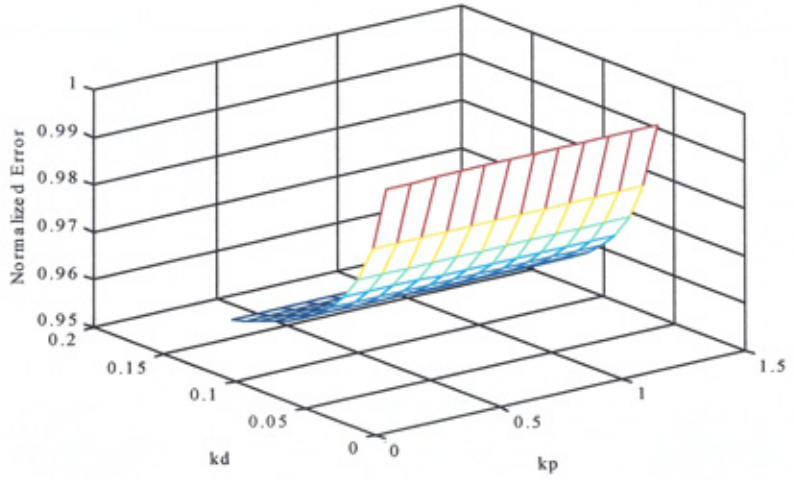

Figure (5.8): Normalised error vs k_p, k_d

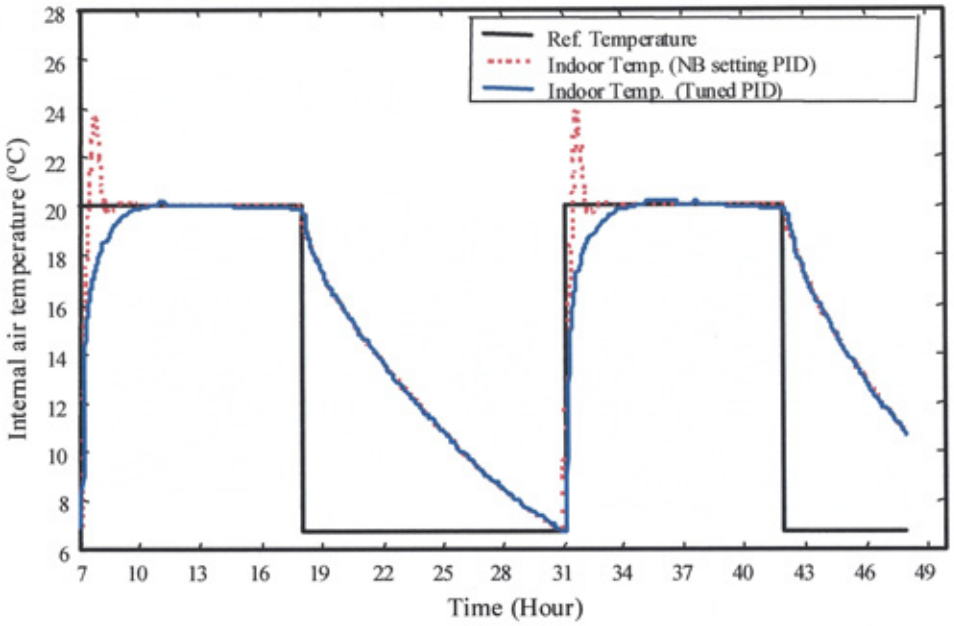

Figure (5.9): Closed loop response with tuned and untuned PID control

5.4.2. Static fuzzy logic control

Good tracking and more robustness to change in the building and climate parameters are the objectives of design with the static fuzzy logic controller.

Although the choice of the number, range and shape of membership functions for a variable is ultimately based on the subjective design choice and evaluation of the resulting system performance, there are some guidelines were kept in mind during this work and were presented by [112,114]. These guidelines are:

1. Symmetrical distribute the fuzzy sets across the defined universe of discourse,
2. Use an odd number of fuzzy sets of each variable-this ensures that some fuzzy set will be in the middle, five or seven fuzzy sets for each system variable is fairly typical,
3. Overlap adjacent fuzzy sets to ensure that no crisp values fails to correspond to any set, and to help ensure that more than one rule is involved in determining the output.
4. The membership function should allow a variable to have a membership value of unity for at least one specific value of the variable in question.

5. Use triangular or trapezoidal membership functions: these two choices can be explained by the ease with which a parametric, functional description of the membership function can be obtained, stored with minimal use of memory, and manipulated efficiently, in terms of real-time requirements, by the inference engine.

A fuzzy control algorithm was developed after some trials in order to verify the fuzzy control rules, membership functions, scaling factors and defuzzification strategy.

The input variables were normalised using different scaling factors of error and change of error ($E_N = g_e \times E$, and $CE_N = g_{ce} \times CE$) to bring all values of the error and change of error within the corresponding UOD. In this application, fuzzy sets are defined by assigning the membership functions to seven fuzzy sets (negative big (NB), negative medium (NM), negative small (NS), zero (ZE), positive small (PS), positive medium (PM), positive big (PB)) as shown in figure (5.10a,b,c) for the inputs and output to simplify the design problem.

Overlapping triangular membership functions were used for inputs (fuzzification) and output (defuzzification), the difference between these being the corresponding scaling factors. The fuzzy control rules were derived by referring to human operator experience and knowledge. There are two selected fuzzy sets each for error and change of error. Therefore, four rules only were fired, represented by the intersection of two rows and two columns in Table (5.1).

Error	Change of error						
	NB	NM	NS	ZE	PS	PM	PB
NB	NB	NB	NB	NB	NM	NS	ZE
NM	NB	NB	NB	NM	NS	ZE	PS
NS	NB	NB	NM	NS	ZE	PS	PM
ZE	NB	NM	NS	ZE	PS	PM	PB
PS	NM	NS	ZE	PS	PM	PB	PB
PM	NS	ZE	PS	PM	PB	PB	PB
PB	ZE	PS	PM	PB	PB	PB	PB

Table (5.1): Applied fuzzy control rules

To make the fuzzy controller more sensitive to the error and change of error, and to get fine resolution of the controller around the setpoint, the membership functions of both inputs and output were narrowed around zero and widen elsewhere as shown in figure (5.10).

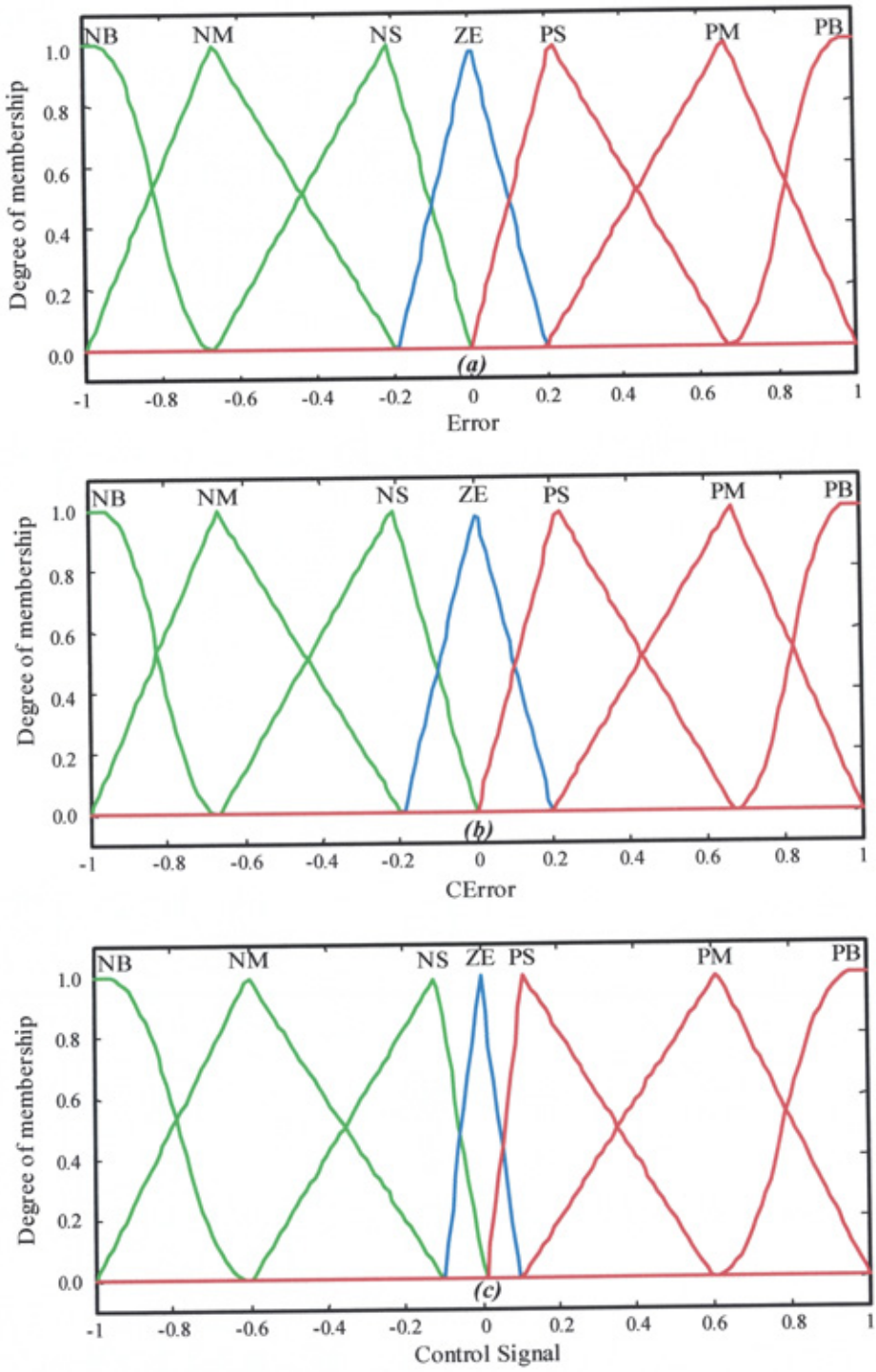

Figure (5.10): *(a)* Membership functions of the error, *(b)* Membership functions of the change of error, *(c)* Membership functions of the control signal

A scaling factor (g_u) was used to convert the crisp control signal from the normalised discourse to the applied range of actual control signals ($U_p = g_u \times U$), which was then applied to the nonlinear valve. The relationship between the inputs and the outputs of the controller (or the controller surface) is shown in figure (5.11).

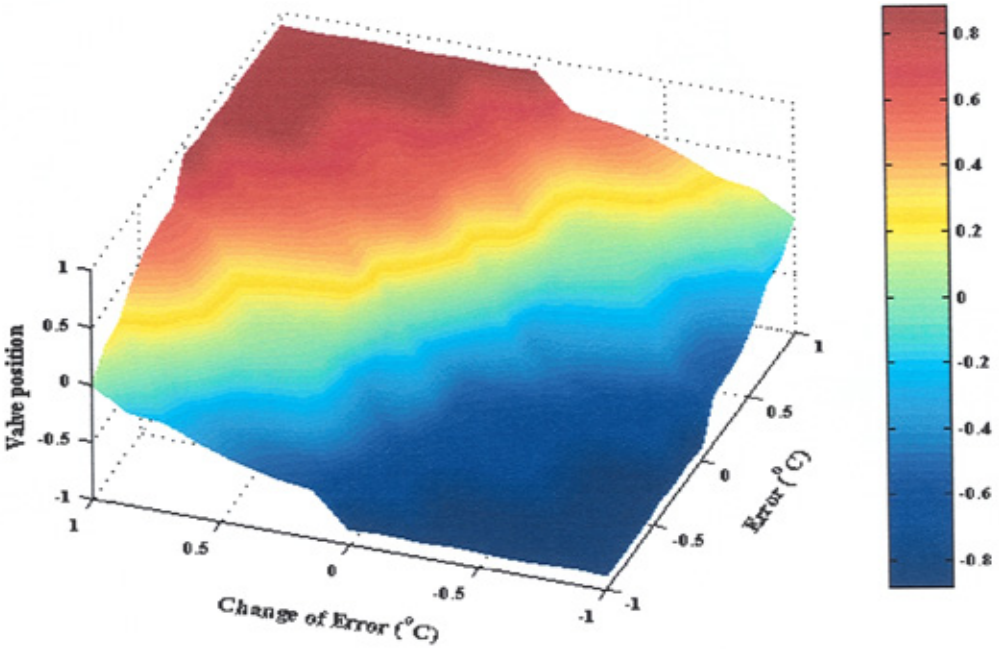

Figure (5.11): Fuzzy controller output surface

Also a saturation block should be added on the overall control signal output value leaving the controller and limit the signal to 0 (minimum); 1 (maximum). This is because the valve model equations are based on a control signal in the fractional range 0→1. Thus any value outside this range is likely to lead to a mass flow rate from the control valve subsystem which is outside the design range hence we adopt a fractional control signal convention accordingly.

5.5. Comparison of controllers

The resulting FLC was applied to the building space and its heating system. Figure (5.12), shows the system response under tuned PID and FLC. As can be seen, the

performance of the FLC is superior to PID controller in terms of tracking of the reference point, and hence, system energy usage and comfort criteria.

In order to test the controllers' performance when system parameters change, the building construction data were changed to those representing a very low thermal capacity structure while keeping the overall thermal transmittance of each element constant. This would have the effect of making the system much more responsive (and, hence control more "difficult"). The controller specifications remained unchanged.

Figure (5.13) reveals that the fuzzy controller maintains excellent tracking of the reference condition whereas the tuned PID gives a reasonable response but with overshoot. Thus a certain amount of robustness of the PID controller is lost requiring it to be re-tuned whereas the robustness characteristic of the FLC is maintained.

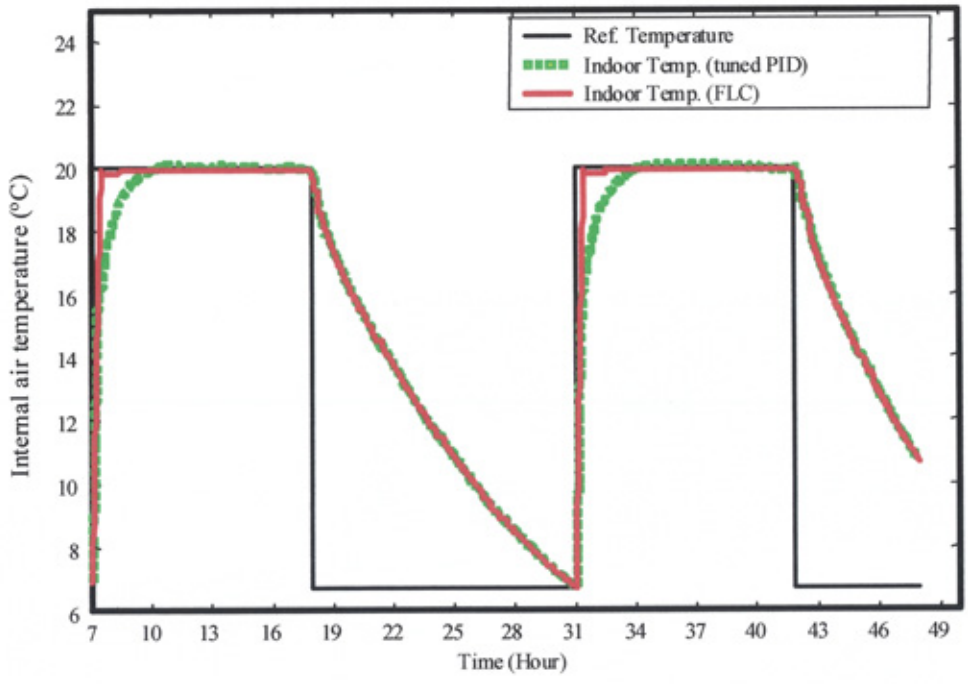

Figure (5.12): Comparison of tuned PID and FLC

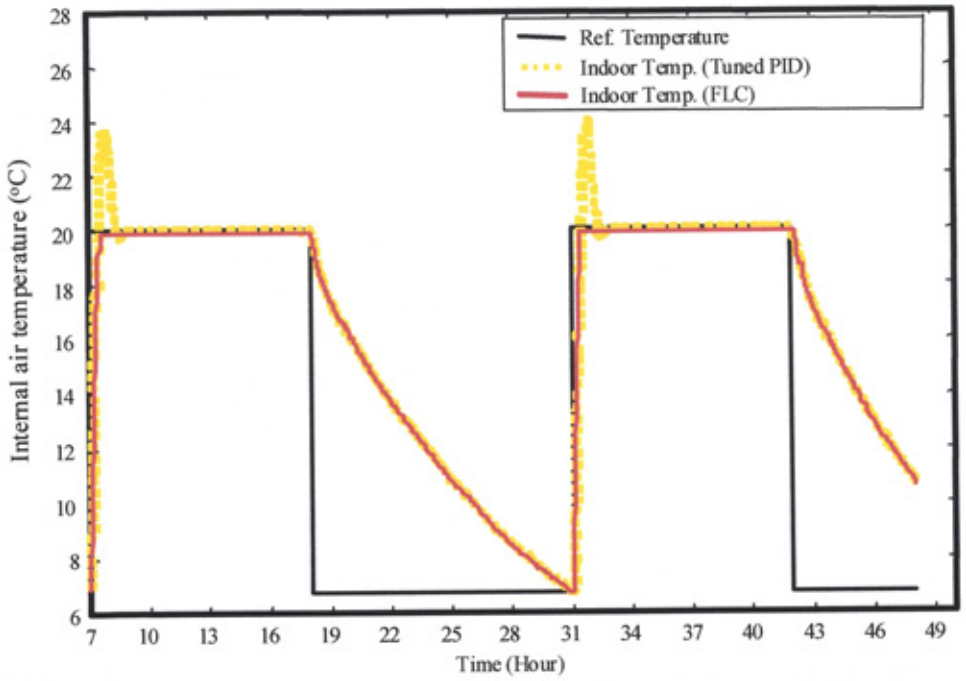

Figure (5.13): Low thermal capacity building's space with tuned PID and FLC

5.6. Conclusions

Most current space heating system controllers continue to be based on the conventional PID regulator. These controllers require 3 tuning parameters which are difficult to optimise *a priori* and which, in any event, are only suited to a finite range of plant response when the plant has nonlinear characteristics.

A fuzzy logic controller has been developed based on a 49-rule rulebase. The FLC was found to give better tracking of the reference control condition than a comparative tuned PID controller as well as better robustness properties when the parameters of the system under control were changed. The FLC has the advantage of requiring no mathematical model of the plant or measurements of plant response as would be required to achieve satisfactory tuning of the PID controller.

Whereas the controllers in this chapter are designed for room air temperature control, on a more fundamental level what is important is comfort, which depends on other factors such as radiant temperature, relative humidity etc. In the next chapter, comfort indices are discussed and a comfort based control system investigated.

Chapter 6

Thermal Comfort based Fuzzy Logic Controller

Chapter 6

Thermal Comfort based Fuzzy Logic Controller

6.1. Introduction

Building space comfort control is a multidimensional problem having no unique solution, particularly in a solar building [143]. Also, the definition of comfort is obscure and depends considerably on the psychosynthesis of the individuals living in the space and on the type of activity they are engaged in [144]. In addition, the same result can be achieved by employing different subsystems, such as ventilation, cooling auxiliary heating thermal stores, etc., and consequently the problem of correcting the environmental conditions corresponds initially to a twofold problem:

(a) the interpretation of the comfort requirement, and (b) the making of a decision on which subsystem or subsystems to use at a particular moment.

Also, most heating, ventilation and air conditioning (HVAC) control systems are considered as temperature control problems. For this reasons the application of the optimal control theory has not resulted in a single, widely applicable solution, but only in sub-optimal systems, operating well only under a certain set of predefined conditions [145-148]. By contrast, the implementation of a fuzzy logic expert system fits the problem well, since it handles naturally the fuzzy comfort concepts and is well suited to provide real-time decisions [149-152]. This approach captures the architect's operation design rules in the form of a knowledge base, i. e. a set of logic rules that would be applied if a human were operating the building controls intuitively. According to Fanger's theory, thermal comfort is determined by personal-dependent and environmental–dependent variables. Thus, the comfort index PMV (predicted mean vote) can be considered as a new indoor climate high-level performance variable [149,152]. This is the main reason behind the necessity to regulate the thermal comfort index rather than the internal air temperature.

The present chapter investigates the problem of designing a widely applicable fuzzy logic system, focusing on the design of the rule base, the fuzzification interface, defuzzification interface and the inference engine [114,153-155]. It should be noted that the expert system works well only if the knowledge embedded in its rule base is sound. An expert system with poor understanding of the requirements will make poor utilisation of resources, just as a poorly trained human operator would. Consequently the more complex the buildings are, with many spaces and many subsystems, so the fuzzy logic system is more appropriate, since the number of comfort requirements and the number of usable subsystems increase [149].

In this chapter, the predicted mean vote (PMV) is used to control the indoor temperature of a space by setting it at a point where the PMV index becomes zero and the predicted percentage of persons dissatisfied (PPD) achieves a maximum threshold of 5%. This is achieved through the use of a fuzzy logic controller that takes into account a range of human comfort criteria in the formulation of the control action that should be applied to the heating system to bring the space to comfort conditions. The

resulting controller is free of the set up and tuning problems that hinder conventional HVAC controllers.

The PMV-based fuzzy logic controller investigated in this chapter starts with the evaluation of the predicted mean vote level and compares this with the required comfort range in order to arrive at a linguistic definition of the comfort sensation. The controller then adjusts the air temperature set point in order to satisfy the required comfort level given the prevailing values of other comfort variables contributing to the comfort sensation.

The objectives of this chapter are thus:

- To further develop the previous model for investigating the comfort sensation control of the heating system in a building space.
- To develop a control strategy which responds to the essentially subjective basis of comfort sensation.
- To compare the developed control strategy with a conventional method of building space heating control.

6.2. Thermal comfort variables

The thermal comfort sensation is expressed using Fanger's predicted mean vote (PMV) and percentage persons dissatisfied (PPD) [156] in which the environmental factors of influence are room air temperature, relative humidity, mean radiant temperature, and air velocity. In this work, for simplicity (besides being difficult to evaluate dynamically) a constant mean was used for the air velocity. In addition, there are human factors associated with activity level, and the thermal resistance of clothing.

According to Fanger's theory [156], PMV and PPD can be defined as follows:

> *"PMV, is an estimation of the average vote of a large group of persons submitted to a given thermal environment. The range of PMV is* -3(too cold) $\leq PMV \leq +3$(too warm) *".*
>
> *"PPD is an estimation of the percentage of persons who would be dissatisfied by a thermal environment (i.e. the number of potential complainers)".*

The relationship between PMV, PPD and the thermal sensation of the occupant is summarised in Table (6.1) [156] based on a neutrality at zero PMV (positive when the thermal sensation is "warm" or "hot" and negative when "cool" or "cold"). The PPD is estimated to be 5% when the PMV is zero and the target indoor temperature is set with respect to this point.

PMV	Thermal Sensation	PPD (%)
+3	Hot	100
+2	Warm	75
+1	Slightly warm	25
0	Neutral	5
-1	Slightly cool	25
-2	Cool	75
-3	Cold	100

Table (6.1): Relationship between PMV, PPD and thermal sensation

ASHRAE Standard 55-81 for thermal comfort gives a psychrometric chart that defines the winter and summer comfort zones. The comfort zone of the 55-81 Standard sets the effective temperature limits of 20 and 23 °C for winter and 23 and 26 °C for summer. Lines of constant dew point temperature bound the upper and lower limits of the comfort zone with 2 °C as the lower limit and 17 °C as the upper limit [143]. These boundaries should be interpreted as fuzzy limits, since small deviations in the borders of a zone do not have a dramatic effect on the comfort felt by the space user [152].

Thermal comfort is expressed in terms of the thermal comfort PMV (predictive mean vote). This thermal sensation ranges between the seven points of the psychophysical scale [from –3 (cold), through 0 (neutral), to +3 (hot)]. Thermal comfort influencing variables are classified in two categories [144]:

(a) Environment-dependent variables, such as air temperature, mean radiant temperature, relative air speed and air humidity. An equivalent representation, with a rather statistical definition, is the predicted percentage of dissatisfied

(PPD). PMV and PPD are related through a one to one correspondence. The comfort zone is defined as the zone in which the PPD is <10% or the zone in which is PMV lies between ± 0.5 units.

(b) Personal-dependent variables, such as activity (metabolism) and thermal resistance of clothing.

6.3. Environmental-dependent variables

A model, which addresses the thermal response of a building space and its heating system, was described in chapter 3 and chapter 4. In principle, three further developments of this model are needed in order to prosecute a full thermal comfort sensation analysis but only two of these were incorporated. The three developments are mean radiant temperature; relative humidity and mean relative air velocity. Only the first two were incorporated in the model developed previously since it was assumed that, for the heated and naturally ventilated case of interest in this work mean relative air velocity would be insignificant in most applications.

6.3.1. Mean radiant temperature

The mean radiant temperature T_{mrt} can be formally defined as follows:

$$T_{mrtb}^4 = \sum_s (F_b T_s^4) \tag{6.1}$$

where T_{mrtb} is the mean radiant temperature of a body in an enclosing space; F_b is the shape or configuration factor between the body and any one surface and T_s is the temperature of that surface. The mean radiant temperature has a significant influence on the body's rate of heat loss and thus its comfort state as defined by the Fanger PMV [156]. Calculation of the mean radiant temperature is complicated by the non-uniform "view" that the body has of the various surfaces making up a room space. Consequently, equation (6.1) was not used to calculate the mean radiant temperature. Thus an approximation has been used in this work, and the mean radiant temperature has been calculated by the following equation based on an area-weighted mean:

$$T_{mrt} = \frac{\sum_{1}^{nc} A_j T_j}{\sum_{1}^{nc} A_j} \tag{6.2}$$

in which nc is the number of enclosing surfaces of the space and A_j, T_j are the area and the temperature of the j^{th} surface respectively.

In practice, most building spaces experience asymmetry in the radiant field at least to some extent. This is particularly evident when the following prevail (either individually or in combination):

- Large spaces.
- Irregularly shaped spaces.
- Where there is a high degree of glazing.
- Where bare heating surfaces form the main method of space heating.

Accounting for these conditions in the assessment of mean radiant temperature (T_{mrt}) is feasible in theory but not easy in a practical situation, in which a single point measurement is generally used to inform control. Part of the problem is concerned with the point of measurement since the occupant sensation of comfort is spatially dependent. In small spaces this is not significant and in a large or more complex spaces it can be dealt with by dividing the space into a number of rectilinear sub-spaces with a point of measurement in each. The present work is confined to a single zone approach for the calculation of the mean radiant temperature (T_{mrt}) but clearly this assumption could be refined when dealing with more complex room space geometries.

6.3.2. Relative humidity

At high temperatures when comfort becomes shortly influenced by perspiration loos from the skin, the relative humidity becomes an important factor. In fact perspiration loss is governed partly by the moisture content or vapour pressure of the air in a space (both of which are functions of relative humidity and dry bulb

temperature). Hence a model of comfort will require a knowledge of the prevailing space relative humidity.

Relative humidity in the space is calculated using standard psychrometric properties of air [157,158]. The uniformity of this parameter within the space is again an issue (see above concerning T_{mrt}) however in most cases the air moisture content (on which the relative humidity is dependent together with prevailing air temperature) will be well mixed unless the space is very large. In any case the relative humidity is less influential on overall comfort sensation than in the case with temperature variables. Again, non-uniformity in relative humidity is not considered in the present work. To calculate the relative humidity of a building space, the internal air enthalpy (H_r) is first calculated from a room air total heat balance as follows:

$$M\dot{H}_r = Q_l + m_o(H_o - H_r) \tag{6.3}$$

The outdoor air enthalpy (H_o) is calculated using the procedure detailed in appendix D. The mass of water vapour in (kg/kg) the internal air is given by:

$$g(T_i) = (H_r - CT_i)/h \tag{6.4}$$

Hence the percentage saturation (to which the relative humidity may be taken as a close approximation) is obtained:

$$\phi_i = 100g(T_i)/g_{ss}(T_i) \tag{6.5}$$

In which $g_{ss}(T_i)$ is obtained in a similar manner as that of $g_{ss}(T_o)$ as given in appendix D.

6.4. Person-dependent variables

These can be defined as the variables associated with the building occupants themselves that have an effect on an individuals comfort.

6.4.1. Activity (metabolic rate)

The metabolic rate is the rate of energy production of the body and is dependent on the activity level of the occupant. As the metabolic rate varies, the environmental conditions in which the occupant feels comfortable will change. With respect to temperature, the higher the activity rate of the person, i.e. metabolic rate, the lower the temperature required for human comfort [156].

The SI unit commonly used for metabolic rate is the met (1 met = 58.2 W/m^2 of body area). Metabolic rates for typical tasks are listed in Table (6.2).

Activity	met	W/m^2
Reclining	0.8	46.6
Seated and quiet	1.0	58.2
Sedentary activity	1.2	69.8
Standing, relaxed	1.2	69.8
Light activity, standing	1.6	93.1
Medium activity, standing	2.0	114.4
High activity (sustained)	3.0	174.6

Table (6.2): Metabolic Rates for typical activity levels [159].

6.4.2. Clothing thermal resistance

Occupants can regulate their thermal comfort by the addition or removal of clothing items. Different types of clothing possess different values of thermal resistance, some examples of which are given in Table (6.3). A commonly used unit for clothing thermal resistance is the Clo (1 Clo = 0.155 m^2K/W).

A detailed methodology for the estimation of thermal insulation of clothing is given in ISO 9920 [160]. For calculation purposes it is assumed that a piece of clothing adds thermal resistance uniformly to the whole body surface. This is not the case but seems to work well in practice [161]. Chair upholstery may contribute as much as 0.2-0.4 Clo to that of an occupant total clothing thermal resistance which is not included in any of the standard methods for estimating clothing thermal insulation [161]. However, in recent years it has become common practice to include a chair's thermal resistance into calculations. An example of the relationship between clothing thermal resistance and comfort temperature is given in [156].

Clothing Ensemble	Clothing Resistance (Clo)
Nude	0
Light Summer Clothing	0.5
Typical business suit	1
Typical business suit and cotton overcoat	1.5
Heavy wool pile ensemble	3 - 4

Table (6.3): Typical thermal resistances of clothing ensembles [156].

6.5. Thermal comfort indices (PMV & PPD)

The thermal comfort indices (PMV and PPD) are calculated as follows [156]:

$$\begin{aligned} PMV = {} & (0.352\exp(-0.42\,Met)+0.032)\times(Met-0.35(43-0.061\,Met-pv) \\ & -0.42(Met-50)-0.0023\,Met(44-pv)-0.0014\,Met(34-T_i) \\ & -3.4\times10^{-8}f_{cl}((T_{cl}-273)^4-(T_{mrt}-273)^4)-f_{cl}h_c(T_{cl}-T_i)) \end{aligned} \quad (6.6)$$

Where T_{cl} is calculated iteratively from the following equation:

$$T_{cl} = 35.7 - 0.032\,Met - 0.18 I_{cl}(3.4\times10^{-8} f_{cl}((T_{cl}-273)^4 - (T_{mrt}-273)^4) + f_{cl}h_c(T_{cl}-T_i) \quad (6.7)$$

$$PPD = 1 - 0.95\exp(-0.003353 PMV^4 - 0.2179 PMV^2) \quad (6.8)$$

6.6. Conventional comfort-based control

In order to identify a reference performance for a comfort-based control strategy, a conventional approach was first developed based on a proportional-plus-integral-plus-derivative (PID) controller, a method commonly used in space heating control [162,163]. The resulting controller and feedback path were added to the system model (including the developments described in section (6.3)) as summarised in Figure (6.1).

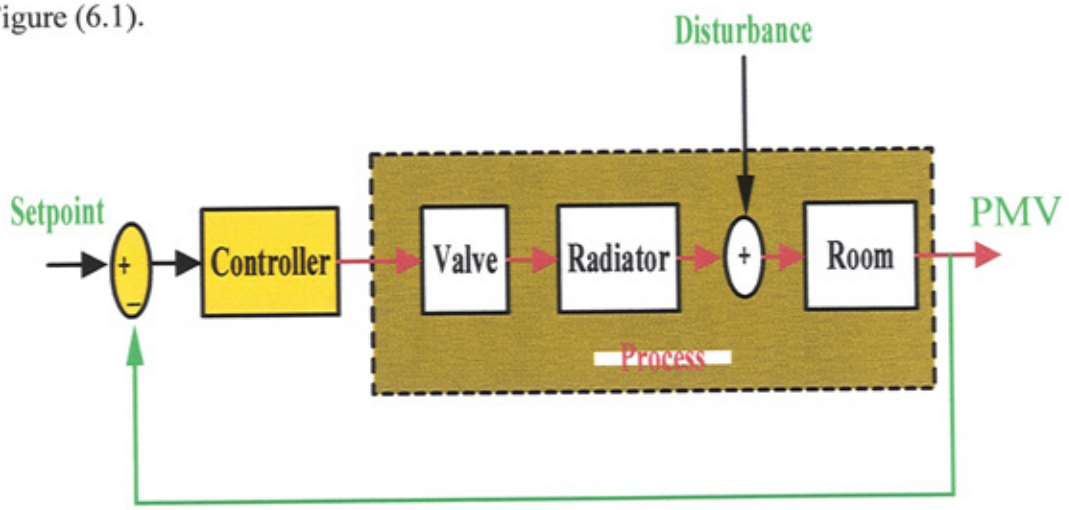

Figure (6.1): Closed Loop System

The controlled variable (PMV) is calculated at each time step from prevailing values of room air temperature, relative humidity and mean radiant temperature with the room air velocity, activity and clothing levels treated as constants. This is compared with a reference value of PMV and the resulting error is applied to the controller. External temperature, solar radiation and casual heat gains act as disturbances, as shown in Figure (6.1). The output of the PID controller is given by:

$$u(t) = k_p e(t) + k_i \int_0^t e(t)dt + k_d \int_0^t de/dt \qquad (6.9)$$

The initial parameters of the controller were based on those actually in use in the building space to which the model was applied (see section 2.3), these values being $0.1K^{-1}$, $0.01K^{-1}s^{-1}$, and $0.5sK^{-1}$ (representing k_p, k_i, k_d respectively). This produced a reasonable response but with overshoot as shown in figure (6.2), leading to sub-optimal thermal comfort and unnecessary use of energy.

A tuning algorithm was adopted to adjust the controller parameters in order to eliminate this overshoot. The MATLAB NON-LINEAR CONTROL DESIGN (NCD) Blockset was used [142] – a gradient-descent based method designed to minimise a cost function (i.e. a weighted maximum constraint violation of the constrained (control) variable) with reference to perturbed values of certain tunable variables (in this case k_p, k_i, k_d). To give initial estimates of the controller parameters, an error mapping method, which described in section (5.4) was used. Using the initial mapped values from within the planes of minimum normalised error to initiate the tuning algorithm, tuned controller parameters of $1.527K^{-1}$, $0.005K^{-1}s^{-1}$, and $0.050sK^{-1}$ were obtained for k_p, k_i, k_d respectively. In this way, the initial mapping resulted in substantial reductions in computational effort needed by the tuning algorithm. The response of the system under tuned PID controller is shown in figure (6.2) showing an improvement over the existing case.

6.7. PMV-based fuzzy logic controller

The PMV-based fuzzy logic controller proposed here evaluates the predicted mean vote (PMV) level and, if this level is out of the comfort range, provides the air temperature set point that should be used by the plant in order to create indoor thermal comfort. The controller uses a linguistic description of the thermal comfort sensation making it easy to apply and generic to a wide range of heating control problems. Overlapping triangular membership functions were used for input (fuzzification) and output (defuzzification) of the fuzzy system.

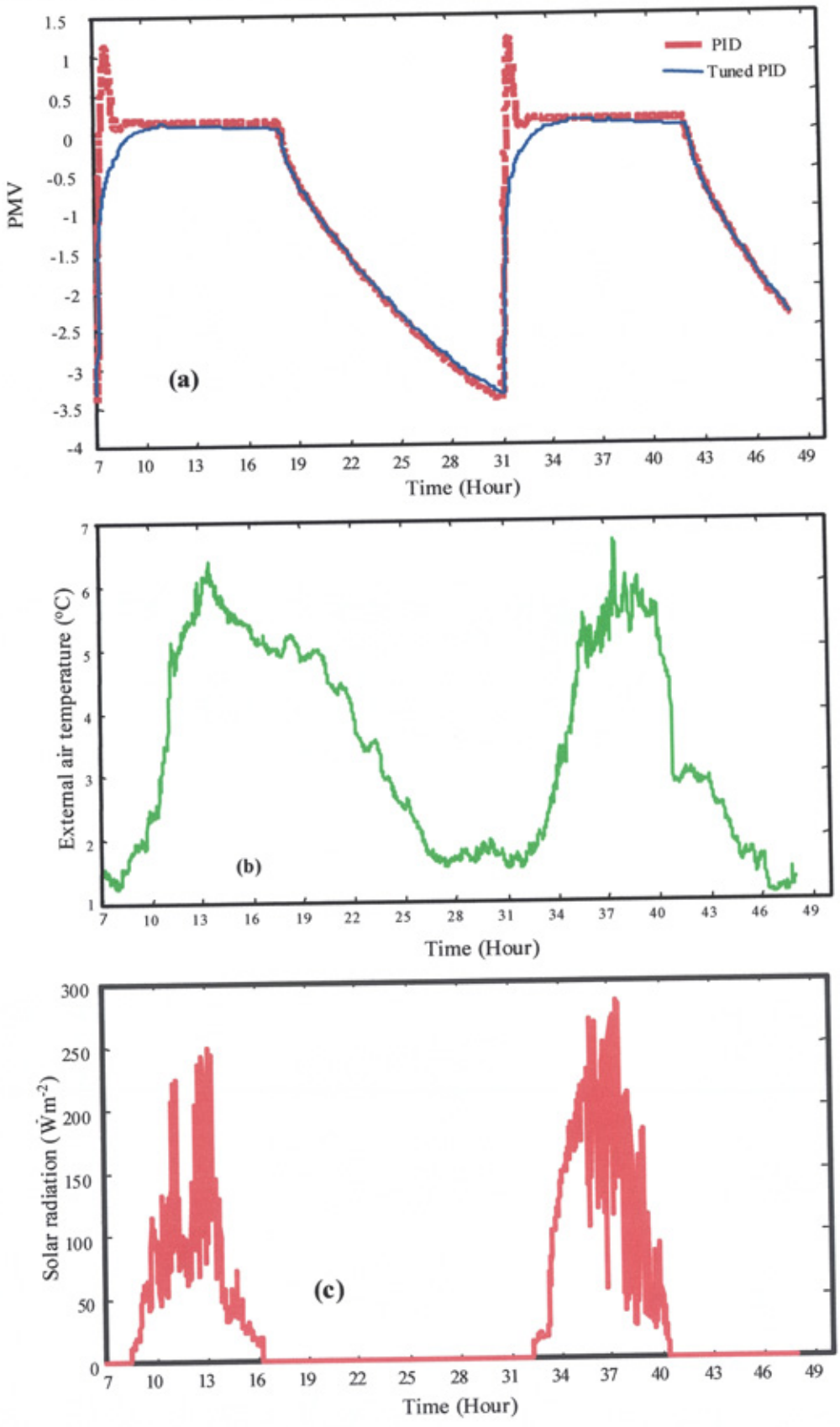

Figure (6.2): Closed Loop Response with PID Control (February)
(a): PMV, (b): External air temperature, (c): Solar radiation

The input membership functions were defined by assigning seven fuzzy input sets to the variables; (*COLD, COOL*, slightly cool (*SCOOL)*, neutral (*NEUT)*, slightly warm (*SWARM)*, *WARM*, and *HOT*), as shown in figure (6.3).

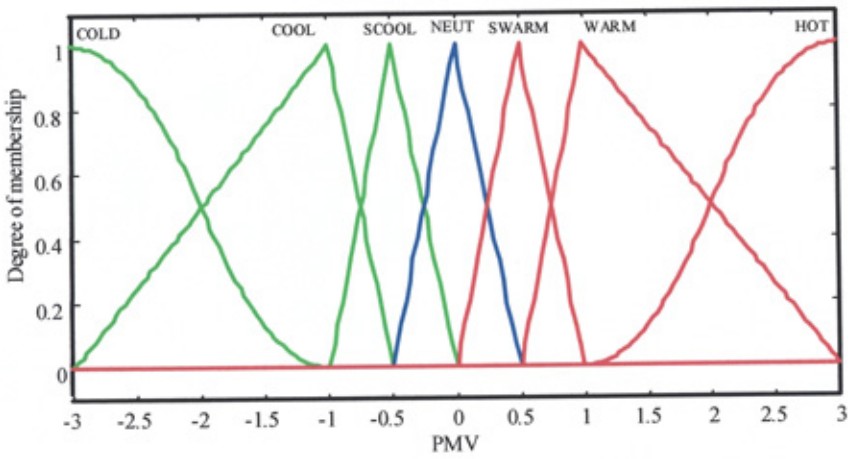

Figure (6.3): Membership functions of the fuzzy controller input

Seven fuzzy sets were ascribed to the output variables; (full closed (FC), closed (CL), slightly closed (SCL), medium (MDL), slightly opened (SOP), open OP, full open (FO)) to form the output membership functions as shown in figure (6.4).

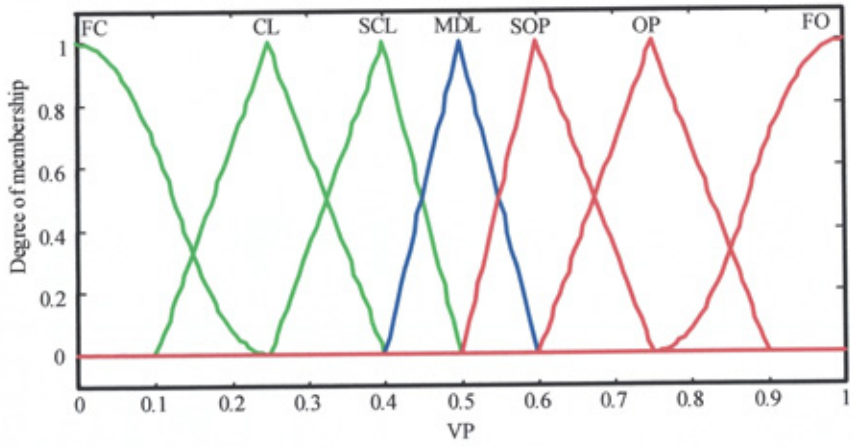

Figure (6.4): Membership functions of the fuzzy controller output

According to the number of the fuzzy sets of the input and the output, seven fuzzy rules were defined as follows:

R1: If PMV is 'COLD' Then Vp is 'FO'

R2: If PMV is 'COOL' Then Vp is 'OP'

R3: If PMV is 'SCOOL' Then Vp is 'SOP'

R4: If PMV is 'NEUT' Then Vp is 'MDL'

R5: If PMV is 'SWARM' Then Vp is 'SCL'

R6: If PMV is 'WARM' Then Vp is 'CL'

R7: If PMV is 'HOT' Then Vp is 'FC'

The relationship between the input and the output of the controller according to these fuzzy rules is shown in figure (6.5). Figure (6.5), shows that when the PMV is in the range of –3 >PMV>-1 (cold area) the valve is open, when PMV is in the range of –1>PMV> +1, the valve in the middle, when the range of PMV is +1>PMV>+3 the valve is closed.

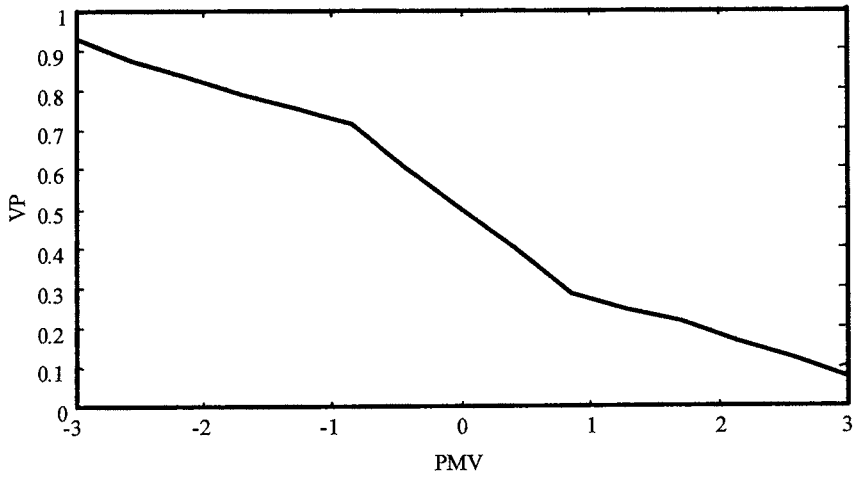

Figure (6.5): Input/output relationship for the fuzzy controller

Using Mamdani's minimum operator method for inference, the control action was a fuzzy set, requiring a defuzzification strategy to obtain a crisp control signal. The COG method was used to convert from fuzzy values to crisp values, forming the actual control signal, which was then be applied to the heating valve.

The overall system (building, heating system, and outdoor climate files) with the PMV based fuzzy logic controller and, for comparison, the PID-based comfort controller is shown in figure (6.6). In which the model of the temperature sensor was included for the data comparison purpose. A switch was added to the model, before the non-linear valve, to select between PID and fuzzy logic control actions. Two different outdoor climate files were prepared and used one in February (winter month, low external air temperature and solar radiation i.e. cloudy sky) and the second in April (spring month, clear sky and significant external air temperature).

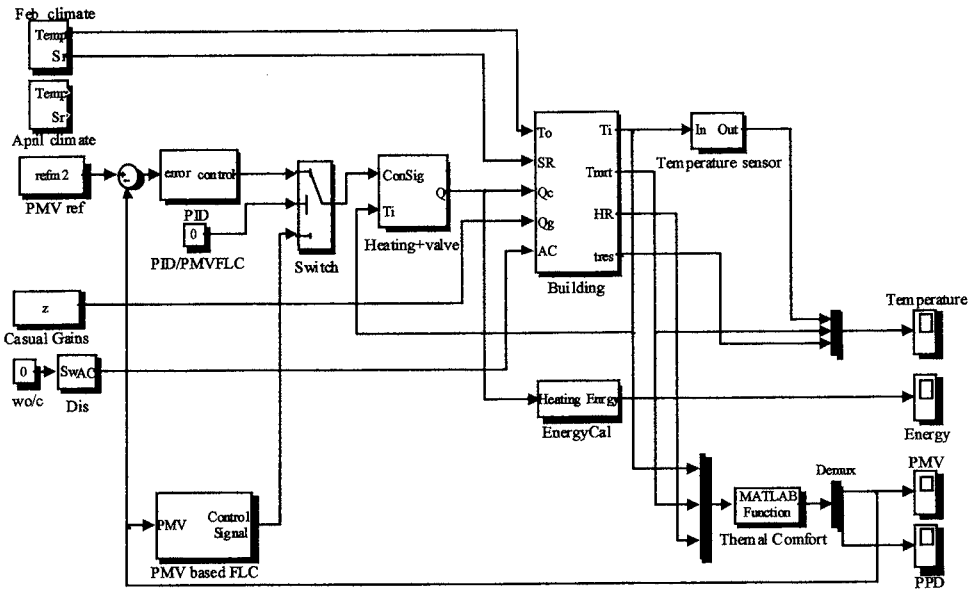

Figure (6.6): Overall model of the building, its heating system, and the controllers

The calculation of the predicted mean vote (PMV) and the predicted percentage of dissatisfied (PPD) was determined using a MATLAB function based on three inputs from the simulation model; the internal air temperature, the mean radiant temperature, and the relative humidity of the internal air. Because the activity and clothing levels are application-dependent, these values were entered as constants (c.f. appendix D).

The resulting PMV based fuzzy logic controller was applied to the building space and its heating system. Figure (6.7), shows the system response under the tuned PID (method described in section (6.6)) and PMV-based FLC. As can be seen, the performance of the PMV based FLC is superior to PID controller in terms of reference point tracking.

In order to test the robustness properties of the two control systems, the building construction data were changed to those representing a very low thermal capacity structure while keeping the overall thermal transmittance of each element the same and the controller specifications unchanged. As described in section (5.5), this would have the effect of making the system more responsive, thus challenging the PID controller originally tuned for a high thermal capacity application. Results, shown in

figure (6.8), reveal that the fuzzy controller maintains excellent tracking of the reference condition whereas the tuned PID controller gives a reasonable response but with significant overshoot. Thus the robustness characteristic of the PMV-based FLC is superior to that of the PID controller. In practice, the PID controller would either have to be tuned for each individual application, or tuned for an expected least-damped case (in which case it would behave sub-optimally in all other applications) whereas the PMV-based FLC would not require this.

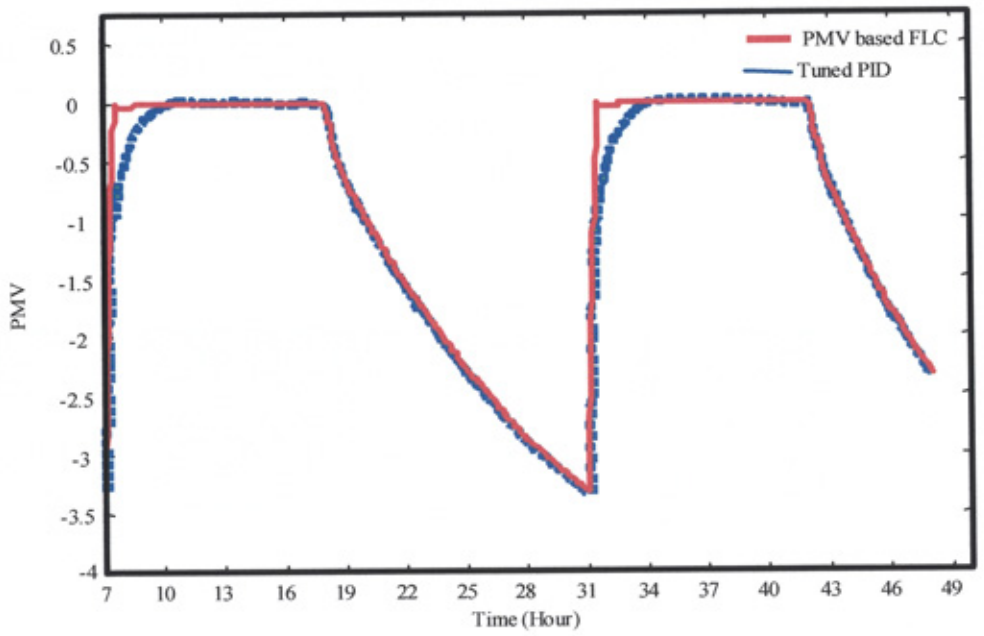

Figure (6.7): Comparison of tuned PID and PMV-based FLC

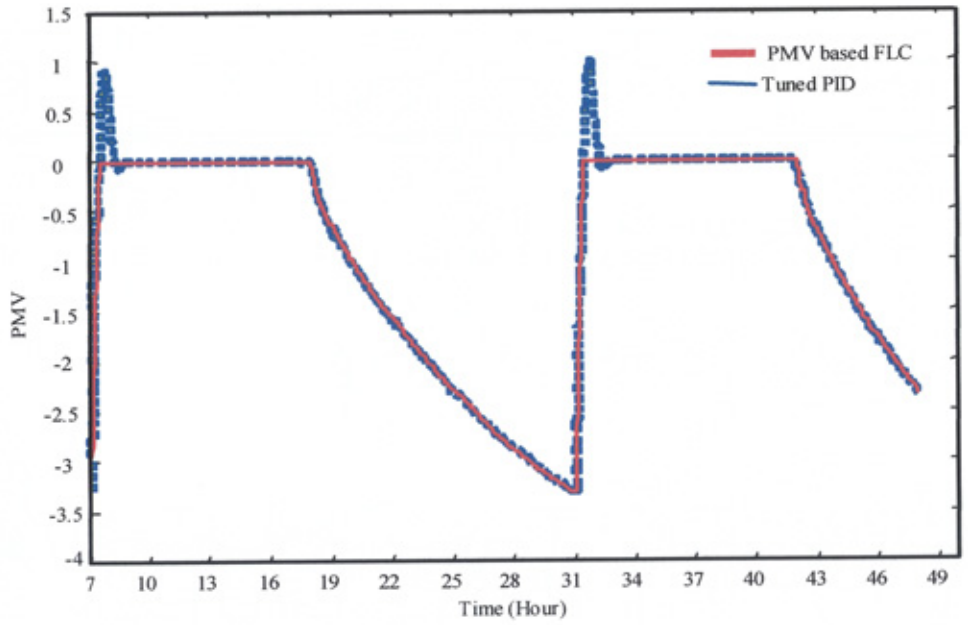

Figure (6.8): Low thermal capacity building with PID control and PMV-based FLC.

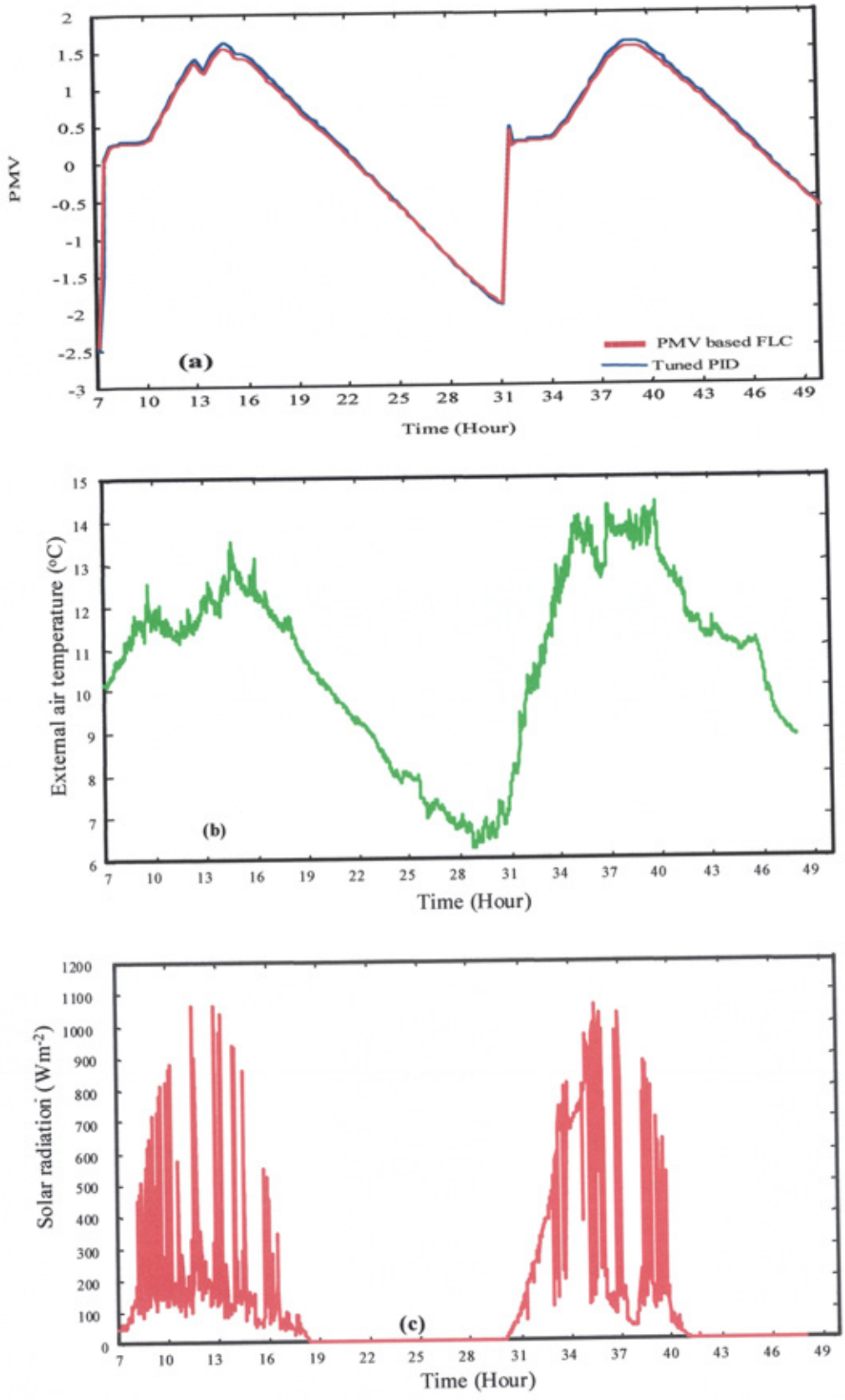

Figure (6.9): Comparison of Tuned PID Control and PMV based FLC (April)
(a): PMV, (b): External air temperature, (c): Solar radiation

In order to test the behaviour of the two control systems when the outdoor climate changes. The outdoor climate data was changed from winter conditions (February) to spring conditions (April) in which the solar radiation and external air temperature were increased. Results, shown in figure (6.9), reveal that both conventional PID and PMV based FLC were not able to adequately compensate for changes in solar radiation inputs.

6.8. Conclusions

In this chapter, a control strategy has been developed for the space heating of a building space in which the comfort sensation as quantified by predicted mean vote forms the control variable. Difficulties associated with the lack of generality inherent in PID control of this problem are identified and an alternative strategy based on a fuzzy logic controller (FLC) is developed. There is a natural appeal in this in that the essentially subjective comfort control problem can be easily mapped onto a universe of discourse of input fuzzy sets and the associated inference which ultimately forms a required control action can be carried out qualitatively. The resulting FLC was compared with a PID controller tuned to give optimal performance for a given case, consisting of a building space with high thermal capacity. A further comparison was then made using the same controller specifications but with a low thermal capacity building space. Results show that the FLC gives better control tracking and robustness than the PID controller for both applications.

This work has addressed the extremes of building space thermal capacity in arriving at these conclusions and further work needs to be done on the applicability of the results to a wider range of construction types, heating system types (and modes) and microclimate conditions.

Whereas it was shown that the thermal comfort based controller worked well, at times of the year when solar gains do not cause overheating, it was clear that some sort of predictive technique would be needed for the spring and autumn heating seasons. It was furthermore decided that in order to simplify the predictive control problem that temperature would be used as a proxy variable for thermal comfort, as real time implementation of the thermal comfort based controller is very difficult to achieve.

Chapter 7

Adaptive Fuzzy Logic Control

Chapter 7

Adaptive Fuzzy Logic Control

7.1. Introduction

A case for the further development of the static comfort based fuzzy logic control was made in chapter 6. Specifically, there is a need for the controller to adapt the adventitious heat gains received by space under control. Instantaneous heat gains (i.e. those arising from internal casual sources) can easily be dealt with by direct feedback but the lagging source due to solar radiation is much less responsive and requires the controller to take on an adaptive role. An adaptive controller form is addressed in this chapter, but first, a brief review of the literature related to adaptive fuzzy logic control of HVAC plant is considered.

Neural networks have been applied in different engineering cases in the fields of the control systems, classification and in modelling complex process transformations [164,165]. Reviews of a number of applications of ANNs in energy systems are presented in [166]. Artificial neural networks (ANNs) have also been investigated for system identification of building specific parameters such as U-values and thermal capacitance [167]. In an investigation by [168], a neural network was trained to determine Z-transfer function coefficients of a building envelope from experimental data. ANNs were used for the estimation of building heating loads using a minimum of input data [169]. ANNs were also used to predict energy use in commercial buildings [38].

The using of a fuzzy controller to create an adaptive controller for use with a home heating system is described by [41]. The controller ensures optimal adaptation to customer heating demands while using one sensor less than a conventional control system.

SO et al. [44] applied FLC to the control of air handling plant VAV systems. Using error and error rate, FLC signals are generated for the air handling plant fresh air damped, fan control, cooling coil, humidifier and reheat coil. In later work, they developed a self-learning FLC using artificial neural networks (ANN) based on the same air handling control problem as their earlier work [45]. The ANN is used to monitor the plant and update the parameters of the FLC, which permits robustness in spite of changes in operating conditions and nonlinearities.

Egilegor et. al. [46] described the results of simulations using a neuro fuzzy controller to adjust the airflow rate through fan coils for three zones of a dwelling to improve thermal comfort. The input variables of zone temperature and humidity are used to calculate the value of Fanger's PMV thermal comfort index, which is then used as a comfort variable. Fuzzy proportional derivative control is used to provide the desired zone conditions while a neural network is trained to tune the fuzzy controller to optimise the fuzzy tuning parameters and improve the control performance for different situations. The simulations carried out for the neuro fuzzy controller, indicate an improvement in the PMV compared to the benchmark simulations using thermostatic control.

7.2. Artificial neural networks, Over-fitting and Generalisation

Artificial neural networks have been adopted in this chapter for modelling the thermal behaviour of the building and its heating system to predict the internal air temperature due to the fact that these are widely accepted as a new technology offering an alternative way to tackle complex mapping problems. They are able to learn from examples, are fault tolerant, can handle noisy and incomplete data, can deal with non-linear problems, and once they are trained can perform prediction and generalisation at high speed [170].

Artificial neural networks (ANNs) or simply Neural Networks (NNs) have been devised as an attempt electronically to model the networks of biological neurons of the human brains. NNs have a large number of highly interconnected processing elements, representing biological neurons, called artificial neurons or simply neurons that operate in parallel and are configured in regular architectures. The collective behaviour of the NN demonstrates the ability to learn, recall and generalise from training data in analogy to human brain [170].

Learning, the fundamental trait of intelligence, is the most important entity in specifying an ANN. A learning algorithm refers to the procedure in which learning rules are used for adjusting the weights and biases of the considered neural network.

One major problem that occurs during neural network training is called overfitting [170]. The error on the training set is driven to a small value, but when new data is presented to the network the error is large. The network has memorised the training examples, but it has not learned to generalised to new situations.

There are many methods for improving the generalisation and overcome the problem of overfitting, one of them is the early stopping method. In this method, the available data were divided into three subsets. The first subset was the training set, used for computing the gradient and updating the network weights and biases. The second subset was used as the validation set. The error on the validation set was monitored during the training process. The validation error will normally decrease during the initial phase of training, as does the training set error. However, when the

network begins to overfit the data, the error on the validation set will typically begin to rise. When the validation error increased for a specified number of iterations, the training was stopped, and the weights and biases at the minimum of the validation error returned.

The test set error generated by the third subset was not used during the training, but was used to compare different models. It was also useful to plot the test set error during the training process. If the error in the test set reached a minimum at a significantly different iteration number than the validation set error, this was taken to indicate a poor division of the data set.

7.3. Singular value decomposition (SVD)

Singular value decomposition (SVD) represents a numerical technique for the analysis of multivariate data [171,172]. SVD can be used as a preliminary stage in most types of multivariate analysis, and can greatly increase the computational efficiency of linear techniques such as key vector analysis, and non-linear techniques such as cluster analysis and neural network analysis. SVD is also an extremely effective technique for the reduction of white noise.

A summary of the principles of SVD follows:

Let the matrix $\mathbf{O}$ (of size $m \times n$, which contains both the current values and the past history) be an observation matrix. The SVD method decomposes this $\mathbf{O}$ matrix into three matrices $\mathbf{W}$, $\mathbf{L}$, and $\mathbf{V}$. The SVD of $\mathbf{O}$ is defined as:

$$\mathbf{O} = \mathbf{WLV} \tag{7.3}$$

where $\mathbf{W}$ and $\mathbf{V}$ are pseudo-unitary containing the first n column eigenvectors of $\mathbf{O}^{\mathrm{T}}\mathbf{O}$ and row eigenvectors $\mathbf{O}\mathbf{O}^{\mathrm{T}}$ respectively. The $\mathbf{L}$ matrix contains the corresponding eigenvalues, in decreasing order of significance, on the leading diagonal. In many cases it is useful to partition the matrices as follows:

$$\mathbf{O} = (\mathbf{W}_1 \mathbf{W}_2) \begin{pmatrix} \mathbf{L}_1 & \mathbf{0} \\ \mathbf{0} & \mathbf{L}_2 \end{pmatrix} \begin{pmatrix} \mathbf{V}_1 \\ \mathbf{V}_2 \end{pmatrix} \tag{7.4}$$

where $\mathbf{W}_1$ contains the first k columns of $\mathbf{W}$, $\mathbf{L}_1$, the first k rows and columns of $\mathbf{L}$ and $\mathbf{V}_1$ the first k rows of $\mathbf{V}$. The $\mathbf{O}$ matrix can then be decomposed into two terms:

$$\mathbf{O} = \mathbf{O}_s + \mathbf{O}_N = \mathbf{W}_1 \begin{pmatrix} \mathbf{L}_1 \\ \mathbf{0} \end{pmatrix} \mathbf{V}_1 + \mathbf{W}_2 \begin{pmatrix} \mathbf{0} \\ \mathbf{L}_2 \end{pmatrix} \mathbf{V}_2 \tag{7.5}$$

where the subscript "S" denotes signal space and "N" noise space. As the value of k increases $\mathbf{O}_s$ becomes a closer approximation to $\mathbf{O}$ and the values in $\mathbf{O}_N$ become smaller. The closeness of the approximation is given by $\mathbf{I}(k)$ defined by the following equation:

$$\mathbf{I}(k) = \frac{\sum_{i=1}^{i=k} \mathbf{L}_{i,i}}{\sum_{i=1}^{i=n} \mathbf{L}_{i,i}} \tag{7.6}$$

The value of $\mathbf{I}(k)$ will increase monotonically to one. If significant correlation is present in the data (the rows and or columns of the $\mathbf{O}$ matrix) the series will rapidly approach the value one. It is this property that is used for dimensional reduction.

7.4. An artificial neural network predictor for indoor temperature

An artificial neural network has been used to model the thermal behaviour of the building and its heating system in open loop mode. The model predicts future internal air temperature as a function of past and present external air temperature, solar irradiance, heating valve position and internal air temperature. These variables were chosen to avoid too much information increasing the network training and preventing the network from learning adequately. Both the input and output data were sampled at 15 minute intervals.

Inputs to neural networks need to be scaled to the range of the non-linear activation function used (such as amplitude one). The scaling, or representation, of data can also

affect the learning speed of a network; a good choice of scaling or data manipulation can dramatically improve learning speed. This could include providing additional information in the form of products of features [173].

Meteorological data was used for T_o and SR but the valve position, V_p, was cycled through a predetermined sequence. As building plant is designed for "worst case" conditions, in normal circumstances this will produce significant overheating in open loop mode. Because of the need to supply historic data, not only the current values $inputs(k)$ were used but also, $inputs(k-1)$, $inputs(k-2)$, ..., $inputs(k-i)$. The value of i was increased by trial and error and it was found that a minimum value of $i=48$ was needed to successfully capture the building dynamics. This effectively provided 12 hours of historic data to the network, but led the unwelcome effect of increasing the number of effective inputs to 196.

These inputs were presented as an observation matrix $\mathbf{O}$ (of size $m \times n$, which contained both the current values and the past history over twelve hours, with a 15 minute sampling time) for each of the 4 variables in each row. Thus there were 48 values associated with each parameter, hence $n=196$. The SVD was calculated using weekly blocks hence $m = 4 \times 24 \times 7 = 672$.

The SVD technique as described before was used to decrease these inputs to 10, as this value was sufficient to keep nearly all the important information in the data. It is found in this application with k=10, $\mathbf{I}(k)$>0.95 as illustrated in figure (7.1). This indicates that more than 95% of the observation signal is contained within the first 10 dimensions. To simplify the neural network structure, information contained in the dimensions higher than 10 has justifiably been ignored.

Various network architectures were investigated, and a number of different network sizes and learning parameters have been tested. The architecture that was ultimately selected is shown in figure (7.2). It is a conventional feed forward multiple layer perceptron type and consists of three layers; an input layer with 10 neurons, 7 neurons in hidden layer, and one neuron for the output layer.

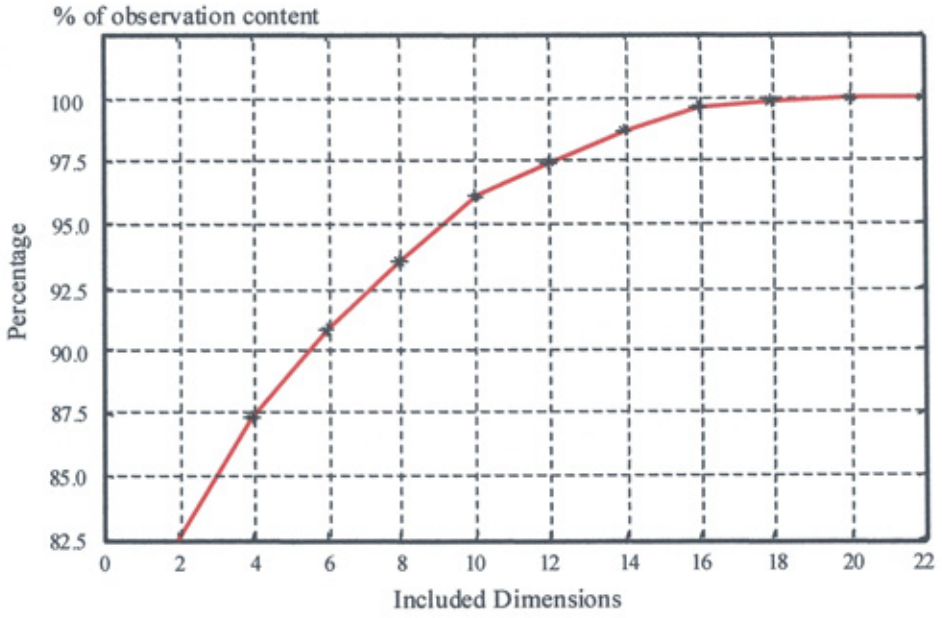

Figure (7.1): Observation information content as a function of included dimension

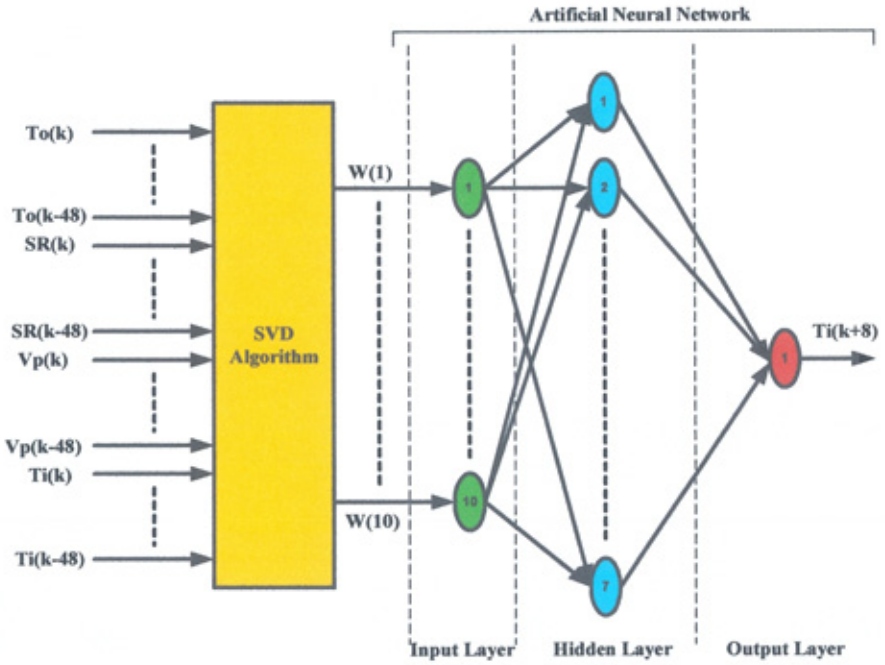

Figure (7.2): Multilayer feed forward neural network with SVD algorithm

In this case the number of hidden neurons was estimated by running the network with different number of hidden neurons and calculating the mean square error using the training, validation and testing data set. Based on this, the number of hidden neurons arrived at was seven as shown in figure (7.3).

The proposed ANN was trained by back-propagation based on the Levenberg-Marquardt (BPLM) algorithm [170]. The activation function used with the input and output neurons was linear, whereas in the hidden neurons a Sigmoid form was used.

The network was trained every weekend, using a data set consisting of the two previous weeks of observation data during a four-month period during the heating season (January-April) to take different heating seasons and different solar angle positions. The training set was the second week of data and the validation set was the data from the first week. These two weeks of data were changed every weekend as shown in figure (7.4). This methodology was chosen in order to capture the slowly varying solar position and consequent solar irradiance profile and any long term seasonal weather effects.

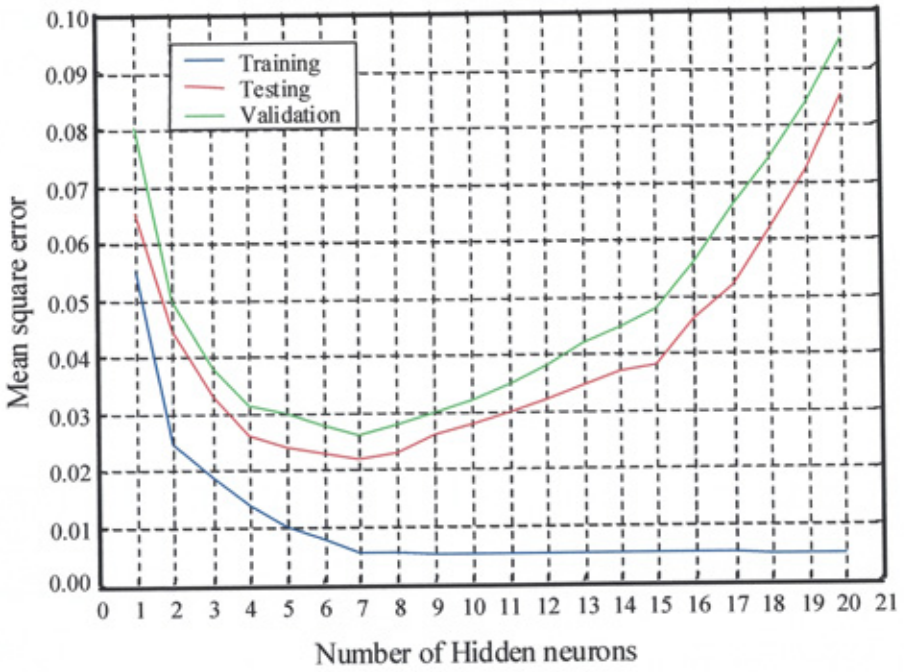

Figure (7.3): Network mean square error

Week1	Week2	Week3	Week4	Week5	.....
Validation	Training	Test	_____	_____	_____
_____	Validation	Training	Test	_____	_____
_____	_____	Validation	Training	Test	.....

Figure (7.4): Training sequences

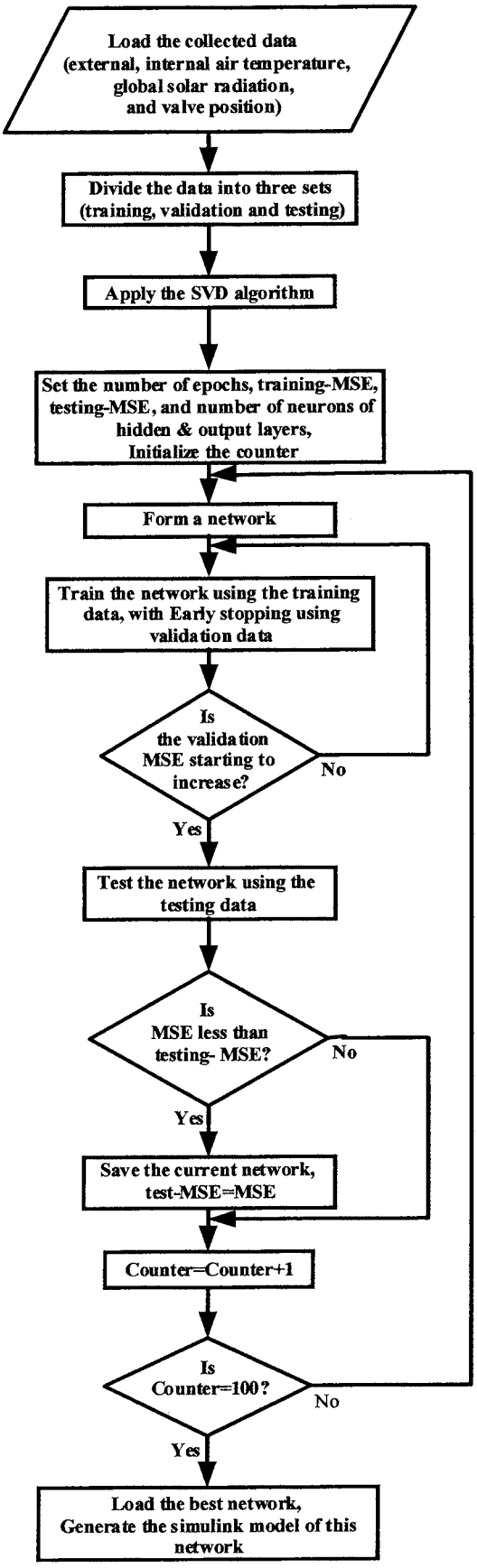

Figure (7.5): Flowchart of the neural network predictor with SVD algorithm

The network was trained using 100 different random starting values for the weights and biases and the one with the lowest mean square error was chosen. This minimised the likelihood of being trapped at a local minimum. The early stopping method was used to overcome the problem of over-fitting and the MATLAB NEURAL NETWORKS TOOLBOX package was used for training, validation and testing [142]. Once a satisfactory degree of input-output mapping was reached, the network training was frozen and a set of test data was applied for verification. The network training procedure is illustrated in figure (7.5). Finally, the trained network was used to predict the indoor temperature of the solar building up to two hours ahead (i.e. 8 time steps ahead).

Excellent agreements were obtained when using this network to predict the internal air temperature of a low thermal capacity building up to one-hour ahead, during a four month period during the heating season (January-April). The results were in excellent agreement during totally clear and overcast days. On days of intermediate solar irradiance, the results were less good due to the stochastic nature of cloud cover and the consequent effect on solar irradiation. Figure (7.6a) and figure (7.7a) show the behaviour over a typical week (week 7) in this period for 30 minute and one hour ahead respectively. A stacked histogram of error during the complete heating season is shown in figure (7.6b) and figure (7.7b) period for 30 minute and one hour ahead respectively (the first week being colour coded in darkest blue and the last week colour coded in darkest red). Most of the error is located in the range ±0.2K – within what might be regarded as a typical measurement uncertainty for practical commercial temperature sensors used in this application.

Results for a 90 minute and a two-hour time horizon (6,8 steps prediction) are also reasonable as shown in figure (7.8a) and figure (7.9a) over the same week but at greater time horizons the error increased significantly. A significant contributor to this error is the stochastic nature of cloud cover during the winter months in northern England with a subsequent stochastic element to the solar irradiance input. Figures (7.8b, and 7.9b) show a stacked histogram of the error during complete heating season (14 weeks) with the start of the heating season (the first week being colour coded in darkest blue and the last week colour coded in darkest red).

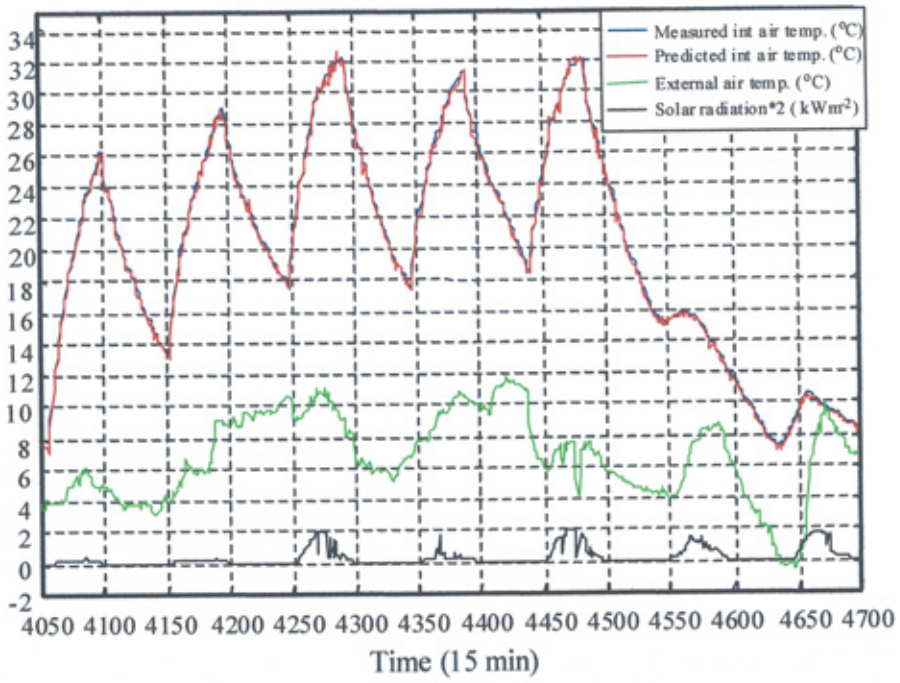

(a)

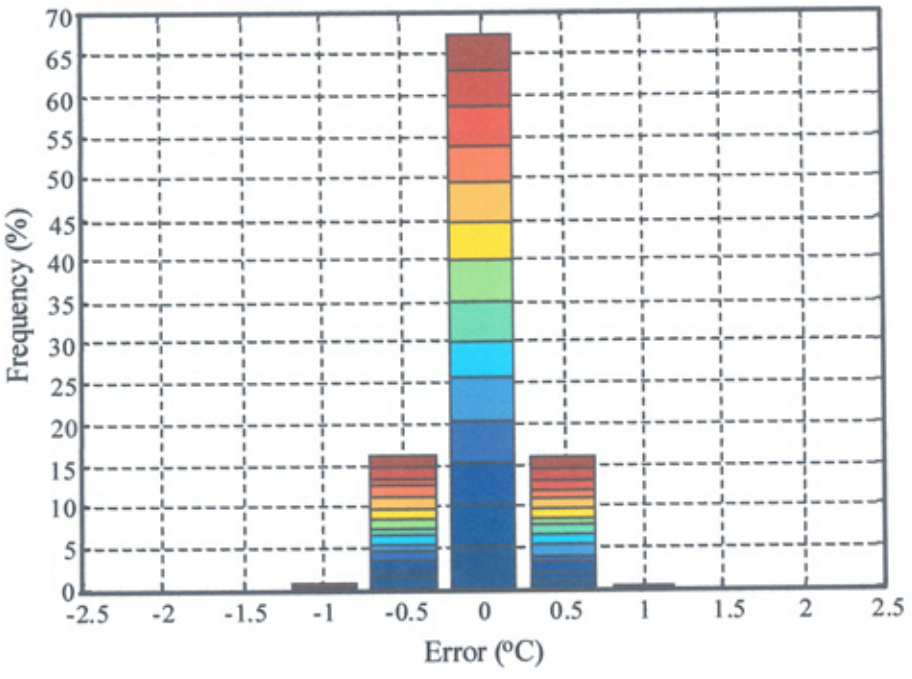

(b)

Figure (7.6): (a) Predicted internal air temperature (30 min. ahead).
(b) Error distribution (30 min. ahead)

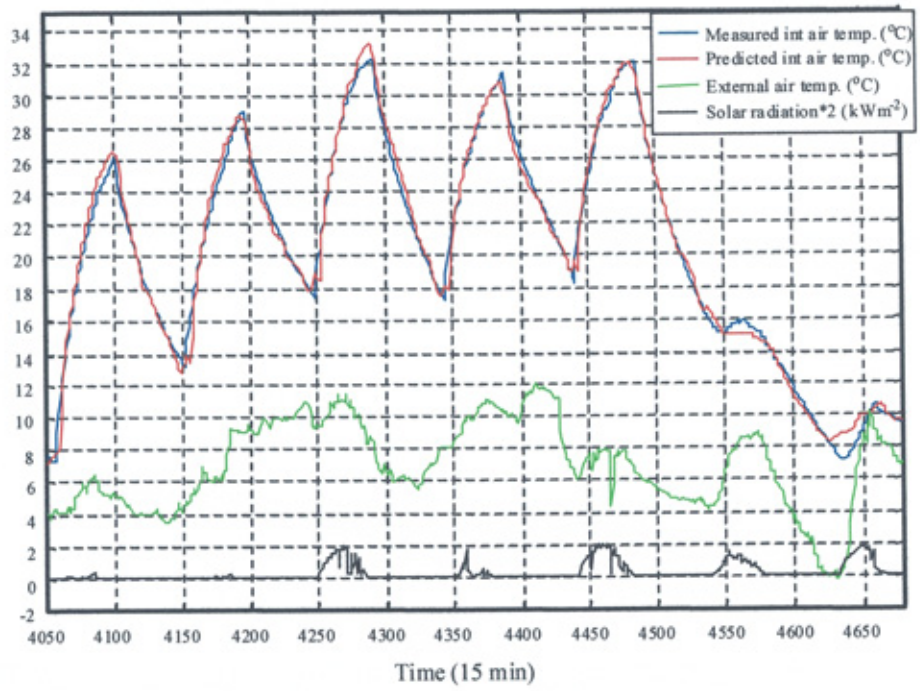

(a)

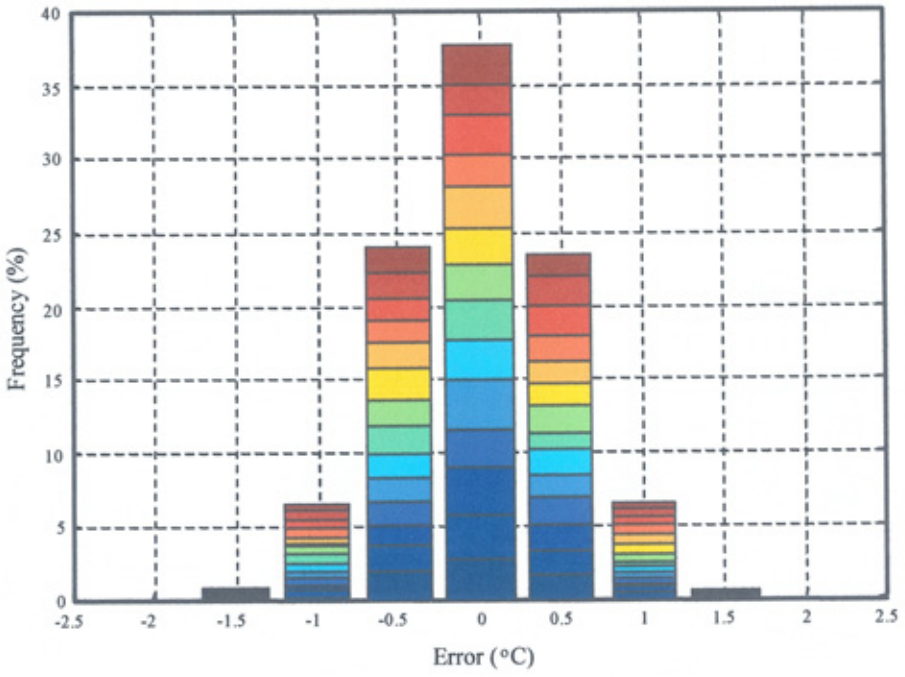

(b)

Figure (7.7): (a) Predicted internal air temperature. (60 min. ahead)
(b) Error distribution (60 min. ahead)

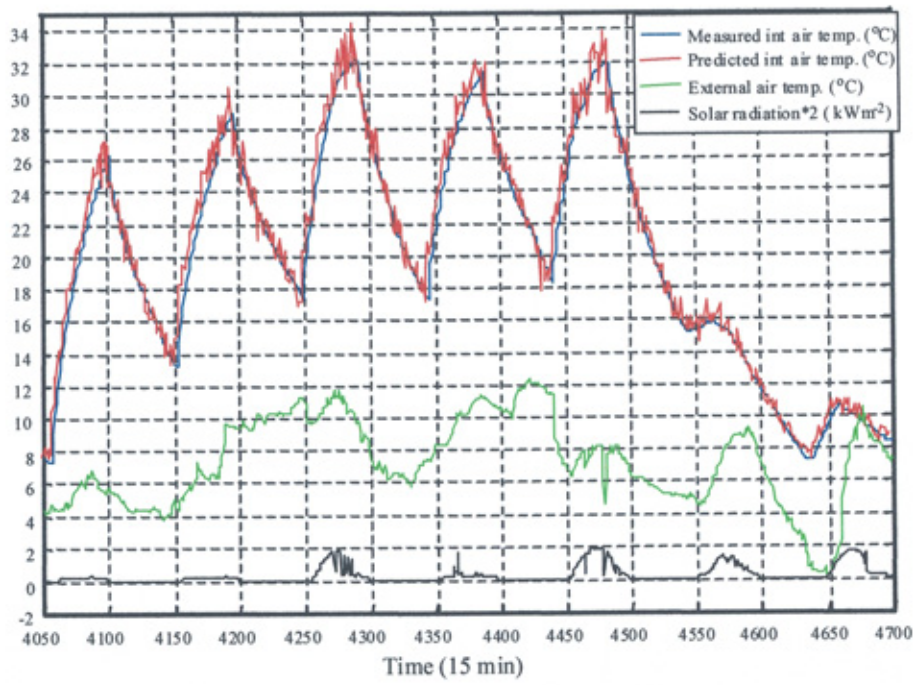

(a)

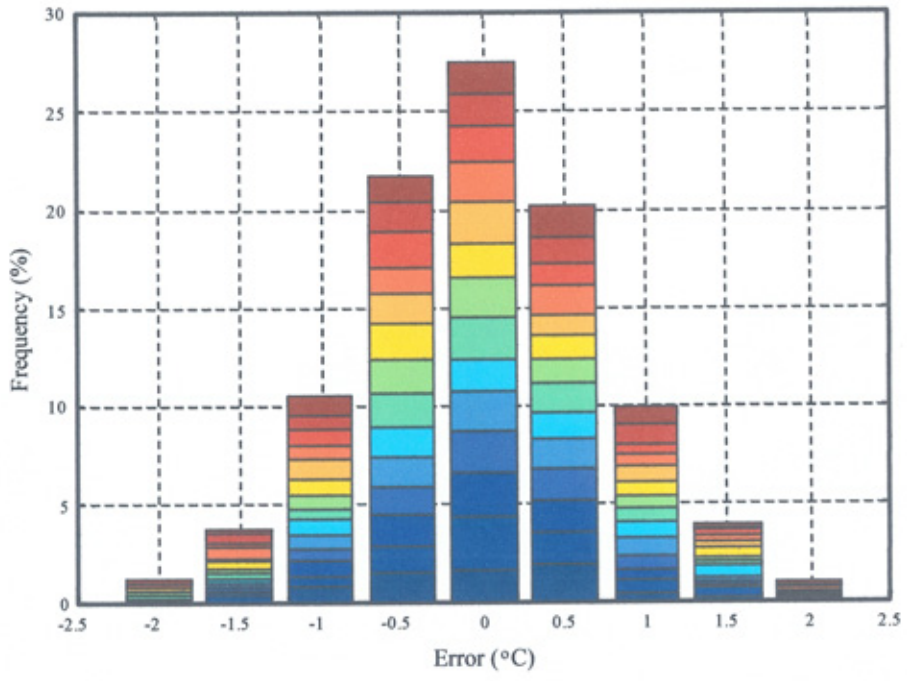

(b)

Figure (7.8): (a) Predicted internal air temperature (90 min. ahead)
(b) Error distribution (90 min. ahead)

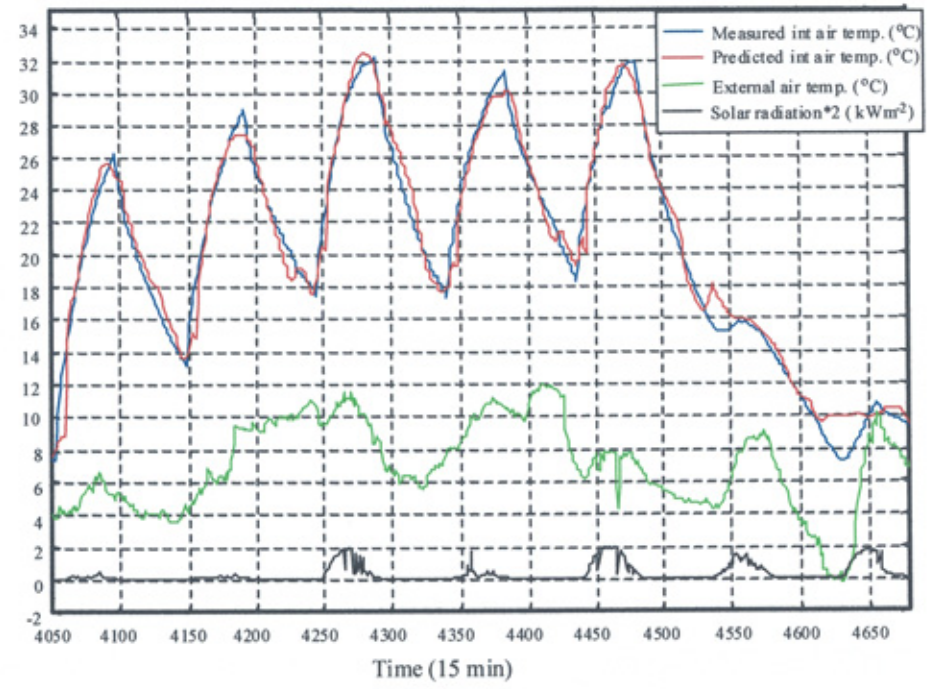

(a)

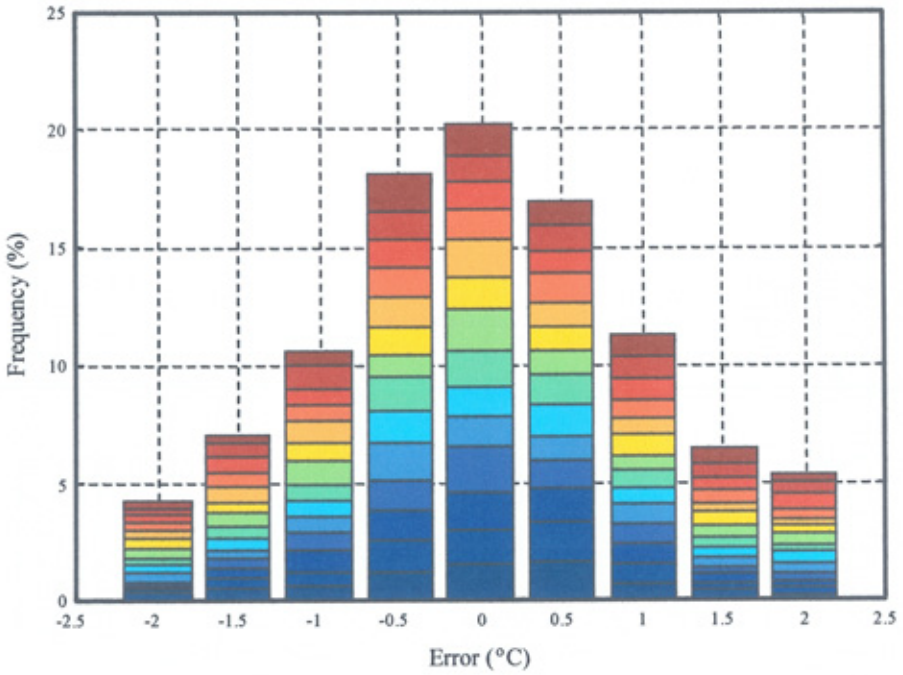

(b)

Figure (7.9): (a) Predicted internal air temperature. (120 min. ahead)
(b) Error distribution (120 min. ahead)

7.5. Proposed quasi-adaptive fuzzy logic controller

A quasi-adaptive fuzzy logic controller is considered in this section. The controller is divided into two main modules; the fuzzy controller and feedforward neural network with SVD algorithm as shown in figure (7.10). The inputs needed for this controller are the setpoint temperature expressed by the user, and the current and past values of external air temperature, solar radiation and the internal air temperature.

Using this neural network model of the building space, the heating controller was able to reduce the heating energy consumption while maintaining acceptable internal temperature tracking by anticipating solar and other heat gains to the space. The error between the internal air temperature and the setpoint temperature was applied as a first input of the fuzzy controller to instantaneously adjust the internal air temperature to the setpoint value. The second input to the fuzzy controller was the predicted future internal air temperature and this enabled the controller to adjust to lagging influences of heat gain sources.

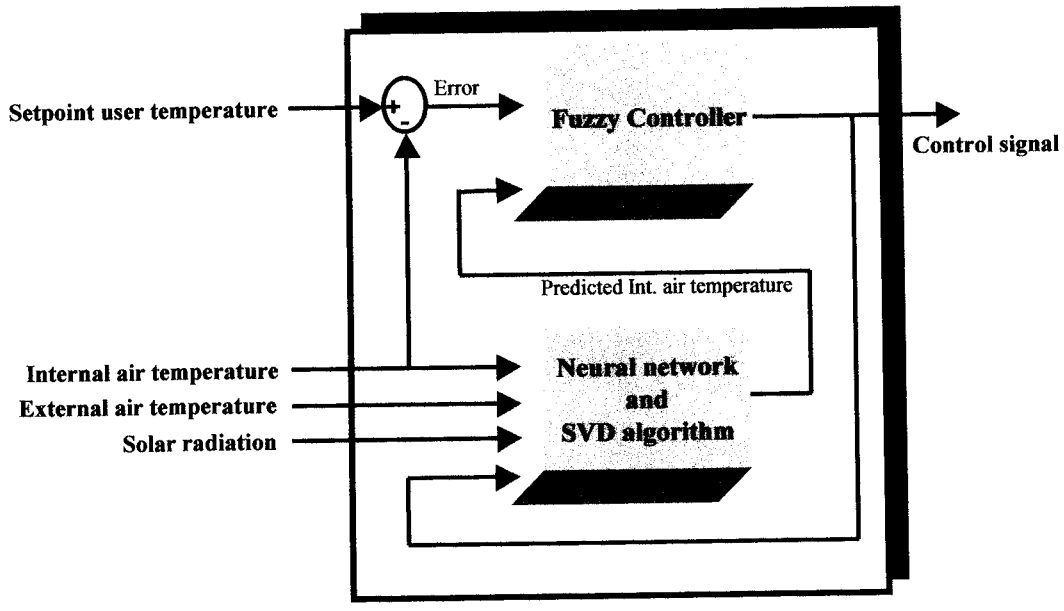

Figure (7.10): A quasi-adaptive fuzzy logic controller

Because the MATLAB NEURAL NETWORK TOOLBOX uses different initial values for the weights and biases each time the network trained, a "best" neural network structure which gives the minimum mean square error using the testing data was chosen from 100 structures with different initial values of weights and biases of the neurons.

Adjustments were needed to the fuzzy control rules, membership functions, and the defuzzification strategy developed earlier. In this application, a fuzzy set was defined by assigning its membership function to five fuzzy sets for both input variables and then seven fuzzy sets for both input variables were chosen.

In the case of five nonlinear membership functions, the controller gave reasonable results but an improvement was obtained when seven membership functions were used. The fuzzy sets of the error were defined as NB *(negative big)*, NM *(negative medium)*, NS *(negative small)*, ZE *(zero)*, PS *(positive small)*, PM *(positive medium)*, and PB *(positive big)*, as shown in figure (7.11a).

The fuzzy sets of the predicted temperature were defined as LW *(low)*, ML *(medium low)*, SL *(slightly low)*, MD *(medium)*, SH *(slightly high)*, MH *(medium high)*, and HG *(high)*, as shown in figure (7.11b).

Overlapping triangular membership functions were used for input (fuzzification) and output (defuzzification) of the fuzzy system. Seven fuzzy sets for the output variable were defined as NB *(negative big)*, NM *(negative medium)*, NS *(negative small)*, ZE *(zero)*, PS *(positive small)*, PM *(positive medium)*, and PB *(positive big)*, as shown in figure (7.11c).

Thus according to the number of the fuzzy sets of the inputs and the output, there are 49 fuzzy rules. There are two selected fuzzy sets each for error and predicted internal air temperature. Therefore, four rules were applied, represented by the interaction of two rows and two columns in Table (7.1).

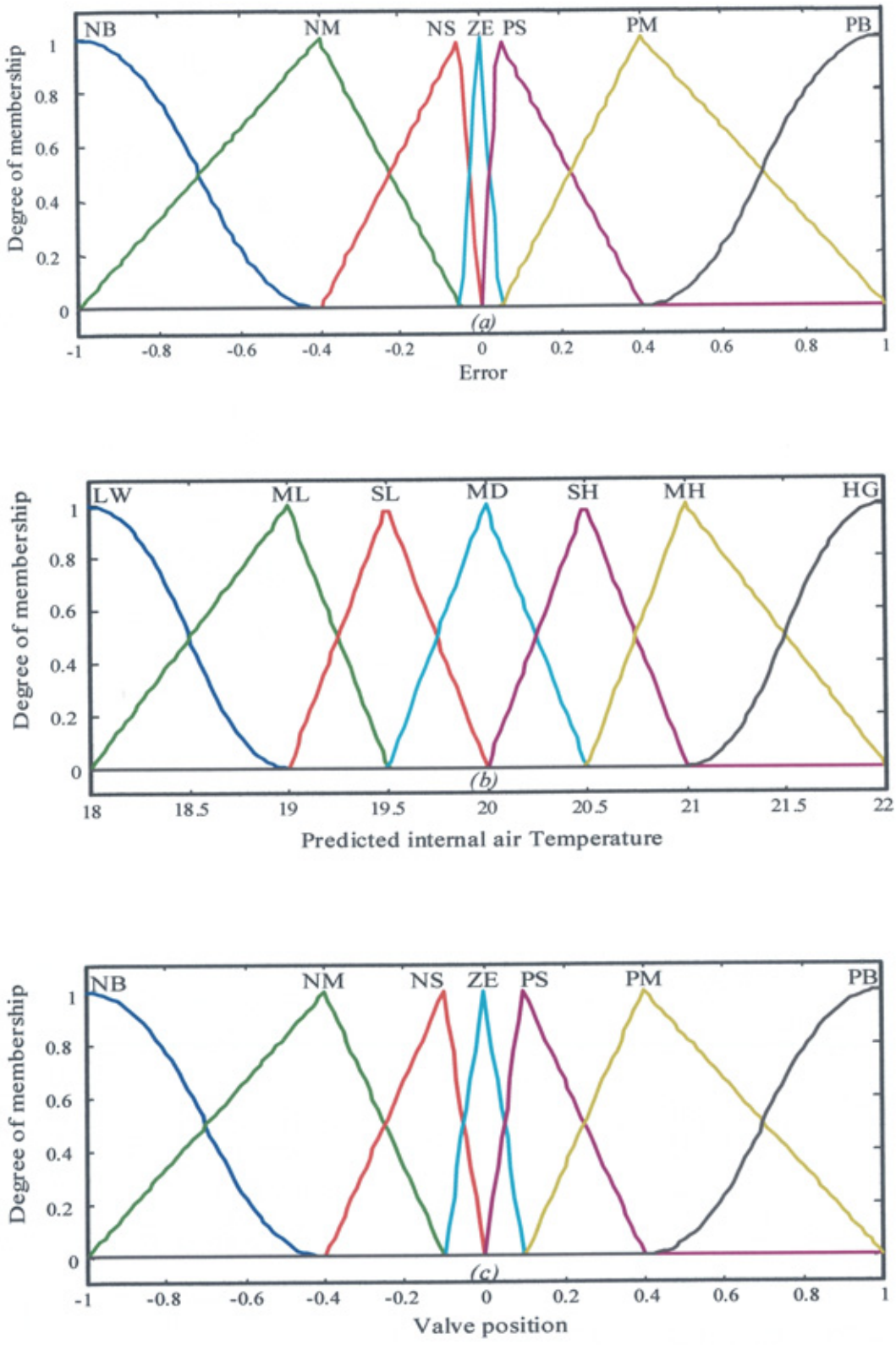

Figure (7.11): *(a)* Membership functions of the error, *(b)* Membership functions of the predicted internal air temperature, *(c)* Membership functions of the control signal

Error	Predicted internal air temperature						
	LW	ML	SL	MD	SH	MH	HG
NB	NB	NB	NB	NB	NB	NB	NB
NM	NB	NB	NB	NB	NB	NB	NB
NS	ZE	NM	NM	NM	NB	NB	NB
ZE	PS	ZE	NM	NM	NM	NB	NB
PS	PM	PS	ZE	NM	NM	NM	NM
PM	PM	PM	PS	ZE	NS	NS	NS
PB	PB	PB	PB	PM	PS	PS	PS

Table (7.1): Applied fuzzy control rules

The relation between the inputs and the output of the controller according to the fuzzy rules is shown in figure (7.12).

Mamdani's minimum operator method was operated for inference, resulting in a control action as a fuzzy set. This was defuzzified to a crisp control signal using the method of center of gravity *(COG)*.

The overall system (building space, hot-water heating system, temperature sensor and outdoor climate files which contain the external air temperature and solar radiation data) with the quasi-adaptive fuzzy logic controller is shown in figure (7.13).

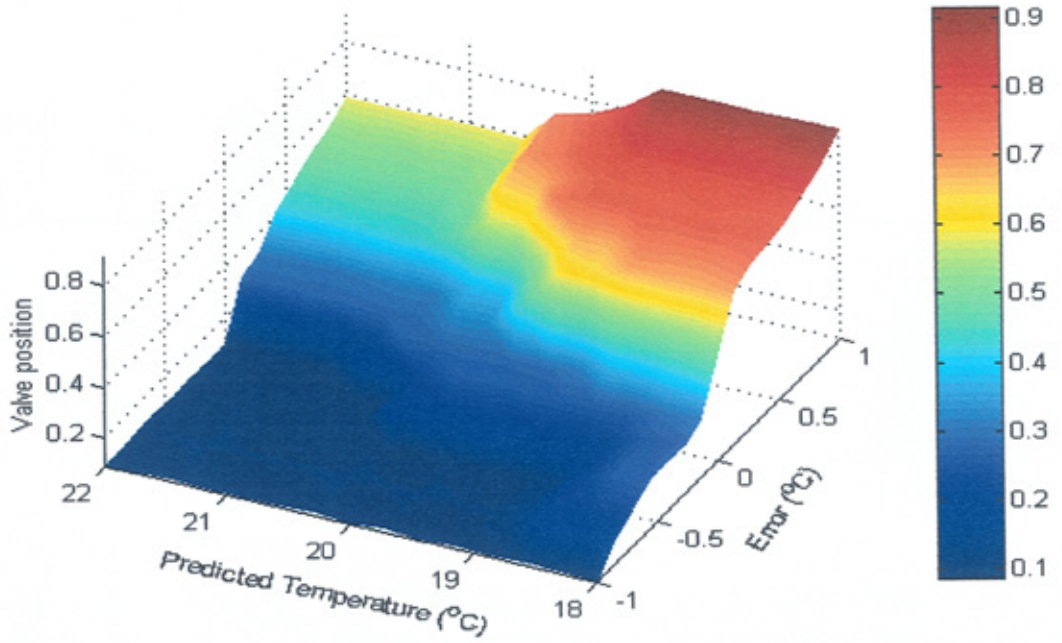

Figure (7.12): Fuzzy controller output surface

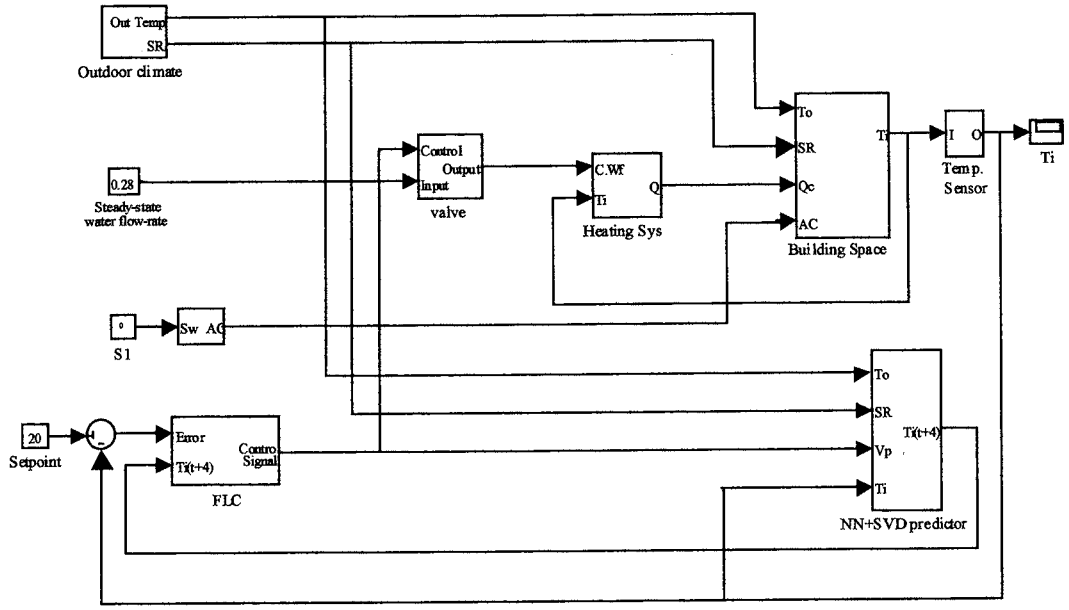

Figure (7.13): The overall system including the quasi-adaptive fuzzy logic controller

7.6. Results

The resulting quasi-adaptive fuzzy logic control (QAFLC) was applied to the building space described in section (3.5) and its heating system described in section (4.3).

Figure (7.14), shows internal air temperature of the building using, conventional PID control (described in section (5.4)) and the proposed controller. As can be seen, the performance of the tuned PID controller is unable to accommodate the lagging heat gain influence of solar radiation (especially evident on day 1, day2). However the quasi-adaptive fuzzy logic controller achieves excellent heating, stability and eliminates solar overheating influences.

7.7. Conclusion

In this chapter, a quasi-adaptive fuzzy logic controller was developed to overcome the problem of the overheating due to the lagging influence of solar heat gain in a space.

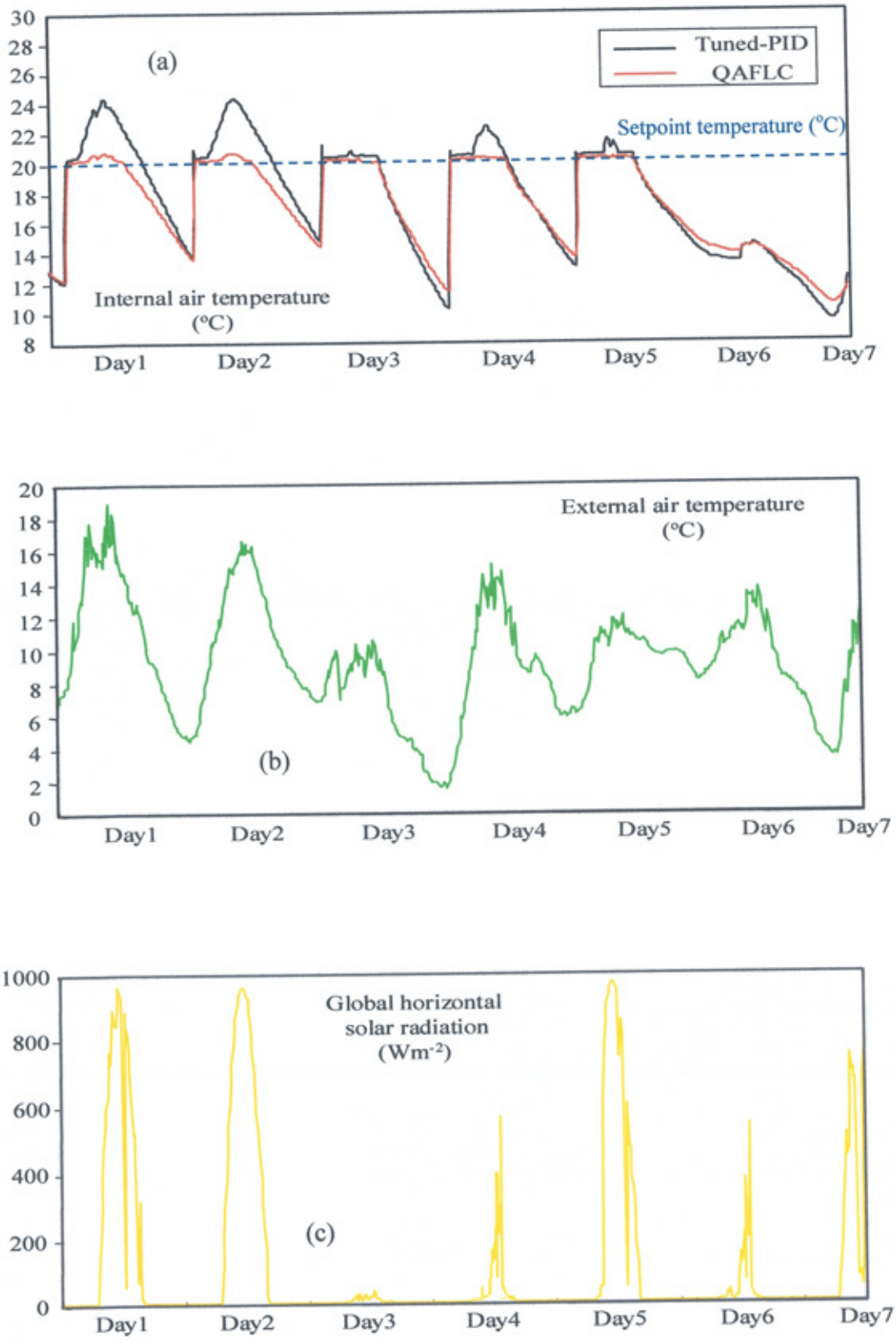

Figure (7.14): (a) Internal air temperature, (b) External air temperature, (c) Solar radiation

The development of the proposed quasi-adaptive fuzzy logic controller was carried out according to a combination of the following steps:

1. Development of a thermal model of the building and its heating system using feedforward neural network to predict future values of internal air temperature,
2. Development of a fuzzy controller with two inputs: the error between the setpoint temperature and the current internal air temperature; and the predicted future internal air temperatures.

Results show that the energy demands in both cases (conventional PID and proposed quasi-adaptive fuzzy logic controller) were integrated to reveal energy saving of approximately 20% due to the quasi-adaptive fuzzy logic controller when compared with conventional tuned PID control.

An artificial neural network was used as the predictive model of the building space and its heating system. Good accuracy for a time horizon of up to two hours has been demonstrated thus the predictive model can be used for providing control intelligence for early shut down of heating plant with resulting energy saving.

The results show that artificial neural networks can be successfully used for predicting the indoor temperature of buildings for several time steps ahead based on only a small number of input variables. The proposed quasi-adaptive fuzzy logic controller has the advantages over conventional PID controller in that it is able to avoid the overheating arising from solar heat gain particularly towards the end of the heating season and, thereby, generate saving in energy use as well as improve thermal comfort.

In simulation it has been shown that the controller works well, however the acid test is whether the controller works in a real situation. This is developed in the next chapter.

Chapter 8
Controller Testing

Chapter 8
Controller Testing

8.1. Introduction

An experimental test was conducted to evaluate the proposed quasi-adaptive fuzzy logic controller under practical conditions. Again, a comparison between the proposed quasi-adaptive fuzzy logic controller and a conventional PID controller formed the basis of the experiment. In this chapter, the experimental equipment for the developed algorithm is described together with the experimental procedure adopted. Then a comparison of results between the proposed controller and the conventional PID controller are presented.

8.2. Cranfield test cell

Controller testing took place at a remote test site at Cranfield University. The test site is situated on the edge of Cranfield airfield, in Bedfordshire. The site location is: latitude=52.07°N, longitude=0.63°W, and altitude=100 m.

An approximately cubical test cell with internal dimensions 3.550m (east west) × 2.995m (north-south) × 2.270m (high), was used, with its glazed wall facing due south as shown in figure (8.1a). Figure (8.1b), shows the internal view of the test room in which air temperature sensors and an oil-filler electric radiator were installed. Due to the fact that, this test cell is a light building, its thermal weight is very responsive compared to the high thermal capacity building (Northumberland building).

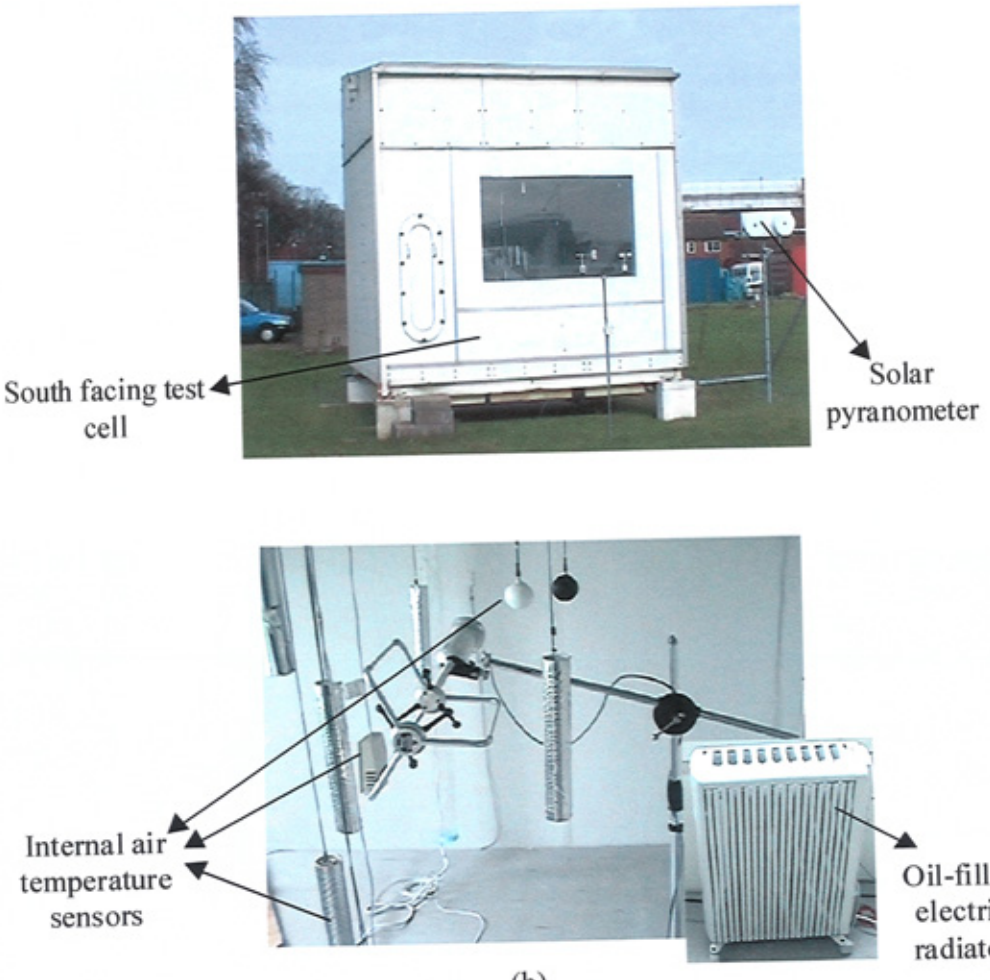

(b)

Figure (8.1): (a) South facing external view of the test cell. (b) Internal view of the test room

The internal volume of the test room was 24.135 m^3, and the window dimensions of 1.200 × 2.000 m. The internal floor surface of the test room was approximately 0.90 m above the ground level.

The tables in appendix "E" give the thermal properties of the east, north, west walls, the ceiling, the floor and the south wall of the test room. The convention adopted for listing the components of the multi-layer construction was to work from the outside inwards. For the purpose of simulation modelling, the model realisation of the test cell is shown in figure (8.2) in which the model parameters optimised using the technique outlined in section (3.4) and are given in appendix "E". The state space model of the test cell can be written as follows:

$$\dot{\mathbf{X}} = \mathbf{AX} + \mathbf{BU} \qquad (8.1)$$
$$\mathbf{Y} = \mathbf{CX} + \mathbf{DU}$$

where **X** is the state vector $[T_1\ T_2\ T_3\ T_4\ T_5\ T_6\ T_7\ T_8\ T_9\ T_{10}\ T_{11}\ T_{12}\ T_i]^T$, **U** is the input vector $[T_o\ Q_s\ Q_p]^T$, **Y** is the output vector (i.e. in this case the internal air temperature, T_i).

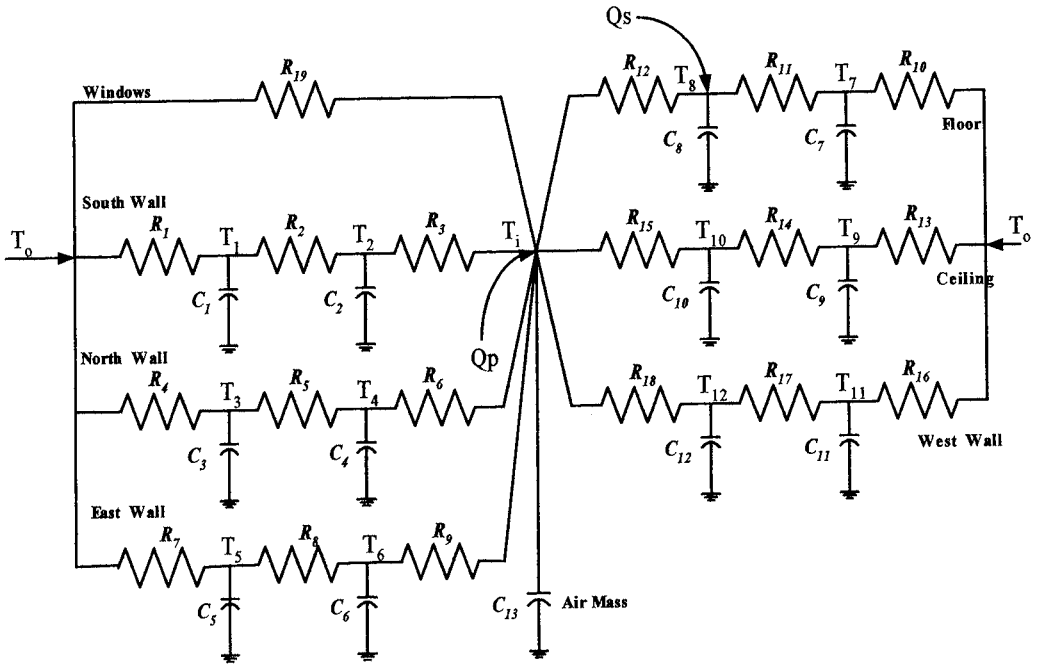

Figure (8.2): Model realisation for the test cell

8.3. Modelling the test cell heating system

The tests described here used an oil-filled electrical radiator, controlled form a personal computer which implemented the proposed control strategy. The mathematical description of the oil-filled electric radiator can be written as follows:

$$\dot{T}_r = [up - k(T_r - T_{ai})^n] / \sum C \tag{8.2}$$

where: T_r is the radiator surface temperature ($^\circ$C), T_{ai} is the room air temperature ($^\circ C$), u is the power controller signal, p is the maximum power emitted from the radiator (kW), $\sum C$ is combined thermal capacitance of the oil and the radiator metal, k and n are constants.

At design, the p and T_{ai} should be known, so the value of the constant k can be calculated from the following expression:

$$p = k(T_r - T_{ai})^{1.3} \tag{8.3}$$

To calculate the heating needed for the test room (and, hence, p) the external air temperature was taken to be $-1^\circ C$ and the designed internal air temperature $20^\circ C$. The ventilation rate was set at 0.5 air change/hour. Note that it was possible to precisely control the ventilation rate in the test cell. Hence:

Wall $U = (0.12 + 0.06 + 0.18 + 0.05/0.035)^{-1} = 0.56$ W/m^{2}K

Floor $U = (1/0.56 + 0.05/1.4)^{-1} = 0.549$ W/m^{2}K

$$\text{Ventilation loss coefficient} = \frac{0.5 \times 3.6 \times 3.0^2}{3} = 5.4 \text{ W/K}$$

Wall loss coefficient $= (2 \times 3.55 \times 2.995 + 2 \times 3^2) \times 0.56 = 22.18$ W/K

Floor loss coefficient $= 3.55 \times 2.995 + 0.549 = 5.93$ W/K

Glass loss coefficient $= 2.8 \times 2.00 \times 1.2 = 7.08$ W/K

$\therefore$ Steady state heat loss $= (20 - (-1))(5.4 + 22.18 + 5.93 + 7.08) = 880.8$ W

Allow 25 % preheat margin $= 880.8 + 0.25 \times 880.8 \cong 1100$ W

8.3.1. Ventilation

The test room features a mechanical ventilation system, which allows a controlled and metered airflow to be directed to the space. For this work incoming air was

drawn into the room through the ventilated window system. The temperature of the air as it entered the room was measured.

Inside the room, ventilated air was extracted through a duct, located vertically midway along the north wall. There were a total of 55 holes in the pipe, each of diameter 10 mm. The pipe was positioned at the centre of the rear wall. This arrangement assisted in ensuring uniformity of air movement in the space.

The ventilation system was designed to maintain a constant volumetric flow at the outlet from the room. Thus the recorded mass flow varied slightly (by about ±0.5%) as the air temperature in the test room varied.

8.4. Data acquisition

A dSPACE DS1102 data acquisition card was used for analogue (control) inputs and the single analogue output required to position the heater. The DS1102 is a single board system, which is specifically designed for development of high-speed multivariable digital controllers and real time simulations in various fields.

It is based on a Texas Instruments TMS320C31 third generation floating-point Digital Signal Processor (DSP), which builds the main processing unit, providing fast instruction cycle time for numeric intensive algorithms. The TMS320C31 is object-code compatible to the TMS320C30 [174].

The DSP contained 128K words of memory (fast enough to allow zero wait state operation). Several peripheral subsystems were implemented to support digital signal processing. Figure (8.3) summaries of the DS1102's hardware [174].

8.4.1. Power control circuit

The power control circuit was designed during the course of the project consisting of two main parts: a pulse width modulator (PWM) and a semiconductor relay (switching circuit) as shown in figure (8.4). The PWM unit consisted of two parts:

(1) A ramp waveform generator operating at constant frequency.

(2) A comparator, for detecting when the ramp voltage exceeds the control signal.

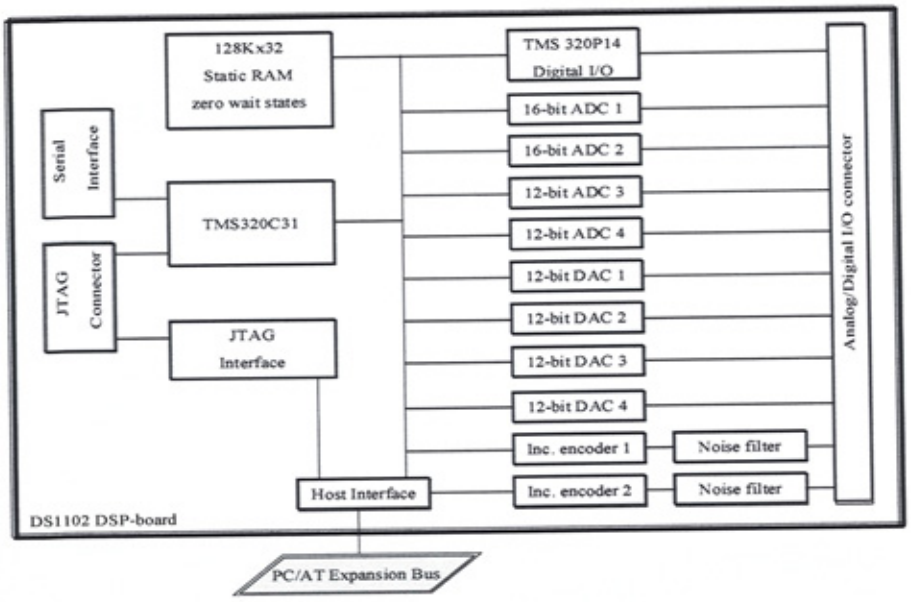

Figure (8.3): Block diagram of the DS1102 [174]

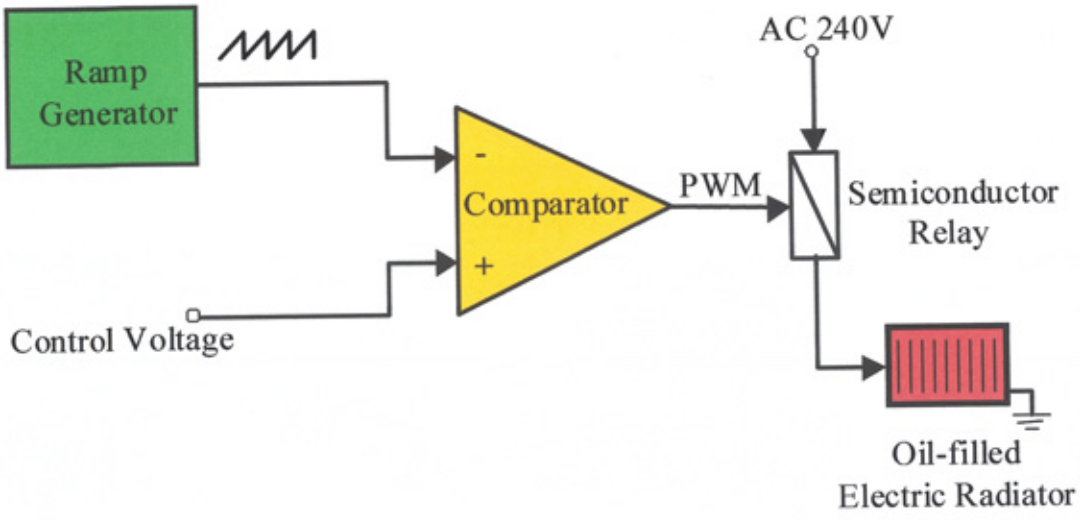

Figure (8.4): Basic organisation of the pulse-width modulation power control system

The ramp generator was implemented by a timer and a transistor. By choosing an appropriate value of RC network, it was possible to set the frequency of the ramp waveform. An operational amplifier to compare between the reference ramp voltage

and the control signal from the data acquisition card was used to generate a modulated pulse applied to the switching device as shown in figure (8.5).

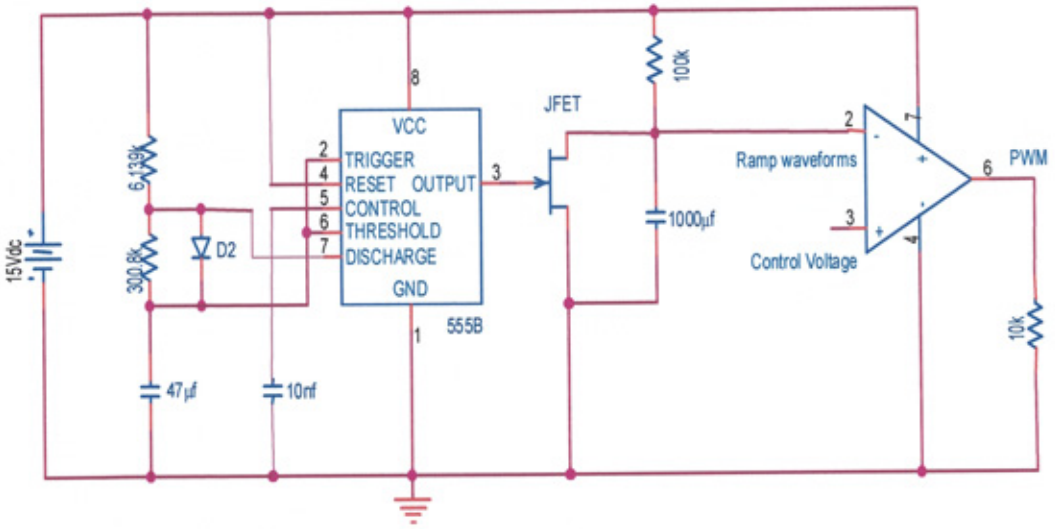

Figure (8.5): Circuit diagram of the pulse width modulation (PWM)

At the moment the ramp began its run-up, the positive control voltage $V_{control}$ exceeded V_{ramp}. Therefore the comparator produced positive saturation, hence turning the semiconductor relay on giving full supply voltage across the oil-filled electric radiator.

For example if $V_{control}$=3V the ramp oscillator, producing an overall load voltage waveform with a 30% duty cycle. This situation is repeated every cycle until the control voltage changed as shown clearly in figure (8.6a). Therefore the average load voltage in figure (8.6a) is given by:

$$V_{LD(avg)} = 0.30 \times V_S \tag{8.4}$$

A larger control voltage is shown in figure (8.6b). So, with a small value of control voltage, the load's duty cycle is low (pulse width is narrow), with a larger value of control voltage the load's duty cycle is higher (pulse width is wider). This delivered greater average electrical power, so the load produced a greater amount of its output product. By varying the control voltage to the PWM, the pulse width to the load was modulated.

Since the rated power of the oil-filled electric heater was 2500W, the duty cycle needed to produce an average power equal to 1100W (i.e. the required design duty), was 44% of the periodic time of the ramp waveform. To get this duty cycle, the output of the data acquisition card (control signal) was fixed at a maximum of 0.44V.

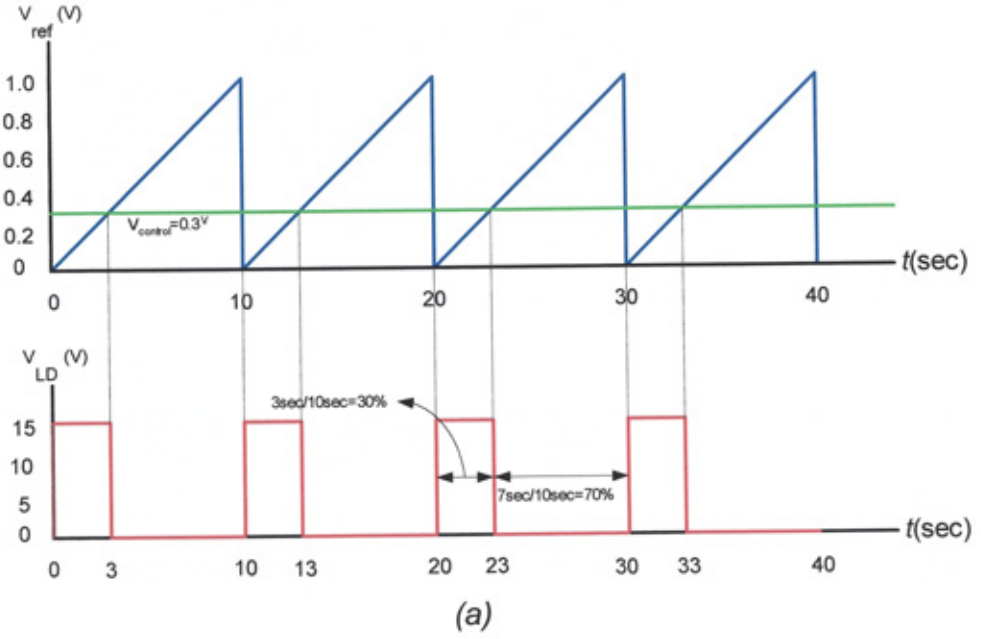

(a)

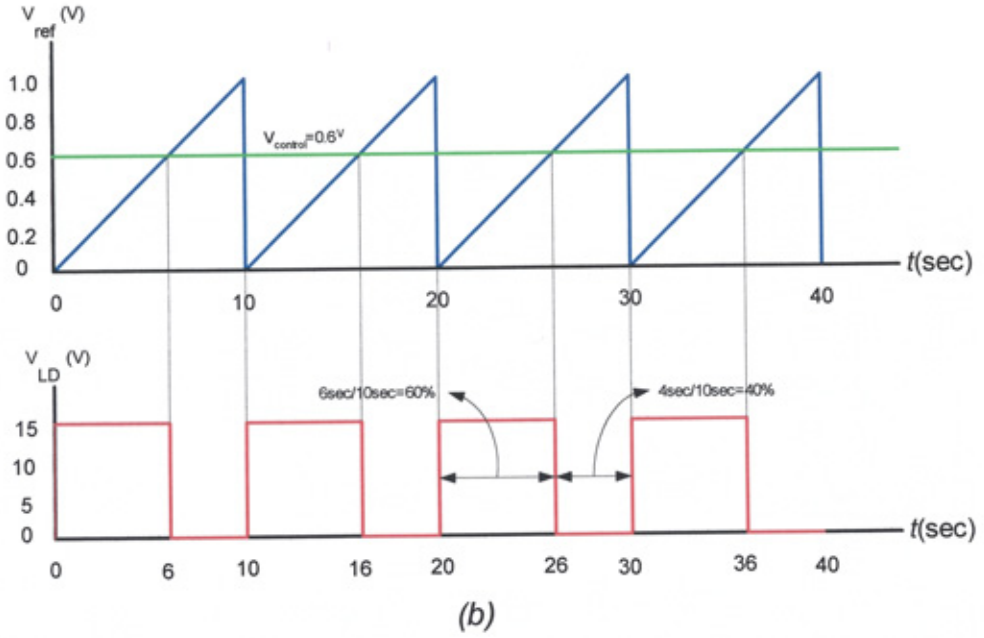

(b)

Figure (8.6): Pulse width modulation waveforms

(a): Small voltage (b): Large voltage

8.4.2. Sensors

Two temperature sensors were used the first measured the internal air temperature and the second measured the external air temperature. The internal air temperature sensor was an integrated circuit based active output temperature sensor, with a 4-20mA output and an uncertainty of ±0.1°C. The internal air temperature sensor was located in the middle of the test cell.

The external air temperature sensor was similar to the internal air temperature sensor but was in a weatherproof enclosure. The external air temperature sensor was located on the top of the north side of the test cell.

Since the data acquisition card inputs were voltages, a high precision resistor (500Ω) was connected in series with the sensors, and a 2200μf capacitor was connected in parallel with this resistor to act as a low pass filter (f_c=0.57 Hz). Both the internal air temperature and external air temperature sensors required a 24V DC supply voltage. The installation circuit is shown in figure (8.7).

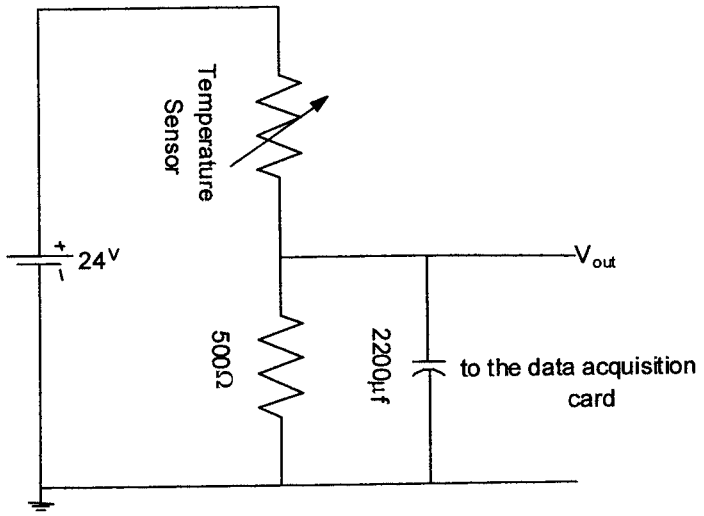

Figure (8.7): The installation circuit of the temperature sensors

The temperature sensors were scaled using the indoor test cell in the school of Built Environment at University of Northumbria. Figure (8.8) shows the relation between the output voltage and the measure temperature by the temperature sensor, it is clearly linear. Therefore, the equation which describe this relation can be written as following:

$$V_{out} = 0.16\,Temp + 3.6 \tag{8.6}$$

This equation was used to reproduce the actual measured temperature in the test cell, as a function of incoming signal.

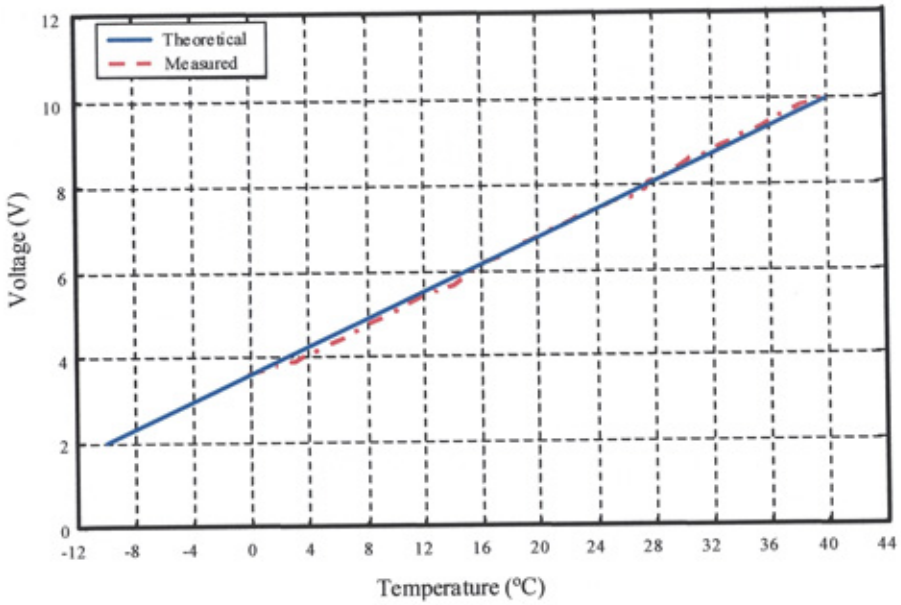

Figure (8.8): Voltage versus temperature of a temperature sensor

A Kip and Zonen LI-200SA pyranometer was used to measure the vertical solar radiation incident on the window. This featured a silicon photovoltaic detector mounted in a fully cosine-corrected miniature head. Current output was calibrated under natural daylight conditions in unit of Watts per square meter (Wm^{-2}). It was found that the pyranometer gave 10μV per Wm^{-2}, so a high precision amplifier was used to amplify this signal to 10 mV per Wm^{-2}.

A local data logging system was used to monitor a full range of variables besides those required for the control system. The data logger and the control system are shown in the figure (8.9).

8.5. Controller implementation

Two controllers were tested in the test cell. The first controller was a PID controller as a benchmark for the proposed controller and also to collect two weeks of

regulated internal air temperature used for training the network in the second controller. The second controller was the quasi-adaptive fuzzy logic controller (described in section (7.6)).

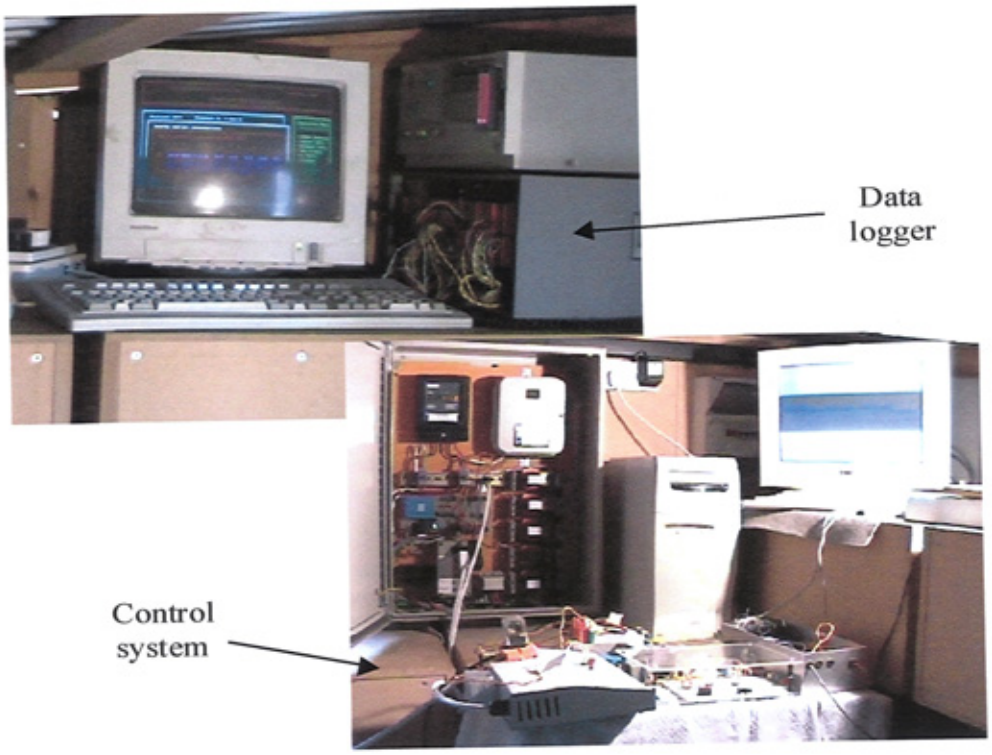

Figure (8.9): Data logger and Control system

8.5.1. PID controller

Although PID controllers are well established, parameters require precise adjustment to obtain optimal performance, and they are heavily dependent on system parameters thus optimality is conditional. The output of a PID was defined in section (5.4).

To avoid the problem of wind-up, there are a few anti-wind-up strategies but they are all based on the same idea – that of retarding the integral term in some way when the actuator reaches saturation. The simplest thing to do is to saturate the integral term to the upper and lower limits of the control signal that correspond to actuator saturation (i.e. 1 and 0 in this case). This strategy was adopted in the present work.

Also a saturation block required to added on the overall control signal output value to limit the signal to 0 (minimum); 1 (maximum). This was because the valve model equations were based on a control signal in the fractional range 0→1. Thus any value outside this range was likely to lead to a mass flow rate from the control valve subsystem outside the design range.

To establish values for the test case PID parameters, a simple test was done using a step change in the reference set point temperature thereby a controller response. The internal air temperature was oscillated around the set point temperature. A maximum overshoot of 1.6 and a periodic time of 12 minutes at a sampling time of one minute were obtained. Hence, Ziegler Nichols method [141] led to: k_p=0.8, integration time τ_i=10 minutes; (integral gain $k_i = k_p / \tau_i$=0.08 /minute), and D-term was set at zero because the test cell is damped system and for simplicity as well.

8.5.2. Proposed quasi-adaptive fuzzy logic controller

The proposed controller was implemented and tested using the test cell. Some modifications were necessary to meet the memory limitation of the data acquisition card:

(1) The number of membership functions representing each variable was reduced to 5 instead of 7 (in simulation there was a little difference, between 5 membership and 7 membership functions).

(2) The number of neural networks formed to choose optimality was reduced to 50 (from100).

These have quite minor implications regarding original controller design in section (7.6).

The sampling time was set at 15 minutes for training and control signal generation. Two weeks of external air temperature, solar radiation and internal air temperature from the corresponding sensor, and control signal generated by the controller, were collected and stored in a matrix to act as a stack. Using the principle of a stack, the data matrix had two weeks of data at each sampling time. The network was trained

and validated using these data after applying the SVD algorithm to generate a one-hour-ahead prediction of the internal air temperature. The SIMULINK representation of the quasi-adaptive fuzzy logic controller using DS1102 real-time workshop is shown in figure (8.10).

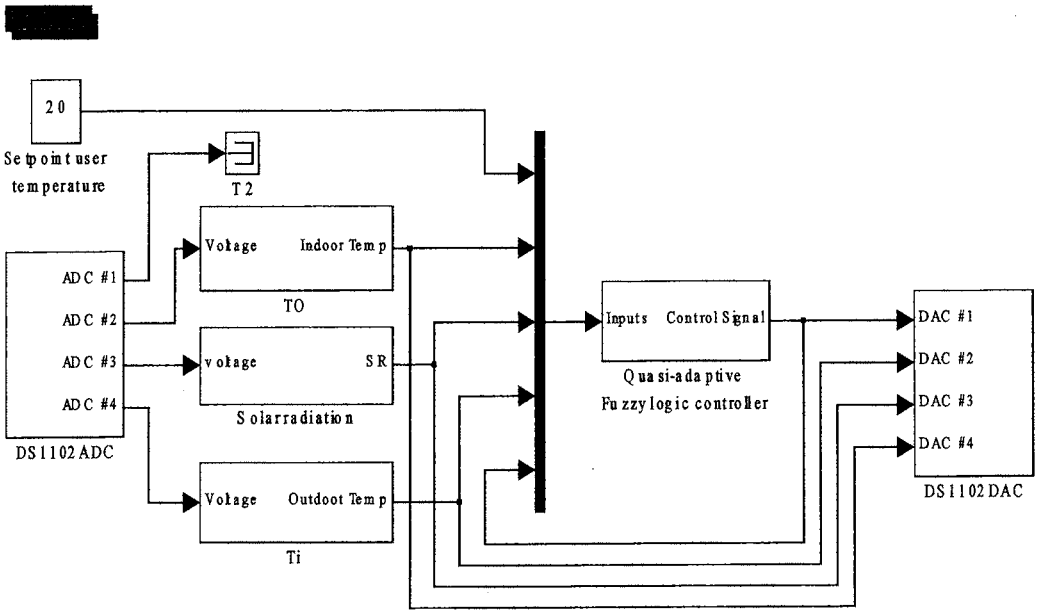

Figure (8.10): SIMULINK model of the quasi-adaptive fuzzy logic controller using DS1102 real-time workshop

The predicted internal air temperature and the error (between the current internal air temperature and the set point reference temperature) were applied to fuzzy logic controller to generate a control signal. This signal was modulated by PWM and then applied to the switching device, which was applied to the oil-filled electric radiator. A flowchart of the implementation is shown in figure (8.11).

8.6. Results

To compare the quasi-adaptive fuzzy logic controller with the benchmark PID controller, two test cells should be used with the same indoor and outdoor climate conditions. Unfortunately there is only one test cell, so a simulation model of the test cell and the oil-filled electric radiator with conventional PID controller was first developed and tested using test cell results. The intention was that the validated

conventional control simulation be used as means of evaluation the practical performance of the proposed quasi-adaptive fuzzy logic controller (QAFLC).

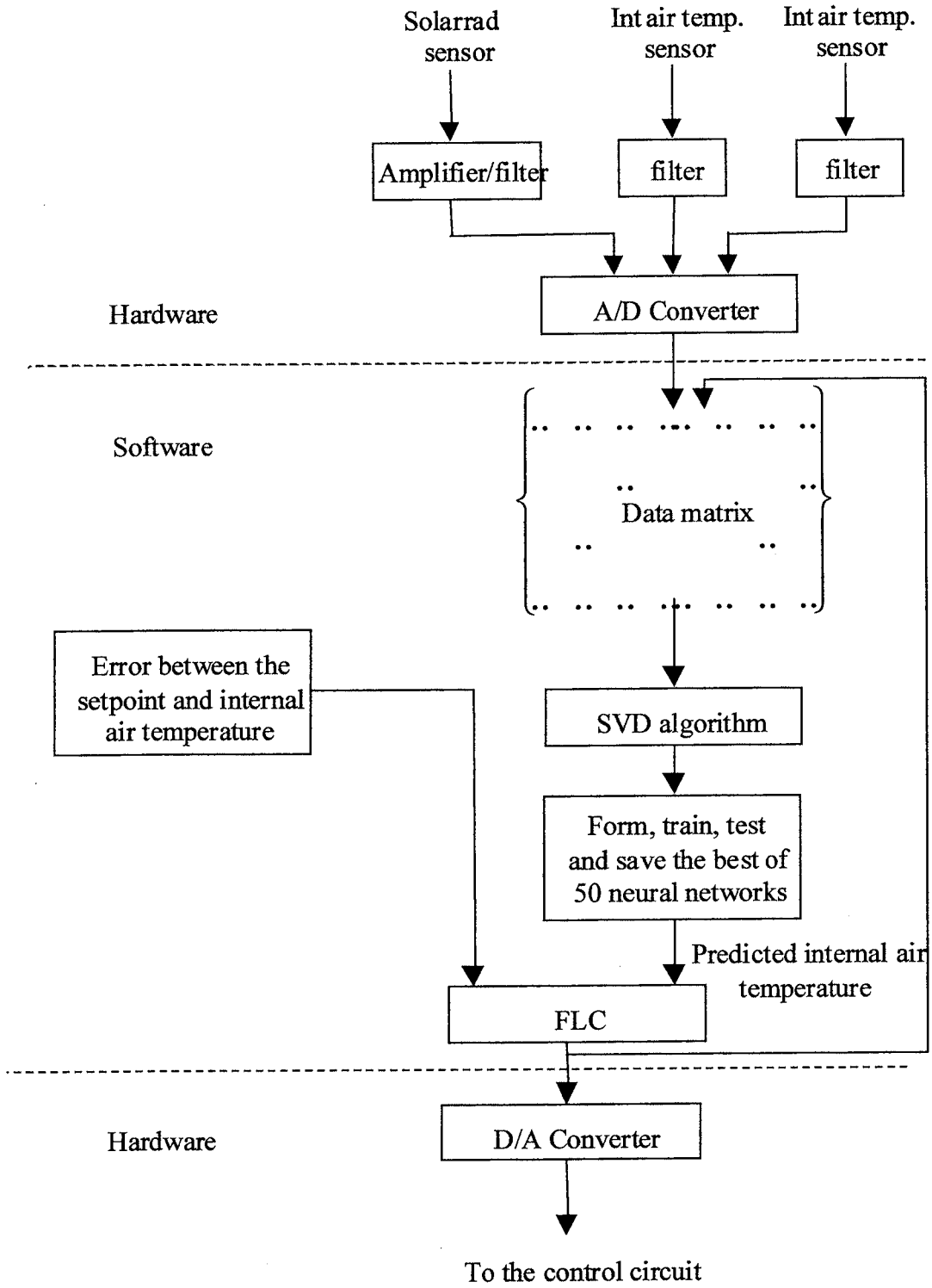

Figure (8.11): Implementation of the proposed controller

Figure (8.12), shows the result of the PID controller (the D-term was set at zero) in real-time compared with a SIMULINK model of the test cell using the same controller.

Results based on the model and the filed measurements compare very favourably and gave a significant agreement.

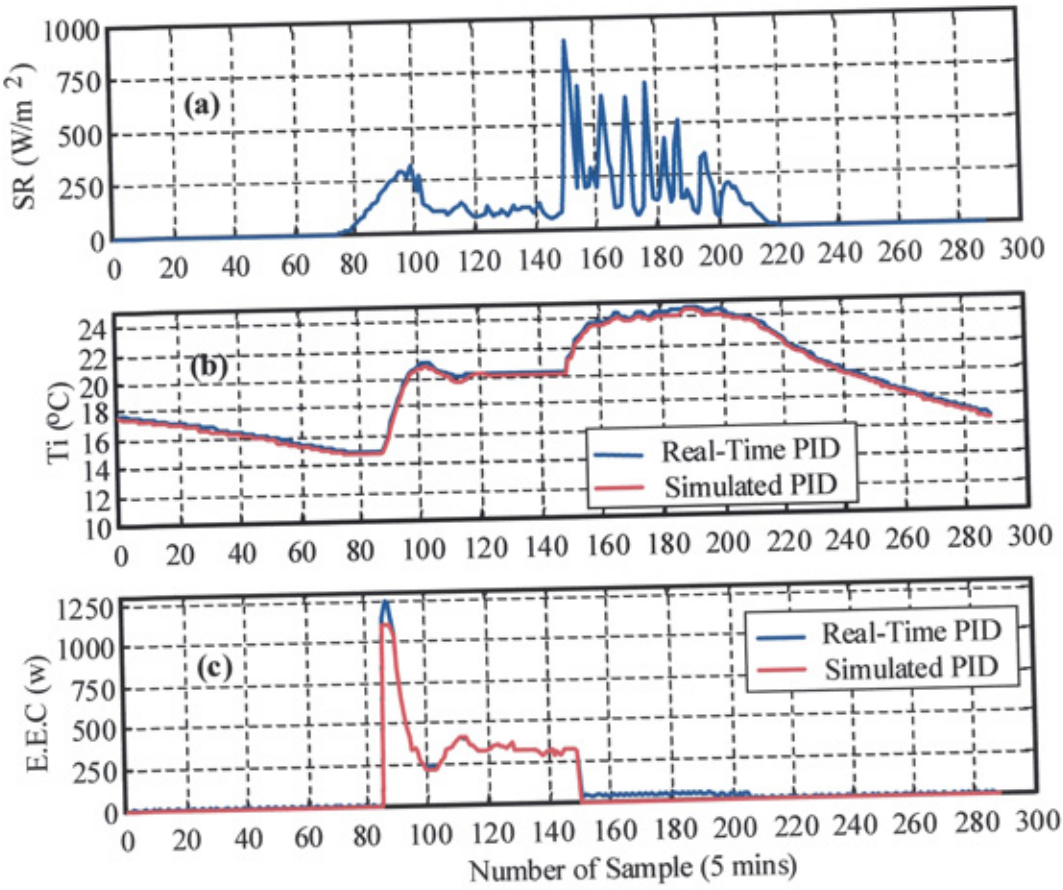

Figure (8.12): Real Time and simulated results of the test cell using PID controller (a): Solar radiation, (b): Internal air temperature, (c): Electric power consumption

The validated model of the test cell with the oil-filled electric radiator was used to compare the conventional PID with the real-time quasi-adaptive fuzzy logic controller. Figure (8.13), shows the real time results using the quasi-adaptive fuzzy logic controller and the simulation results of the conventional PID controller. Quasi-adaptive fuzzy logic controller gave good tracking to the set point reference temperature, reduce the overheating risk and then save a significant amount of energy.

8.7. Conclusions

In this chapter, the quasi-adaptive fuzzy logic controller was implemented using a test cell to be evaluated and compared with benchmarking conventional PID.

The quasi-adaptive fuzzy logic controller was carried out based on a combination between an artificial neural network and fuzzy logic control. A feedforward neural network used to predict future values of internal air temperature. A fuzzy controller had two inputs: the error between the setpoint temperature and the current internal air temperature; and the predicted future internal air temperatures.

The methodology of performance comparison by combining simulation and experiments was applied successfully to the test cell. On this test cell, the proposed controller gave good tracking to the set point reference temperature and reduced the overheating risk as shown in figure (8.13b) and then saves a significant amount of energy. Results shown in figure (8.13c) confirmed that the energy demands in both cases (conventional PID and proposed quasi-adaptive fuzzy logic controller) were integrated in the limited time horizon used to reveal energy saving of approximately 20% for this particular day, due to the quasi-adaptive fuzzy logic controller when compared with conventional PID control, with an improved thermal comfort and reduced overheating risk.

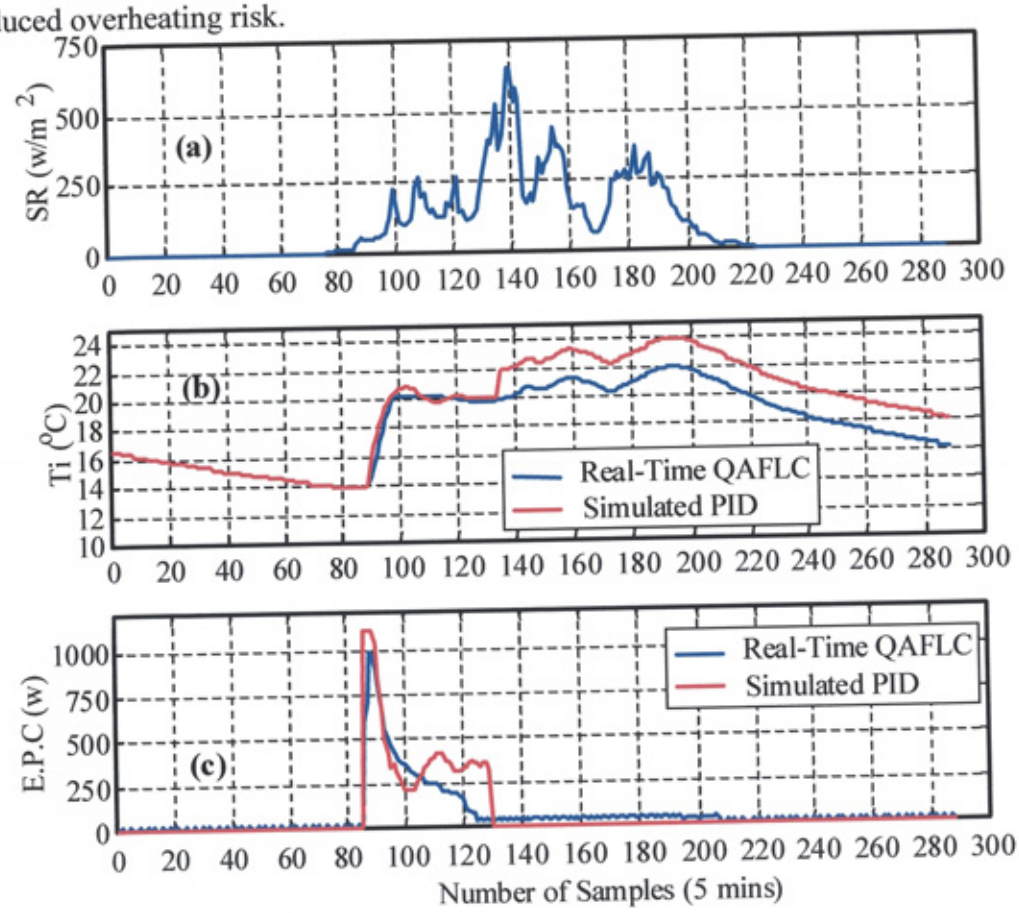

Figure (8.13): Real Time and simulated results of the test cell using PID controller (a): Solar radiation, (b): Internal air temperature, (c): Electric power consumption

Chapter 9

Conclusions and Future work

Chapter 9

Conclusions and Future work

9.1. Conclusions

The aims of this thesis were to develop and test an adaptive control method for space heating in buildings with significant solar input. The proposed control strategy have many properties such as consideration of solar radiation in the control strategy, self-adaptation of the controller to building and climate parameter changes (through using on-line learning neural network predictor), robust and reduced commissioning over the conventional controller.

The following main contributions have been made:

- As, the method of Lorenze & Masy [1] was not suitable for building control investigation, so an approach for the optimisation of reduced-order lumped capacity modelling of the dynamic thermal behaviour of building spaces was presented. The method was appropriate for simplified and computationally efficient building envelope model descriptions of the type needed for short-term analysis of energy and environment in buildings, such as plant and control system simulations.

- The analysis of several construction types of mixed materials according to apply the above method, suggests that the innermost-to-outermost resistance fractions for the optimised second-order model to be typically 0.1, 0.4 and 0.5 of the total thermal resistance of the construction element respectively. The corresponding innermost and outermost capacitance fractions are typically 0.15 and 0.85 of the total thermal capacitance of the construction element respectively respectively.

- A suitable model of a hot water heating system which, when coupled to the room space model developed above, could facilitate the study of nonlinear control laws was developed. Nevertheless, it may be concluded that the model was simple, computationally efficient and sufficiently accurate to have potential for applications to short time-scale simulations appropriate to control system analysis.

- PID controllers require three tuning parameters which are difficult to optimise *a priori* and which, in any event, are only suited to a finite range of plant response when the plant has nonlinear characteristics. Since, the architecture and the principles in the design of the static fuzzy logic controller (FLC) was developed for the control of the internal air temperature. The FLC was found to give better tracking of the reference control condition than a comparative tuned PID controller as well as better robustness properties, when the parameters of the system under control were changed.

- A control strategy for the space heating of a building space in which the comfort sensation, as quantified by predicted mean vote, forms the control variable was

developed. There was a natural appeal in this in that the essentially subjective comfort control problem can be easily mapped onto a universe of discourse of input fuzzy sets and the associated inference which ultimately forms a required control action can be carried out qualitatively. The resulting FLC was compared with a PID controller tuned to give optimal performance for a given case, consisting of a building space with high thermal capacity and low thermal capacity, but did not cope with the overheating risk.

- A quasi-adaptive fuzzy logic controller was developed to overcome the problem of the overheating due to the lagging influence of solar heat gain in a space. The development of the proposed quasi-adaptive fuzzy logic controller was carried out based on a combination of artificial neural network and fuzzy logic control. A feedforward neural network was used to predict future values of internal air temperature. A fuzzy controller with two inputs: the error between the setpoint temperature and the current internal air temperature and the predicted future internal air temperatures. The quasi-adaptive fuzzy logic controller has the advantages over conventional PID controller in that it is able to avoid the overheating arising from solar heat gain and, thereby, generate saving in energy use as well as improve thermal comfort.

- The quasi-adaptive fuzzy logic controller was implemented using a test cell to be evaluated and compared with benchmarking conventional PID. The methodology of performance comparison by combining simulation and experiments was applied successfully to the test cell. On this test cell, the proposed controller gave good tracking to the set point reference temperature and reduced the overheating risk and then saves a significant amount of energy. Results confirmed that the energy demands in both cases (conventional PID and proposed quasi-adaptive fuzzy logic controller) were integrated in the limited time horizon used to reveal energy saving of approximately 20% due to the quasi-adaptive fuzzy logic controller when compared with conventional PID control, with an improved thermal comfort and reduced overheating risk.

To give direct figures to justify a substantial energy saving (KWh) of the adaptive fuzzy logic controller over conventional PID controller, the integration of the power curve (as shown in figure (8.13c)) has been done for different five days. Table (9.1) gives a quantitative data of the energy saving (KWh).

As can be seen from table (9.1), the energy savings of around 20% was achieved using adaptive fuzzy logic controller over the conventional PID control.

	Day1	Day2	Day3	Day4	Day5
Simulated PID	1.2	1.1	1.15	1.0	1.18
Real-time QAFLC	0.96	0.902	0.9315	0.82	0.944

Table (9.1): Quantitative data of energy saving

9.2. Recommendations for further works

A further possibility for those spaces exhibiting one or more of the features mentioned above is to implement a model-assisted strategy in which a thermal model of the space is used to offset measurements made at a single point. None of these avenues have been explored in the present work and form the basis of further work in the field.

- Further work needs to be done to adapt the modelling method based on the optimization technique to whole space simulations, the treatment of building ventilation rates, an analysis of the model performance when applied to occupied spaces with plant, introduction of a library of surface convection coefficients, and introduction of a method to treat longwave and shortwave radiation.

- For practical application in HVAC (Heating, Ventilating and Air Conditioning) control, further work needs to be done to address the wide range of training cases and diversity of building construction types.

- For more saving in energy, further work needs to be done to increase the predicted time horizon for internal air temperature using the neural network with small amount of data.

- To increase the applicability of the proposed controller, further work needs to be done to expand the application of the proposed controller to control the cooling systems and storage room.

- Another important research area needing attention is to design a fault diagnosis system for building energy management system via a simulation environment since air dynamics in rooms can be known from simulation models. A possible way of implementing this could be to apply a set of input and output related data from a normally operating system as a reference and then training a neural network using faulty input/output data. This trained neural network can actually predict the system outputs under normal and failed conditions, and hence can be used to detect a variety of faults. This can be further extended to designing a control reconfiguration system in the case of system failure so that the overall system remains functional.

References

References

[1] Lorenz F and G. Masy, "Méthodé d'évaluation de l'économie d'energie apportéé par l'intermittence de chauffage dans les bâtiments. Traitement par différences finies d'un modélé a deux constantes de temps", *Report No. GM820130-01*, Faculte des Sciences Appliquéés, University de Liége, Liége, Belgium, 1982.

[2] Thomas Herzog, "Solar energy in architecture and urban planning", ed. Prestel Verlag, New York, 1996.

[3] Mathews, E.H, C. P. Botha, D. C. Arndt, and A. Malan, "HVAC control strategies to enhance comfort and minise energy usage", Energy and Building, 33, pp. 853:863, 2001.

[4] Ronald Thomas "Photovoltaics and architecture", ed., Spon Press, London, 2001.

[5] John , R. W, A. L Dexter, "Intelligent controls for building services", Building Services Engineering Research and Technology, 10 (4), pp. 131-141, 1989.

[6] Zaheer-uddin, M, "Optimal, sub-optimal and adaptive control methods for the design of temperature controllers for intelligent buildings", Building and Environment, 28 (3), pp. 311-322, 1993.

[7] Dexter, A. L, P. Haves, "A robust self-tuning predictive controller for HVAC applications", ASHRAE Transaction, 95 (2), pp. 431-438, 1989.

[8] Levermore, G. J, "Building Energy Management Systems-An Application to heating control", ed., E & FN Spon, London, 1992.

[9] Coley, D. A., J. M. Penman, "Simplified thermal response modelling in building energy management. Part III: Demonstration of a working controller", Building and Environment, 31 (2), pp. 93-97, 1996.

[10] Murdoch, N., J. M. Penman, and G. J. Levermore, "Empirical and theoretical optimum start algorithms", Building Services Engineering Research and Technology, 11 (3), pp. 97-103, 1990.

[11] Birtles A. B., R. W. John, "A new optimum start control algorithm", Building Services Engineering Research and Technology, 6 (3), pp. 117-122, 1985

[12] Jota, F. F., A. L. Dexter, "Self-tuning control of an air handling plant", Proceedings of the IEE International Conference-Control'88, IEE, London, IEE Conf. Publ. no. 285, 1985.

[13] Brandt, S.G. "Adaptive control implementation issues", ASHRAE Transactions, 92 (2B), pp. 211-219, 1986.

[14] MacArthur, J. W., E. W. Grald, and A. F. Konar, "An effective approach for dynamically compensated adaptive control", ASHRAE Transactions, 95 (2), pp. 415-423, 1989.

[15] Wellborg, A.O., "A new self-tuning controller for HVAC systems", ASHRAE Transactions, 97 (1), pp. 19-25, 1991.

[16] Attia, A. E, S. F. Rezeka, "Quantitative robust control of temperature and humidity in hot and dry climates", ASME Transactions: Journal of Dynamic systems, Measurements and Control, 116 (2), 286-292, 1994.

[17] Dexter, A. L., D. W. Trewhella, "Building control systems: fuzzy rule based approach to performance assessment", Building Service Engineering Research and Technology, 11 (4), pp. 115-124, 1990.

[18] Dounis, A.L., M. J. Sanatamouris, C. C. Lefas, and A. Arigirious, "Design of a fuzzy set environment comfort system", Energy and Buildings, 22, pp. 81-87, 1995.

[19] Haung, S., R .M. Nelson, "A PID law combining fuzzy controller for HVAC applications", ASHRAE Transactions, 97 (2), pp. 768-774, 1991.

[20] Haung, S., R. M. Nelson, "Rule development and adjustment strategies of fuzzy logic controller for an HVAC system; part one-analysis", ASHRAE Transactions, 100 (1), pp. 841-850, 1994a.

[21] Haung, S., R. M. Nelson, "Rule development and adjustment strategies of fuzzy logic controller for an HVAC system; part two-experiment", ASHRAE Transactions, 100 (1), pp. 851-856, 1994b.

[22] So, A. T. P., T. T. Chow, W. L Chan, and W. L. Tse, "Fuzzy Air Handling System Controller", Building Serv. Res. Technol, vol. 15, Part 2, pp. 95-105, 1994.

[23] Willey, H. B, "Fuzzy Theory and Environmental Control in Buildings", Environment and Planning, vol. 6, pp. 279-291, 1979.

[24] Geng, G., and A. L. Dexter, "Fuzzy Gain Scheduling Control of a Non-linear HVAC System", Proceedings of the 28th Annual Allerton Conference on Communication, Control and Computing, October 3-5, University of Illinois, pp. 1044-1052, 1990.

[25] Ling, K.V., A. L. Dexter, G. Geng, and P. Haves, "Self-Tuning Control with Fuzzy Rule-Based Supervision for HVAC Applications", IAFC Synopsism Intelligent Tuning and Adaptive Control (Ed. Devanathan, R.) 15-17 Jan, Pergamon Press, pp. 205-209, 1991.

[26] Clarke, D.W., C. Mohtadi, and P. S. Tuffs, "Generalised Predictive Control - Parts 1 and 2", Automatica, vol. 23, pp. 137-160, 1987.

[27] Clarke, D.W., C. Mohtadi, "Properties of Generalised Predictive Control", Automatica, vol. 25, pp. 859-875. 1989.

[28] Dounis, A. I., M. J. Santamouris, and C. C. Lefas, "Implementation of Artificial Intelligence Techniques in Thermal Comfort Control for Passive Solar Buildings", Energy Convers. Management, vol. 33(3), Pergamon Press, pp. 175-182, 1992.

[29] MacConnell, P. F, D. H. Owens, "Intelligent Fuzzy Regulation of Residential Buildings", Proceedings of Control '94, 21-24 March, pp. 1379–1384, 1994.

[30] Dounis, A. I., M. J. Santamouris, C. C. Lefas, and D. E. Manolakis, "Thermal Comfort Degradation by a Visual Comfort Fuzzy-Reasoning Machine Under Natural Ventilation", Applied Energy, vol. 48, pp. 115-130, Elsevier Science Ltd, UK, 1994.

[31] Miller, R.C., J. E. Seam, "Comparison of artificial neural networks with traditional methods of predicting return time from nigh or weekend setback", ASHRAE Transactions, 97 (2), pp. 500-508, 1991.

[32] Anstett, M., J. F. Kreider, "Application of neural networking models to predict energy use", ASHRAE Transactions, 99(1), pp. 505-517, 1993.

[33] Curtiss, P.S., J. F. Kreider, and M. J. Brandemuehl, "Energy management in central HVAC plants using neural networks", ASHRAE Transactions, 100(1), pp. 476-493. 1993.

[34] Huang, S. H., R. M. Nelson, "Delay time determination using as artificial neural network", ASHRAE Transactions, 100(1), pp. 831-840, 1994c.

[35] Curtiss, P. S., J. F. Kreider, and M. J. Brandemuehl, "Adaptive control of HVAC processes using predictive neural networks", ASHRAE Transactions, 99 (1), pp. 496-504, 1993.

[36] So, A. T. P., T. T. Chow, W. L. Chan, and W. L. Tse, "A neural network based identifier/controller for modern HVAC control", ASHRAE Transactions, 101 (2), pp. 14-31, 1995.

[37] Curtiss, P. S., "Experimental results from a network assisted PID controller", ASHRAE Transactions, 102 (1), pp. 1157-1168, 1996.

[38] Krieder J. F., X. A. Wang, "Artificial neural networks demonstration for automated generation of energy use predictors for commercial buildings",

Habert J S, Nelson R M, Culp C. C, editors. "The use of artificial intelligence in building systems", ASHRAE, pp.193-198, 1995.

[39] Curtiss P. S, M. J. Brandemuehl, and J. F. Kreider, "Energy management in central HVAC plants using neural networks", Habert J S, Nelson R M, Culp C C, editors. "The use of artificial intelligence in building systems", ASHRAE, pp. 199-216, 1995.

[40] Ling, K.V., A. L. Dexter, "Expert Control of Air-Conditioning Plant", Automatica, vol. 30(5), Elsevier Science Ltd., pp. 761–773, 1994.

[41] von Altrock, C., "Fuzzy Logic and Neurofuzzy Applications", Prentice Hall, New Jersey, ISBN 0-13-368465-2, 1995.

[42] Ross, T. J. "Fuzzy Logic with Engineering Applications", Mc-Graw Hill, London, 1995.

[43] Dounis, A. I., M. Bruant, G. Guarracino, and P. Michel, "Indoor Air-Quality by a Fuzzy-Reasoning Machine in Naturally Ventilated Buildings", Applied Energy, vol. 54, no. 1, pp. 11-28, Elsevier Science Ltd, UK, 1996.

[44] So, A. T. P., T. T. Chow, W. L .Chan, and W. L. Tse, "Fuzzy air handling system controller", Building Services Engineering Research and Technology, 15 (2), pp. 95-105, 1994.

[45] So, A. T. P., T. T. Chow, and, W. L. Tse, "Self-tuning fuzzy air handling system controller", Building Services Engineering Research and Technology, 18 (2), pp. 99-108, 1997.

[46] Egilegor, B., J. P. Uribe, G. Arregi, E. Pradilla and L. Susperregi, "A Fuzzy Control Adapted By A Neural Network To Maintain A Dwelling Within Thermal Comfort", Proceedings of Building Simulation '97, vol. 2, pp. 87-94, 1997.

[47] Chou S. K., W. L. Chang, "Effect of multi-parameter changes on energy use of large buildings", International Journal of Energy Research, 17; pp. 885-903, 1993.

[48] Price B. A., T. F. Smith, "Thermal response of composite building envelopes accounting for thermal radiation", Energy Consumption Management, 36 (1), pp. 23-33, 1995.

[49] Mathews E. H., P. G. Richards, and C. Lombard, "A first order thermal model for building design", Energy and Building, 21 pp. 133-145, 1994.

[50] Hagghighat F, H. Liang, "Determination of transient heat conduction trough building envelopes-a review", ASHRAE Trans., 98, pp. 284-290, 1992.

[51] Athientities A. K., "A methodology for integrated building HVAC system thermal analysis", Building Environment, 28(4), pp. 483-96, 1993.

[52] Richards P. G, E. H. Mathews, "A thermal design tool for building in ground contact", Building Environment; 29(1), pp.73-82, 1994.

[53] Krieder J. F, J. S. Haberl, "Predicting hourly building energy use: the great energy predictor shootout-overview and discussion of results", ASHRAE Journal of Heat, Refrigerating and Air-Conditioning, 36 (6), pp. 72-86, 1994.

[54] Reddy T. A, D. E. Claridge, "Using synthetic data to evaluate multiple regression and principal component analysis for statistical modeling of daily building energy consumption", Energy and Building, 21,pp. 35-44, 1994.

[55] Kajl S, P. Malinowski, E. Czogala, and M. Balazinski, "Fuzzy logic and neural networks approach to thermal description of buildings", Proceedings of EUFIT'95, Aachen, Germany, pp. 299-302, 1995.

[56] Judkoff R. D, J. S. Neymark, "A procedure for testing the ability of whole building energy simulation program to thermally model the building fabric", Journal of Solar Energy Engineering, 117, pp. 7-15, 1995.

[57] Lam J. C, S. C. M. Hui, "Sensitivity analysis of Energy performance of office buildings", Build Environment, 31(1), pp. 27-39, 1996.

[58] Tuomaala P, J. Rahola, "Combined air flow and thermal simulation of buildings", Building Environment, 30(2), pp. 255-265, 1995.

[59] Clark J. A, P. A. Strachan, "Simulation of conventional and renewable building energy systems", Renew Energy, 5, pp. 1178-1789, 1994.

[60] Scott M, L. E. Wrench, and D. L. Hadley, "Effects of climate change on commercial building energy demand", Energy sources, 16, pp.317-332, 1994.

[61] Cammarata G, A. Fichera, and L. Marletta, "Sensitivity analysis for room thermal response", International Journal Energy Research, 17, pp. 709-718, 1993.

[62] Bojic M. L, M. Milovanovic, and D. L. Loveday, "Thermal behaviour of a building with slanted roof", Energy and Building, 26, pp. 145-151, 1997.

[63] Norford L. K., R. H. Socolow, E. S. Hsieh, and G. V. Spadaro, "Two to one discrepancy between measured and predicted performance of a low-energy

office building: insight from a reconciliation based on the DOE-2 model", Energy and Building, 21, pp. 121-131, 1994.

[64] US Department of Commerce, "DOE-2 Reference manual, Parts 1 and 2, (Version 2.1)", Springfield, VA 22161, USA: US Department of Commerce, National Technical Information Service.

[65] BLAST Support Office, "The building analysis and system thermodynamics program, Version 3, Users Manual", Urbana, Champaign, IL, USA: University of Illinios.

[66] Klein S. A., "TRNSYS, a Transient Simulation Program", Solar Energy Laboratory, University of Wisconsin, 1994.

[67] Moller S. K, M. J. Wooldridge, "User's Guide for computer BUNYIP: Building Energy Investigation Package, ver 2.0, Technical Report TR6", CSIRO, Victoria, Australia: Divison of Energy Technology.

[68] ASHRAE Handbook of Fundamentals, Georgia: American Society of Heating, Refrigerating and Air Conditioning Engineers, 1993.

[69] Gouda M. M, S. Danaher, and C. P. Underwood, "Modelling the Heating of A Building Space Using Matlab-Simulink", 3rd Mathematical and Modelling Conference (3rd MATHMOD), Vienna University, Vienna, Austria, 2000.

[70] Gouda M. M, S. Danaher, and C. P. Underwood "Low Order Model for the Simulation of a Building and Its Heating System", Building Services Engineering Research and Technology, 2000.

[71] Laret L, "Use of general models with a small number of parameters: Part 1– theoretical analysis", Proc. 7th Int. Congress of Heating and Air Conditioning CLIMA 2000, Budapest 1980

[72] Crabb J. A, N. Murdoch and J. M. Penman, "A simplified thermal response model", Building Services Engineering Research & Technology, 8, pp. 13-19, 1987.

[73] Dewson T, B. Day and A. D. Irving, "Least squares parameter estimation of a reduced order thermal model of an experimental building", Building and Environment, 28(2), pp. 127-137, 1993.

[74] Tindale A, "Third-order lumped-parameter simulation method", Building Services Engineering Research & Technology, 14(3), pp. 87-97, 1993.

[75] Achterbosch G. G. J, P. P. G. de Jong, C. E. Krist-spit, S. F. van der Meulen and J. Verberne, "The development of a convenient thermal dynamic building model", Energy & Buildings, 8, pp. 183-196, 1985.

[76] Hudson G, C. P. Underwood, "A simple building modeling procedure for MATLAB/SIMULINK", Proc. IBPSA Building Simulation '99 Kyoto, pp. 776-783, 1999.

[77] Moore B. C, "Principal component analysis in linear systems: Controllability, observability and model reduction", IEEE Trans. Auto. Contr, AC-26, pp. 17-32, 1981.

[78] Lucas T N, "Linear system reduction by impulse energy approximation", IEEE Trans. Auto. Contr., AC-30, pp. 784-786, 1985.

[79] Mijangos E and N. Nabona, "On the first-order estimation of multipliers from Kuhn-Tucker systems", Jnl. Computers & Op. Res, 28, pp. 243-270, 2001.

[80] Conn A. R, N. Gould, A. Sartenaer and P. L. Toint, "Convergence properties of an augmented Lagrangian algorithm for optimization with a combination of general quality and linear constraints", SIAM Jnl. on Optimization, 6(3), pp. 674-703, 1996.

[81] Schittowski K, "NLQPL–a FORTRAN subroutine solving constrained nonlinear programming problems", Annals of Operations Research, 5, pp. 485-500, 1985.

[82] Biggs M. C. "Constrained minimization using recursive quadratic programming", Towards Global Optimization, (Dixon L W C and Szergo G P eds.), North-Holland, 1975.

[83] Han S. P, "A globally convergent method for nonlinear programming", Jnl. Opt. Theory & Appl., 22, 1977.

[84] Powel M. J. D, "A fast algorithm for nonlinearly constrained optimization calculations", Numerical Analysis Lecture Notes in Mathematics vol. 630, Watson G A ed., Berlin, Springer Verlag, 1978.

[85] Powel M. J. D, "The convergence of variable metric methods for nonlinearly constrained optimization calculations", Nonlinear Programming 3, O.L. Mangasarian O L, Meyer R R and Robinson S M eds., Academic Press, 1978.

[86] Fletcher R, "Practical Methods of Optimization", Vols. 1 & 2, New York, John Wiley and Sons, 1980.

[87] Gill P. E, W. Murry and M. H. Wright, "Practical Optimization", London: Academic Press, 1981.

[88] Powel M. J. D, "Variable metric methods for constrained optimization Mathematical Programming: The State of Art", Bachem A, Grtschel M, and Korte B eds., Berlin: Springer Verlag, 1983.

[89] Hock W, K. Schittowski, "A comparative performance evaluation of 27 nonlinear programming codes", Computing, 30, pp. 335, 1983.

[90] Horne M, "Modeling photovoltaic-clad facades", Build. Serv. Eng. Res. & Tech., 19(4), pp. B10-B12, 1998.

[91] Skartveit A, J. A. Olseth, "A model for the diffuse fraction of hourly global radiation", Solar Energy, 38(4), 1987.

[92] Liu B. Y. H, R. C. Jordan, "The long term average performance of flat-plate solar energy collectors", Solar Energy, 7(2), 1963.

[93] Jones A. D. "PhD thesis", University of Northumbria at Newcastle, 1999.

[94] Florez, J, "Temperature prediction models and their application to the control heating systems", Ph.D. Thesis, Control Systems Centre, UMIST, Manchester, United Kingdom, 1985.

[95] TRNSYS "A transient system simulation program-Volume 1", Reference manual. Madison, WI: Solar Energy Laboratory, University of Wisconsin, Germany, 1996.

[96] Clark, D R. "HVACSIM+ Building system and equipment simulation-Program reference manual", NBSIR 84-2996, Gaithersberg: National Institute of Standard Technology, 1985.

[97] Underwood C P, "Documentation of TRNSYS component models for HVAC applications", University of Northumbria at Newcastle, Built Environment Research Group, 1994.

[98] Dexter A. L, M. M. Eftekhari, P. Haves, and F. G. Jota, "The use of dynamic simulation models to evaluate algorithms for building energy control: experience with HVACSIM+", Proc. ICBEM'87 International Vongress on Building Energy Management, Lausanne, 1987.

[99] Metcalf R. M, R. D. Tylor, C. O. Pedersen, R. J. Liesen and D. E. Fisher, "Incorporating a modular simulation program into a large energy analysis program; the linking of IBLAST and HVASIM+", Proc. Building

simulation'95, Madison, WI: International Building performance simulation Association, 1995.

[100] Simulink: Dynamic system simulation for MATLAB, Natick, MA: Mathworks Inc., 1996.

[101] Holman J. P. "Heat Transfer", New York, McGraw Hill, 1997.

[102] Underwood C. P, "HVAC Control Systems: Modelling, Analysis and Design", E&FN SPON, London, 1999.

[103] CIBSE Applications Manual–Automatic Controls and their Implications for system design, Chartered Institution of Building Service Engineers, London.

[104] Underwood C. P, J. S. Edge, "Flow characteristics in circuits using three-port modulating control valves", Building Services Engineering Research and Technology, 16(3), pp. 127-132, 1995.

[105] Clark, J, "Computer Applications in the design of energy conscious buildings", Computer Aided Design, 14(1), pp. 3-9, 1982.

[106] Bowman N T, K. J. Lomas, "Empirical Validation of Dynamic thermal Computer models of Buildings", Building Service Engineering Research and Technology, 6(4), pp. 153-162, 1985.

[107] Haines R. W, "HVAC Systems Design Handbook", TAB Books, USA, 1988.

[108] Georgescu C, A. Afshari, and G. Bernard, "Fuzzy Predictive PID controllers: a heating control application", Proc. IEEE International Conference on Fuzzy Systems, 2, pp. 1091-1098, 1993.

[109] King P. J, E. H. Mamdani, "The Application of Fuzzy Control Systems to Industrial Processes", Automatica, 13, pp. 235-242, 1977.

[110] Yan, D, M. Saif, "Neural Network Based Controller for Nonlinear Systems", Control and Computer, 23, pp. 73-78, 1995.

[111] Patyra, M. J, D. M. Mlynek, (eds), "Fuzzy Logic Implementation & Applications", Wiley & Teubner, 1996.

[112] Mamdani, E.H., "Twenty years of fuzzy control: Experiences gained and lessons learned", Proc. Of 2nd IEEE International Conference on Fuzzy systems, pp. 339-344, 1993.

[113] Marks, R. J., "Fuzzy logic technology and applications". II ed., IEEE press, NY, 1994.

[114] Lee, C. C., "Fuzzy logic in control systems: Fuzzy logic controllers – Part I&II", IEEE Transactions on Systems, Man and Cybernitics, vol. 20, no. 2, 1990.

[115] Maiers, J, Y. S. Sherif, "Application of fuzzy set theory", IEEE Transaction on Systems Man and Cybernitics, vol. SMC15, pp. 175-189, 1985.

[116] Tong, R. M., "A retrospective view of fuzzy control systems", Fuzzy Sets and Systems, no. 14, pp. 199-210, 1984.

[117] Zimmermann, H. J, "Fuzzy set theory and its applications", 2nd Rev., Edn., Boston, 1991.

[118] Katayama, R., "Neuro, Fuzzy and Chaos Technology and its applications to SANYO consumer electronics", Japanese-European Symposium on Fuzzy Systems, 1992.

[119] Quail, S, S. Adnan, "State of the art in household appliances using fuzzy logic". Proc. Of the 2nd international workshop in Industrial fuzzy control and intelligent systems, IEEE press, pp. 204-213, 1992.

[120] Okey, C. h, "Fuzzy logic control for EPRI microwave clothes dryer", Proc. Of the 3rd IEEE International Conference on Fuzzy Systems, pp. 1348-1353, 1994.

[121] Steinmuller, H, O. Wiek, "Fuzzy and NeuorFuzzy applications in European Washing Machines", Proc. EUFIT'93. Aachen, pp. 1031-1035, 1993.

[122] Altrock, C. V, "Fuzzy Logic & NeuroFuzzy Applications Explained", Prentice Hall, NJ, 1995.

[123] Ross, T. R., "Fuzzy Logic with Engineering Applications". McGraw Hill Inc., 1995.

[124] Badami, V., "Fuzzy Logic Supervisory Control for Steam Turbine Pre-warming Automation", Proc. Of 3rd International Conference on Fuzzy Systems, pp 1045-1050, 1994.

[125] Cox, E., "Fuzzy Logic for Business and Industry", Charles River Media Inc., Massachusetts, 1995.

[126] Altrock, C. V, "Fuzzy Logic Technologies in Automative Engineering", Proc. Of Embeded Systems Conference, vol. 2, pp. 407-422, 1944.

[127] Yasunobu, S, S. Miyamoto, "Automatic Train Operation by Predictive Fuzzy Control", Sugeno (ed.), Industrial Applications of fuzzy Control, pp. 1-18, 1985.

[128] Jamshidi, M., N. Vadiee, and T. Ross, "Fuzzy Rule Based Expert Systems I&I.", (ed.) Fuzzy Logic and Control: Software and Hardware applications, pp. 137-149, Prenice Hall, NJ, pp. 51-111, 1993.

[129] Kaufmann, A., M. M. Gupta, "Introduction to Fuzzy Arithmetic", NewYork, Van Nostrand, 1985.

[130] Dubois, D., H. Prade, "Unfair Coins and necessity measures: Toward a possibilistic interpolation of histograms", Fuzzy Sets and Systems, vol. 10, no. 1, pp. 15-20, 1985.

[131] Bharathi, B., S. Sarma, "Estimation of Fuzzy membership from histograms", Information Science, vol. 35, pp. 43-59, 1985.

[132] Takagi, T., M. Sugeno, "Derivative of Fuzzy Control Rules From Human Operator's Control Actions", Proc. Of IFAC Symp. On Fuzzy Information, Knowledge Information and Decision Analysis, France, pp. 55-60, 1983.

[133] Lin, C. T., G. Lee, "Neural Fuzzy Systems: A Neuro-Fuzzy Synergism to Intelligent Systems", Prentice Hall, NJ, 1996.

[134] Hopfield, J. J, "Neural Networks and Physical Systems with Emergent Collective Computational Abilities", Proc. of the national academy of Science of the USA, vol. 79, pp. 2554-2558, 1982.

[135] Sugeno, M., M. Nishida, "Fuzzy Control of Model Car", Fuzzy Sets and Systems, no. 16, pp. 103-113, 1985.

[136] Sugeno, M., K. Tanaka, "Sucessive identification of fuzzy Model and its applications to predictions of complex systems", Fuzzy Sets and Systems, no. 42, pp. 315-344, 1991.

[137] Procyk, T. J., E. H. Mamdani, "A linguistic Self-organizing Process Controller". Automatica, vol. 15, no. 1, pp. 15-30, 1979.

[138] Sugeno, M., "An Introduction Survey of Fuzzy Control", Information Sciences, no. 36, pp. 59-83, 1985.

[139] Hellendoorn, H., C. Thomas, "Defuzzification in Fuzzy Controllers", Intelligent and Fuzzy Systems, vol. 1, pp. 109-123, 1993.

[140] ASHRAE, "Systems handbook", ASHRAE Inc., GA, 1984.

[141] Ziegler J. G., N. B. Nichols, "Process Lags in Automatic Control Circuits", ASME Transactions, 65, 1943.

[142] MathWorks, "Matlab User Manual", Natick, MA, 1993.

[143] ASHRAE, "Handbook of fundamentals, physiological principles, comfort and health", chapter 8, 1985.

[144] Fanger P. O., "Thermal comfort, Analysis and application in environmental engineering", Florida: Publishing Company Malabar, 1982.

[145] Benard C, B Guerrier, M. M. Rosset-Louerat, "Optimal building energy management: Part II-control", ASME Journal of Solar Energy Engineering, 114, pp. 13-22, 1992.

[146] Liem S. H, P. L. Lute, A. H. C van Paassen, and M. Vrwaal, "Passive building-control system", CEC-project "pastor", Delft University of Technology, 1989.

[147] Winn C. C, "Controls in Solar energy systems Advances", Solar Energy, 1, pp. 209-220, 1982.

[148] Dounis A. I, C. C Lefas, and A. Argirious, "Knowledge-based versus classical control for solar-building design", Applied Energy; 50(4), pp. 81-87, 1995.

[149] Dounis A. I, M. I. Santamouris, and C. C. Lefas, "Implementation of Artificial Intelligent techniques in thermal comfort control for passive solar buildings", Energy Conversion and Management, 33(3), pp. 175-182, 1992.

[150] Dounis A. I, M. I. Santamouris, and C. C. Lefas, "Building visual comfort control with fuzzy reasoning". Energy Conversion and Management, 34(1), pp. 17-28, 1993.

[151] Dounis A. I, M. I. Santamouris, C. C. Lefas, and D. E. Manolakis, "Thermal Comfort degradation by a visual comfort fuzzy reasoning machine under natural ventilation", Applied Energy, 48(2), pp. 115-130, 1994.

[152] Dounis A. I, M. I. Santamouris, C. C. Lefas, and A. Arigiou, "Design of a fuzzy set environment comfort system", Energy and Buildings, 22, pp. 81-87, 1995.

[153] Gupta M. M, J. B. Kiszka, and G. M. Rojan, "Multivariable Structure of fuzzy control systems", IEEE Transaction Systems Man Cybernetics 16(5), pp. 638-655, 1989.

[154] Mamdani E. H. "Application of fuzzy logic to approximate reasoning using linguistics synthesis", IEEE Transaction in Computers, 26(12), pp. 1182-1191, 1977.

[155] Kosko B, "Neural Networks and fuzzy systems", Prentice Hall, 1992.

[156] Fanger P. O., "Thermal comfort, Analysis and application in environmental engineering", McGraw-Hill, 1972.

[157] CIBSE Guide part C, section C1.

[158] Psychrometrics: Theory and Practice, American Society of Heating, Refrigerating, and Air-Conditioning Engineers, Inc, 1996.

[159] ASHRAE, "Ventilation for Acceptable Indoor Air Quality. ASHRAE Standard 62-1989", American Society of Heating, Refrigerating and Air-Conditioning Engineers, Atlanta, USA, 1989.

[160] ISO 9920, "Ergonomics of the Thermal Environment - estimation of the thermal insulation and evaporative resistance of a clothing ensemble", International Organisation for Standardisation, Switzerland, 1995.

[161] Nicol, F, "Thermal Comfort - a handbook for field studies toward an adaptive model", University of East London, 1993.

[162] ASHRAE, "Systems handbook", ASHRAE Inc., GA, 1984.

[163] Haines R. W, "HVAC Systems Design Handbook", TAB Books, USA, 1988.

[164] Kalogirou S. A, C. E. Neocleous, and C. N. Schinzas, "Artificial neural networks for the estimation of the performance of a parabolic trough collector steam generation system", Stockholm, Sweden: Proceedings of the International Conference EANN'97, pp. 227-232, 1997.

[165] Kalogirou S. A, C. E. Neocleous, and C. N. Schinzas, "Artificial neural networks for modelling the starting-up of a solar steam generator", Applied Energy, 60, pp. 89-100, 1998.

[166] Kalogirou S. A, "Application of artificial neural networks in energy systems: a review", Energy Conference Management, 40 (3), pp.1073-87, 1999.

[167] Bloem H., M. deGraaf, J. F. Kreider, and U. Norlen, "The first system identification competition", Proceedings of the ASME ISEC, Albuquerque, NM, 1998.

[168] Chen Y., Z. Chen, "A neural network based experimental technique for determining z-transfer function coefficients of a building envelope", Build Environ., 35, pp. 181-189, 2000.

[169] Kalogirou S. A, C. E. Neocleous, and C. N. Schinzas, "Heating load estimation using artificial neural networks", Brussels, Belgium: Proceedings of CLIMA 2000 Conference on CD-ROM, 1997.

[170] Haykin S, "Neural networks: a comprehensive foundation", New York: Macmillan, pp. 177, 1994.

[171] Golub G. H., C. F. Van Loan, "Matrix Computations", John Hopkins Univ. Press, Baltimore, MD, 1983

[172] Danaher S., G. Herries, T. Selige and M. Mac Suirtan, "A comparison of the Characterisation of Agricultural Land using Singular Value Decomposition and Neural Networks", Journal of Remote Sensing, 1998.

[173] Pao, Y. H, "Adaptive pattern recognition and neural networks", New York: Addison Wesley, 1989.

[174] DS1102 User's Guide Vs 3.0, dSPASE digital signal processing and control engineering GmbH Technologiepark 25, D-33100, Paderborn, Germany, 2001.

Appendices

Appendix A: High thermal capacity building's elements properties

Two rooms have been selected to demonstrate and validate the modelling and control methods through this thesis. Room 302, in the third floor of "Northumberland Building" in the city campus of University of Northumbria at Newcastle, it is a south facing room. Room 301, in the same floor in the same building, but it is a north facing room. Both rooms have the same areas, the same construction element properties, and they are computer laboratories as shown in the third floor plane. Northumberland building is a high thermal capacity building, it has been the subject of extensive research into photovoltaic cladding. The properties of various construction elements of the selected spaces are given in Table A1.

Element	Layering	Thickness (m)	Thermal Conductivity ($Wm^{-1}K^{-1}$)	Specific heat Capacity ($kJkg^{-1}K^{-1}$)	Density (kgm^{-3})
External Wall 1 (17.91 m^2)	Brick	0.122	0.84	800	1700
	Insulation	0.05	0.03	1764	30
	C-Block	0.112	0.510	1000	1400
	Plaster	0.013	0.160	1000	600
External Wall 2 (7.36 m^2)	Aluminium	0.003	0.160	896	2800
	Air space	0.100	-------	1025	1.2
	Insulation	0.075	0.035	1000	30
	Cast concrete	0.185	1.130	1000	2000
	Plaster	0.013	0.160	1000	600
Internal partitions (43.10 m^2)	Plaster	0.013	0.160	1000	600
	C-Block	0.122	0.510	1000	1400
	Plaster	0.013	0.160	1000	600
Internal floor/ceiling (63.00 m^2)	Carpet	0.009	0.060	2500	160
	Screed	0.065	0.410	840	1200
	Concrete	0.125	1.130	1000	2000

Table A1: Construction element properties (high thermal capacity building)

The parameters of the 6th order model of the high thermal capacity building space based on Lorenze & Mesy method are given in Table A2.

R_1=	0.060731 ($W^{-1}K$)	R_7=	0.003211 ($W^{-1}K$)	C_2=	2853468 (JK^{-1})
R_2=	0.067285 ($W^{-1}K$)	R_8=	0.009007 ($W^{-1}K$)	C_3=	35854560 (JK^{-1})
R_3=	0.335941 ($W^{-1}K$)	R_9=	0.007444 ($W^{-1}K$)	C_4=	35854560 (JK^{-1})
R_4=	0.037407 ($W^{-1}K$)	R_{10}=	0.007444 ($W^{-1}K$)	C_5=	8033840 (JK^{-1})
R_5=	0.009007 ($W^{-1}K$)	R_{11}=	0.010834 ($W^{-1}K$)	C_6=	1104000 (JK^{-1})
R_6=	0.003211 ($W^{-1}K$)	C_1=	5967003 (JK^{-1})		

Table A2: Parameters of 6th order model (high thermal capacity building)

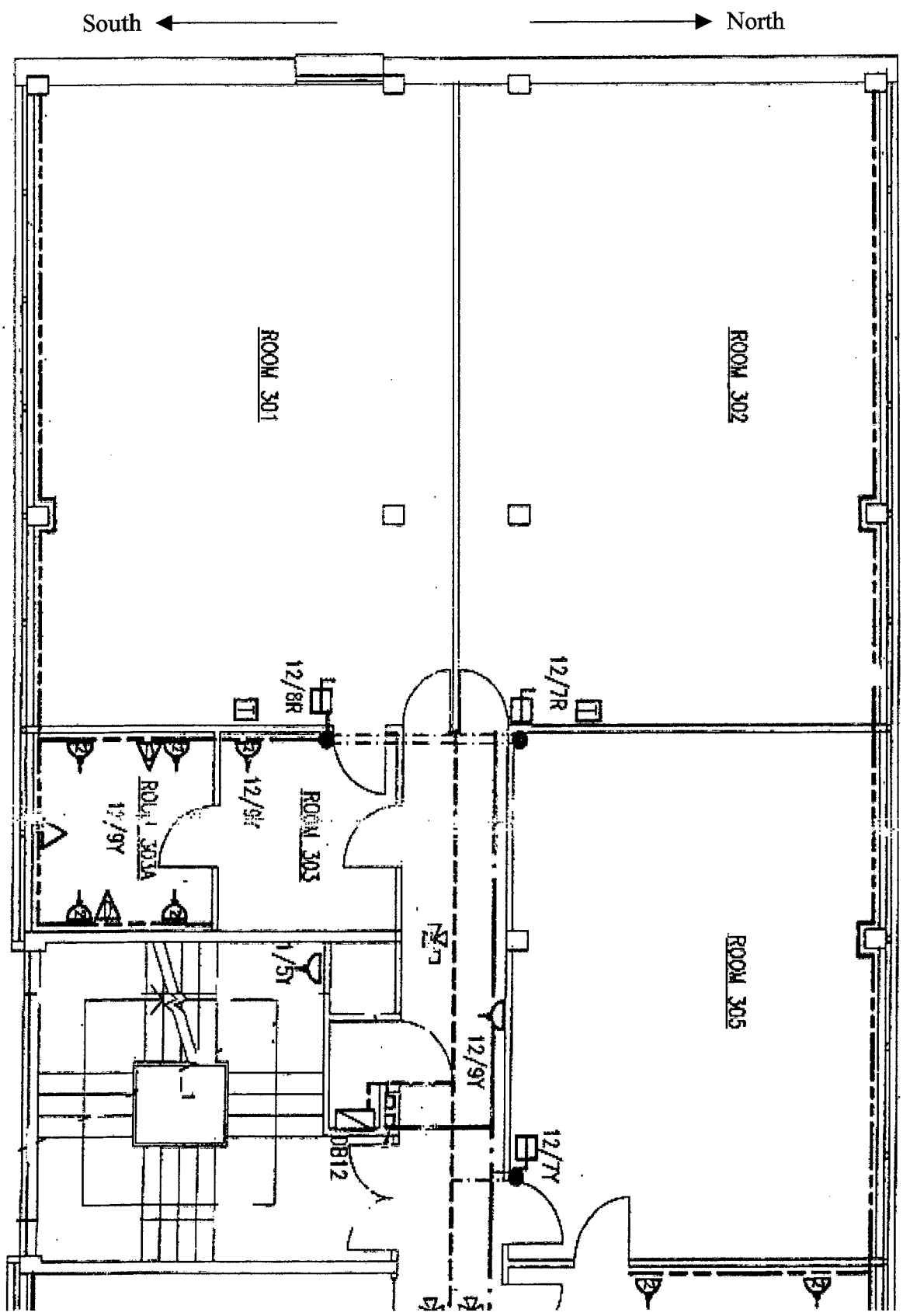

Figure (A1): Part of the third floor in Northumberland Building at University of Northumbria at Newcastle

Appendix B: Low thermal capacity building's elements properties

The above room was adopted to be a low thermal capacity building space but all construction elements were replaced using combinations of material choices with low capacity. Table B1, shows the construction element properties of low thermal capacity building.

Element	Layering	Thickness (m)	Thermal conductivity ($Wm^{-1}K^{-1}$)	Specific heat Capacity ($kJkg^{-1}K^{-1}$)	Density (kgm^{-3})
External Wall 1 (17.91 m^2)	Aluminium	0.0030	160	896	2800
	Air gap	0.0250	-----	1025	1.2
	Min. Wood	0.0433	0.04	1000	16
	L/w block	0.1120	0.19	1000	600
	Air gap	0.0100	-----	1025	1.2
	Plaster	0.0130	0.16	840	950
External Wall 2 (7.36 m^2)	As external wall 1 but with mineral wood insulation thickness of 0.0615 m				
Internal partitions (43.10 m^2)	Plaster	0.0177	0.16	840	950
	Air gap	0.1000	-----	1025	1.2
	Plaster	0.0177	0.16	840	950
Internal floor/ceiling (63.00 m^2)	Timber	0.025	0.14	1200	650
	Air gap	0.200	-----	1025	1.2
	Plaster	0.027	0.16	840	950

Table B1: Construction element properties (low thermal capacity building)

The parameters of the 6th order model of the high thermal capacity building space based on Lorenz & Masy method are given in Table A2.

R_1=	0.087900 ($W^{-1}K$)	R_7=	0.005861 ($W^{-1}K$)	C_2=	614951.5 (JK^{-1})
R_2=	0.040116 ($W^{-1}K$)	R_8=	0.006358 ($W^{-1}K$)	C_3=	2621506 (JK^{-1})
R_3=	0.269425 ($W^{-1}K$)	R_9=	0.007444 ($W^{-1}K$)	C_4=	2621506 (JK^{-1})
R_4=	0.103923 ($W^{-1}K$)	R_{10}=	0.007444 ($W^{-1}K$)	C_5=	1225249 (JK^{-1})
R_5=	0.006358 ($W^{-1}K$)	R_{11}=	0.010834 ($W^{-1}K$)	C_6=	1104000 (JK^{-1})
R_6=	0.005861 ($W^{-1}K$)	C_1=	1491221 (JK^{-1})		

Table B2: Parameters of 6th order model (low thermal capacity building)

Appendix C: Hot-water heating system parameters

The fin and tube natural convector consists of mild steel tube of 32mm and 35.52mm inside and outside diameter, respectively. The length of the tube is 9.2m. The thermal properties of the tube materials are as follows:

Density (ρ)	7860 kgm^{-3}
Specific heat capacity (C_p)	0.42 $kJkg^{-1}K^{-1}$
Thermal conductivity (k)	63 $Wm^{-1}K^{-1}$

Each of the aluminium fins are 90mm long and 83mm wide, with a thickness of 0.28mm and there are 90 fins per meter. The thermal properties of aluminum are taken to be as follows:

Density (ρ)	2710 kgm^{-3}
Specific heat capacity (C_p)	0.913 $kJkg^{-1}K^{-1}$
Thermal conductivity (k)	201 $Wm^{-1}K^{-1}$

Boundary conditions and design parameters of the convector are as follows:

T_{wi}	80 °C
T_{wo}	70 °C
A_w	0.925 m^2
A_a	25.039 m^2
Pr	2.53
μ_w	0.0004 $kgm^{-1}s^{-1}$
k_w	0.662 $Wm^{-1}K^{-1}$
m_w	0.28 kgs^{-1}
n	1.5
h_e	158 $Wm^{-2}K^{-1}$

Appendix D: Calculation of relative humidity

To calculate the relative humidity of the internal air of the selected building's space, firstly the internal air enthalpy (H_r) have been calculated from the room energy balance as following:

$$m\dot{H}_r = Q_l + m_o(H_0 - H_r) \qquad \text{D.1}$$

The outdoor air enthalpy (H_o) is calculated using the following set of equations:

$$g_{ss}(T_o) = \frac{0.624 Pw_{sat}(T_o)}{101.325 - 1.004 Pw_{sat}(T_o)} \qquad \text{D.2}$$

where Pw_{sat} can calculate from the following two equations (D.3,D.4):

The saturation pressure Pw_{sat} over ice for the temperature range of –100°C to 0°C is

$$lin(Pw_{sat}) = \sum_{i=0}^{5} a_i T^{i-1} + a_6 lin(T) \qquad \text{D.3}$$

where

$a_0 = -5674.5359$ $a_1 = 6.3925247$ $a_2 = -0.9677843e^{-2}$ $a_3 = 0.622157e^{-6}$

$a_4 = 0.20748e^{-8}$ $a_5 = 0.948402e^{-12}$ $a_6 = 4.1635019$

The saturation pressure over liquid water for temperature range of 0°C to 200°C is

$$lin(Pw_{sat}) = \sum_{i=-1}^{3} b_i T^{i-1} + b_4 lin(T) \qquad \text{D.4}$$

where:

$b_{-1} = -5800.2206$ $b_0 = 1.3914993$ $b_1 = -0.048640239$

$b_2 = 0.41764768e^{-4}$ $b_3 = -0.14452093e^{-7}$ $b_4 = 6.5459673$

From the measured outdoor air relative humidity (ϕ_{ext}), the mass of water vapour of the mixture (g) of the outdoor air can be calculated from the following equation:

$$\phi_{ext} = \frac{100 g(T_o)}{g_{ss}(T_0)} \qquad \text{D.5}$$

And then the enthalpy of the outdoor air (H_o) can be calculated from the following equation:

$$H_o = h * g(T_o) + C * T_o \qquad \text{D.6}$$

The mass of water vapour of the mixture (g) of the internal air can be calculated from the following equation:

$$g(T_i) = \frac{H_r - C * T_i}{h} \qquad \text{D.7}$$

Then the relative humidity of the internal air calculated form the following equation:

$$\phi_{\text{int}} = \frac{100 g(T_i)}{g_{ss}(T_i)} \qquad \text{D.8}$$

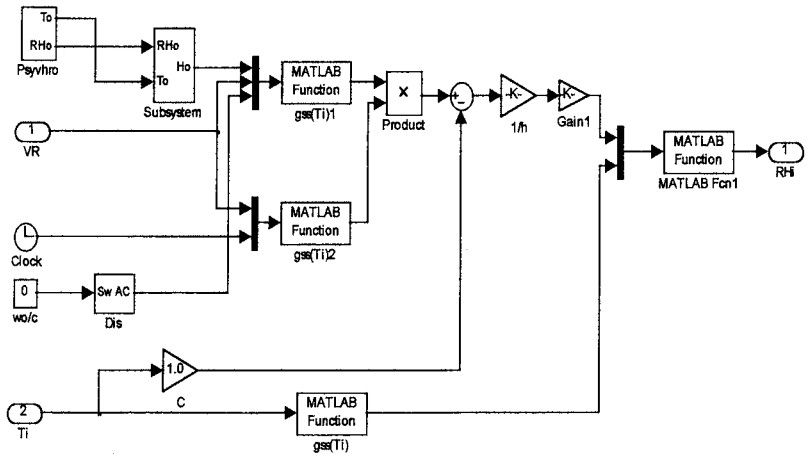

Figure (D.1): Model realisation of the relative humidity

The constants used to calculate PMV and PPD are given in the following table:

Constant	Value
Met (Specific metabolic activity in met)	1.2 met
pv (air velocity in m/s)	0.2 m/s
Clomin (minimal closing thermal resistance in clo)	0.75 clo
Clomax (maximal closing thermal resistance in clo)	1.25 clo

Appendix E: Cranfield test cell's elements properties

The construction elements properties of the test cell at Cranfield University as fellows:

Element	Layering	Thickness (m)	Thermal Conductivity ($Wm^{-1}K^{-1}$)	Specific heat Capacity ($kJkg^{-1}K^{-1}$)	Density (kgm^{-3})
East, West walls ($6.79865\ m^2$)	MDF	0.0090	0.080	1000	750
	Styrofoam	0.0504	0.033	1400	028
North wall ($8.0585\ m^2$)	Plasterboard	0.0126	0.160	0840	950
External Ceiling ($10.6323\ m^2$)	MDF	0.0090	0.080	1000	750
	Styrofoam	0.0504	0.033	1400	028
	Plasterboard	0.0126	0.160	0840	950
External Floor ($10.6323\ m^2$)	MDF	0.0120	0.080	1000	0750
	Styrofoam	0.0504	0.033	1400	0028
	Slab	0.0360	1.280	0920	2100
	Vinyl	0.0020	0.220	1.260	1600
South wall ($5.6585\ m^2$)	Cladding	0.003	0.170	1300	1300
	Styrofoam	0.010	0.027	1400	0028
	Cladding	0.003	0.170	1300	1300
Window ($2.4\ m^2$)	Glass	0.004	0.105	750	2500
	Air Gap	0.012	-------	-----	------
	Glass	0.004	0.105	750	2500

Table E1: Construction element properties of Cranfield test cell

The parameters of the optimized model of Cranfield test cell as shown in the following table:

R_1=	0.0103502 ($W^{-1}K$)	R_{17}=	0.11170000 ($W^{-1}K$)
R_2=	0.0517151 ($W^{-1}K$)	R_{18}=	0.02792500 ($W^{-1}K$)
R_3=	0.0414008 ($W^{-1}K$)	R_{19}=	1.08333333 ($W^{-1}K$)
R_4=	0.1177965 ($W^{-1}K$)	C_1=	8939.29800 (JK^{-1})
R_5=	0.0942372 ($W^{-1}K$)	C_2=	50656.0220 (JK^{-1})
R_6=	0.0235593 ($W^{-1}K$)	C_3=	128641.125 (JK^{-1})
R_7=	0.1396250 ($W^{-1}K$)	C_4=	22701.3750 (JK^{-1})
R_8=	0.1117000 ($W^{-1}K$)	C_5=	108259.615 (JK^{-1})
R_9=	0.0279250 ($W^{-1}K$)	C_6=	19152.2850 (JK^{-1})
R_{10}=	0.0890910 ($W^{-1}K$)	C_7=	727178.825 (JK^{-1})
R_{11}=	0.0712728 ($W^{-1}K$)	C_8=	128325.675 (JK^{-1})
R_{12}=	0.0178182 ($W^{-1}K$)	C_9=	169582.480 (JK^{-1})
R_{13}=	0.0892810 ($W^{-1}K$)	C_{10}=	29926.3200 (JK^{-1})
R_{14}=	0.0714248 ($W^{-1}K$)	C_{11}=	108529.615 (JK^{-1})
R_{15}=	0.0178562 ($W^{-1}K$)	C_{12}=	19152.2850 (JK^{-1})
R_{16}=	0.1396250 ($W^{-1}K$)	C_{13}=	29686.3052 (JK^{-1})